

ACTIVE VIBRATION CONTROL OF PIEZO-LAMINATED CIRCULAR PLATE

A DISSERTATION

*Submitted in partial fulfillment of the
requirements for the award of the degree
of*

MASTER OF TECHNOLOGY

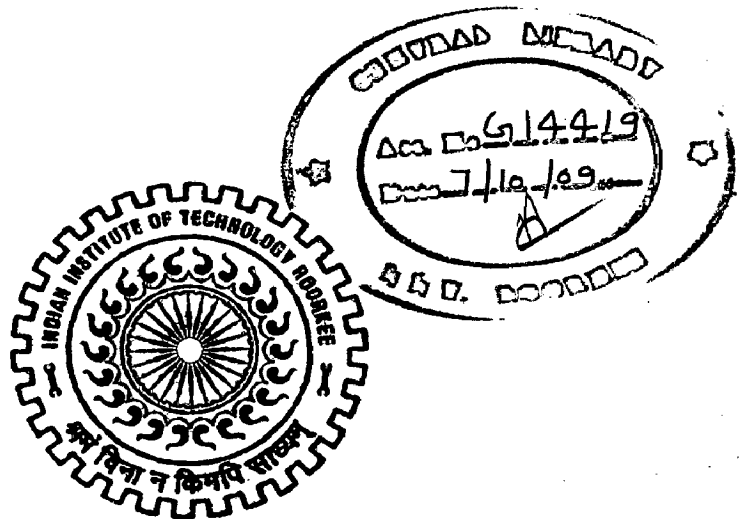
in

MECHANICAL ENGINEERING

(With Specialization in Machine Design Engineering)

By

MOHAMMAD ARIF



DEPARTMENT OF MECHANICAL AND INDUSTRIAL ENGINEERING
INDIAN INSTITUTE OF TECHNOLOGY ROORKEE
ROORKEE - 247 667 (INDIA)

JUNE, 2009

CANDIDATE'S DECLARATION

I here by declare that the work, carried out in this dissertation titled "**ACTIVE VIBRATION CONTROL OF PIEZO-LAMINATED CIRCULAR PLATE**" is presented in behalf of partial fulfillment of the requirement for the award of the degree of "**Master of Technology**" in Mechanical Engineering with specialization in **Machine Design Engineering**, submitted to the Department of Mechanical and Industrial Engineering, Indian Institute of Technology, Roorkee, is an authentic record of my own work under the supervision and guidance of **Dr. B.K.Mishra**, Professor and **Dr. V. H. Saran**, Assistant Professor, Department of Mechanical & Industrial Engineering, IIT, Roorkee, India.

I have not submitted the record embodied in this report for the award of any other degree or diploma of this or any other institute.

Date: 23. 06. 2009

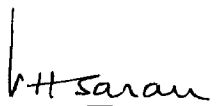
Place: Roorkee



MOHAMMAD ARIIF

This is to certify that the above statement made by the candidate is correct to the best of our knowledge.

Date: 23/6/9

Place: Roorkee


(Dr. V.H.Saran)
Assistant Professor
Department of Mechanical &
Industrial Engineering
I.I.T, Roorkee


(Dr. B.K.Mishra)
Professor
Department of Mechanical &
Industrial Engineering
I.I.T, Roorkee

ACKNOWLEDGEMENT

First and foremost I wish to thank, the one and almighty for his mercy and blessings, without which I can't be able to precede a single step in any direction.

I wish to express my sincerest gratitude to my supervisors **Dr. B. K. Mishra**, Professor and **Dr. V.H. Saran**, Assistant Professor, Department of Mechanical and Industrial Engineering, Indian Institute Of Technology, Roorkee for their consistent advice, guidance and encouragement in this work. Their timely help, constructive criticism, and painstaking efforts made it possible to bring the work contained in this report in its present form. Working under their guidance was a privilege and an excellent learning experience that I will cherish for a long time.

I am very much grateful to **Prof. Pradeep Kumar**, Prof and Head of the department of Mechanical and Industrial Engineering, for his encouragement and overall supervision in bringing out this dissertation report.

I would also like to thanks **Dr. S.P.Harsha**, Assistant Professor & O.C., Mechanical Vibration & Noise Control Laboratory, for his kind and generous support and fruitful discussions during the course of this work. In spite of his busy schedule he has rendered guidance whenever needed, giving golden suggestions and holding informal discussions.

I would like to extend my thanks to all the teachers of the department who had been source of inspiration to me and also to Md. Shaukat Ali, Saad Alam, A.A. S. Gazi, Rehan Sadique and Md. Asif for their continuous encouragement and motivation.

I would like to express my gratitude to my parents, their blessings; motivation and inspiration have always provided me a high mental support. I am also grateful to my friends who are actively involved in providing me a vital support and encouragement whenever I needed.

At last but certainly not least, I would like to express my sincere thanks all those who were attached to me and helped me at any level during my stay at Roorkee.

MOHAMMAD ARIF

CONTENTS

TITLE	PAGE NO.
CANDIDATE'S DECLARATION AND CERTIFICATE	i
ACKNOWLEDGEMENT	ii
ABSTRACT	v
LIST OF SYMBOLS	vii
LIST OF FIGURES	ix
LIST OF TABLES	xi
Chapter 1. INTRODUCTION	1
1.1 Motivation	1
1.2 Preamble	4
1.3 Organization of the thesis	5
Chapter 2. BACKGROUND	6
2.1 Perspective in smart structure	6
2.1.1 Shape memory alloy	8
2.1.2 Piezoelectric material	11
2.1.3 Electrostrictive material	12
2.1.4 Magnetostrictive material	13
2.1.5 Electro-rehostatic and Magneto-rheostatic fluids	13
2.1.6 Fiber optics	14
2.2 Piezoelectric material	14
2.2.1 Classification of piezoelectric materials	19
2.2.2 Piezoelectric constitutive relations	19
2.2.3 PZT manufacturing processes	21
2.3 Active control strategy for vibration suppression	22
Chapter 3. LITERATURE REVIEW	24
3.1 Vibration control	25
3.2 Experimental work	29

3.3 FEM Formulation	31
3.4 Optimal sensor/Actuator placement	34
Chapter 4. BASIC EQUATIONS AND FORMULATIONS	38
4.1 Classical Plate Theory	38
4.2 Modeling of Circular Plate with Piezoelectric patches	39
4.3 Constitutive Equations of Piezoelectric materials	45
4.3.1 Linear strain-displacement relations	46
4.3.2 Isoparametric quadratic element	47
4.3.3 Electric field-electric voltage relations	48
4.3.4 Governing equation of motion	49
4.3.5 Sensor Voltage	50
4.3.6 Actuator Forces	52
4.4 The Control Law	53
Chapter 5. EXPERIMENTATION	56
5.1 Equipments	56
5.2 Experimental setup	59
5.2.1 Piezoelectric material (PZT patch)	60
5.2.2 USB based data acquisition	61
5.2.3 Piezo sensing and actuation system	63
5.2.4 Computer with LabVIEW software	64
5.3 Procedure	68
Chapter 6. RESULTS AND DISCUSSION	70
6.1 Optimal placement of sensor/actuator pair	75
6.2 Experimental work	80
Chapter 7. CONCLUSION AND FUTURE SCOPE	94
7.1 Conclusion	94
7.2 Scope for future work	95
REFERENCES	96

ABSTRACT

This work deals with the experimental study of vibration suppression of circular annular plate clamped at the inner boundary and free at the outer boundary using piezoelectric patches. Piezoelectric material is used, both as a sensor and actuator. Proportional feed back control system is used in this experiment. In the proportional feed back control method, the feed back voltage is generated as a function of position like quantity (i.e. strain). As the plate deforms, due to external excitation, the PZT film (sensor) attached to it also deforms and due to its characteristics, it develop a voltage proportional to the applied force. The voltage is amplified by the control system, to obtain the feedback voltage. This feedback voltage is applied to the actuator which develops counteractive deformation of the plate. This action is used to suppress the vibration of the plate.

First of all, a brief description about objective of active vibration control methods are discussed which mainly focus on the reduction of vibration is done by automatic modification of the system structural response. Active vibration control is widely used because of its broad frequency response range, low additional mass, high adaptability and good efficiency.

Subsequently, theoretical background of smart structures and smart materials are discussed in details which contents shape memory alloy, electrostrictive materials, magnetostrictive materials, fiber optics and piezoelectric materials. In which piezoelectric materials are discussed in details. Further a brief review of the available literatures on active vibration control of beams and circular plates are presented. In which optimum location of PZT patches are also discussed. After that, basic equations and formulations are presented in detail, which contents classical plate theory, modeling of circular plate with piezoelectric patches, constitutive equations of piezoelectric materials, governing equation of motion and sensor voltage relations.

First the optimal locations of the sensor/actuator pairs are investigated by *ANSYS* simulation, because sensor/actuator pairs have a critical influence on the vibration suppression of smart structures. Hence, sensor/actuator pairs must be placed in high strain

regions and away from areas of low strains. An experimental set-up is developed which consist of circular annular plate, PZT patches, DAQ, signal conditioner and computer system with LabVIEW software. The plate is clamped at the inner boundary and excited by impulsive force at the outer boundary. The sensor readings are recorded in the computer with the help of data acquisition card and the vibration of the structure is controlled by the Piezo-actuation system by increasing the gain further logarithmic rate of decay are calculated for comparison purpose. Natural frequency with different aspect ratio are theoretically calculated and compared with the available literature. Mode shape with PZT patch and without PZT patches both are presented.

Finally, experimental and numerical simulation shows that a combination of sensor-actuator-controller can be used to suppress the vibration in the plate.

LIST OF SYMBOLS

DSP	: Digital Signal Processing
PZT	: Piezo-electric (Lead Zirconate Titanate)
PVDF	: Polyvinylidene fluoride
SMA	: Shape Memory Alloy
LQG	: Linear Quadratic Gaussian
SSA	: Self Sensing Actuator
LQR	: Linear Quadratic Regulator
CPT	: Classical plate theory
MIMO	: Multi-input and multi-output
GA	: Genetic algorithms
VEM	: Viscoelastic material
PCLD	: Passive constrained layer damping
h	: Plate thickness
q	: Distributed transverse load
u	: Displacement vector (in x-axis)
v	: Displacement vector (in y- axis)
w	: Displacement vector (in z-axis)
t	: Time
γ	: Shear strain
G	: Control gain
N	: Force resultant
M	: Moment resultant
P	: Load
F_s	: Reaction force of elastic foundation
D_{ij}	: Bending stiffness
D	: Flexural stiffness
I_o	: Principal inertia

I_2	: Rotary Inertia
J_n	: Bessel function of first kind
Y_n	: Bessel function of second kind
I_n	: Modified Bessel function of first kind
K_n	: Modified Bessel function of second kind
V	: Shear force
r_0	: Outer radius
r_i	: Inner radius
k	: Elastic foundation modulus

Greek symbols:

Ω_0	: Mid-plane of the plate
ε	: Strain field
σ	: Stress field
∇	: Del operator
ν	: Poisson ratio
α	: Co-efficient of thermal expansion
ω	: Angular frequency
ρ	: Mass density

Subscripts:

r	: Refers to r direction
0	: Refers to a point on the mid plane (i.e., $Z = 0$)
θ	: Refers to θ direction
z	: Refers to Z direction
S	: No of nodal circle
s	: Refers to sensor
a	: Refers to actuator
n	: No of nodal diameter

LIST OF FIGURES

FIGURE NO.	TITLE	PAGE NO.
1.1	A multi-layer actuator	3
1.2	A schematic of a 1-3 connectivity composite	4
2.1 (a)	Components of a smart structural system	7
2.1 (b)	Components of a smart structural system	7
2.2	The shape memory effect	8
2.3	Microscopic and Macroscopic Views of the Two Phases of SMA	9
2.4	The Dependency of Phase Change Temperature on Loading	10
2.5	Microscopic Diagram of the Shape Memory Effect	10
2.6	Displacement Vs Voltage behavior of piezoelectric and electrostrictive materials	12
2.7	Piezoelectric effect	15
2.8	Crystal structures of PZT ceramics above and below their T_c	16
2.9	Random orientation of polar domain prior to polarization	16
2.10	Polarization in DC electric field	17
2.11	Remanent polarization after electric field is removed	17
2.12	Axis configuration of piezoelectric patch	20
4.1	Moment and shear force resultant on an element of a circular plate	40
4.2	Definition of displacement and rotations	46
4.3	Circular plate with sensor and actuator	54
5.1	Block diagram of experimental setup of proportional feedback control	59
5.2	Experimental setup of the proportional control system	60
5.3	Aluminum plate clamped at the inner boundary with PZT patches	61
5.4 (a)	NI make DAQ card-NI 6009	62
5.4 (b)	NI DAQ card connection unit	63
5.5	Piezo sensing and Piezo actuation system	64
5.6 (a)	LabVIEW main screen (at the time of starting)	65
5.6 (b)	LabVIEW main screen	66
5.7 (a)	Front panel of the LabVIEW VI programme	66

5.7 (b)	Block diagram of the LabVIEW VI programme	67
5.8	DAQ assistant parameter dialogue box	67
5.9	Band pass filter block	69
6.1-6.10	Comparison of natural frequency of annular plate for different aspect ratio.	73-74
6.11	Boundary condition imposed on the plate	78
6.12	Normal elastic strain of circular annular plate	79
6.13	Uncontrolled response of amplitude of vibration with respect to time	80
6.14	Best fit curve (Uncontrolled response) crossing the peak level of amplitude	81
6.15	Controlled response (Gain-1) of amplitude of vibration with respect to time	81
6.16	Best fit curve crossing the peak level of amplitude for Gain-1	82
6.17	Controlled response (Gain-2) of amplitude of vibration with respect to time	82
6.18	Best fit curve crossing the peak level of amplitude for Gain-2	83
6.19	Controlled response (Gain-3) of amplitude of vibration with respect to time	83
6.20	Best fit curve crossing the peak level of amplitude for Gain-3	84
6.21	Bar chart to show the logarithmic decrement	85
6.22	Uncontrolled response of amplitude of vibration with respect to frequency	86
6.23	Controlled response (Gain-1) of amplitude of vibration with respect to frequency	86
6.24	Controlled response (Gain-2) of amplitude of vibration with respect to frequency	87
6.25	Controlled response (Gain-3) of amplitude of vibration with respect to frequency	87
6.26	Combined plot in between uncontrolled response and controlled response (Gain-3)	88
6.27	Six mode shape of circular annular plate without PZT patches	90
6.28	Mode shape of circular annular plate with PZT patches	93

LIST OF TABLES

TABLE NO.	TITLE	PAGE NO.
5.1	Material properties of plate specimen	56
5.2	Properties of the piezoelectric sensor and actuator (PZT patches)	57
5.3	USB based Data acquisition card by National Instrument Inc	57
5.4	Properties of vibration control unit by Spranktronics Inc	58
6.1	Properties of Piezoelectric patch and plate	70
6.2	Comparison of natural frequency (Hz) of annular plate (clamped at inner boundary and free at outer boundary) for different $\frac{h}{r_o}$ ratio and $\frac{r_i}{r_o} = 0.3$	71
6.3	Comparison of natural frequency (Hz) of annular plate (clamped at inner boundary and free at outer boundary) for different aspect ratio and $\frac{h}{r_o} = 0.001$	72

1.1 Motivation

The trend in aeronautical, mechanical and civil design requires structures to become lighter, stronger and more flexible. In aeronautical applications for example, the advantages of lighter weight structures are attained through cost savings and increased capacity to carry a greater payload. However, light weight flexible structures can be more easily influenced by unwanted vibrations, which may lead to problems such as fatigue, instability and performance reduction; these problems may eventually cause damage to the highly stressed structure. Vibration problems may also cause acoustic disturbance (noise nuisance) due to the coupling of structural vibration and the acoustic field. Acoustic disturbance caused by structural vibration can be annoying and harmful to health, and in some cases illegal. Hence controlling vibration is one of the challenging practical problems. With appropriate control, structural problems associated with unwanted vibration can be reduced, and the corresponding noise radiation from the vibrating structure can also be attenuated.

In the past few decades, various control techniques have been developed in different fields to attenuate structural vibration disturbance. Among these techniques, traditional passive control is used widely in industries and commercial products. In passive control technique, the material properties of structures such as damping and stiffness are modified so as to change the response of structure. The two most essential components of passive vibration isolator are its load-supporting means (stiffness) and its energy dissipating means (damping). Typical passive isolator employs metallic springs, elastomers, wire cables, pneumatic springs. They don't require external power in order to function properly. They are very effective in the middle to high frequency range. However, passive control approaches become ineffective when the dynamics of the system and/or the frequencies of the disturbance vary with time. They are often impractical to implement in the low frequency range, where the disturbance wavelength is relatively long and the passive control methods require bulky/heavy installations. In many applications, such as in aeronautical industries where minimizing the structural weight is paramount in the system design, the large and

heavy passive control appendages are impractical. Hence due to these drawbacks active vibration control technique is very much frequently used in order to eliminate the undesired vibration. Particularly during the recent years, due to the progresses in electronic technology and the availability of low cost electronic components, they experienced a dramatic gain in interest. Their use can be considered as under-exploited in the 20th century. The most evident advantage of active systems is given by the lower weight. Active vibration isolation systems are currently being successfully used to solve actual on-site industrial vibration problem. The use of smart structures is experiencing a tremendous growth in actively controlling the vibration.

In the last two decades, due to exponential development in the field of space structures and high-performance light weight flexible mechanical system has stimulated extensive research in the area of smart/intelligent materials and structures. The main reasons to draw attention in the field of smart structure is the ability to sense, measure, process and diagnoses at critical locations for any change in selected variables and to command suitable action to restore structural integrity and continue to perform the required function. The variable may be deformation, temperature, pressure, and change in state and phase, and may be optical, electrical, magnetic, chemical or biological. In addition to carrying mechanical loads, smart structures may alleviate vibration, reduce acoustic noise, monitor their own condition and environment, automatically perform precision alignments, or change their shape or mechanical properties.

On the threshold of 21st century, peoples are entering into research and development of the next generation of smart materials and structural system which provides excellent new opportunities for radical changes in the design and development of adaptive structures and high performance structures. The next generation of smart material systems will focus towards thermo-electro-mechanical coupling, functionality, intelligent and miniaturization (down to nano length scales.) [61].

Recent studies in the areas of smart structures inclined more attention towards piezoelectric materials as compared to conventional discrete sensing and control systems. Piezoelectric materials act as a coupling in between mechanical and electrical properties which convert electrical to mechanical energy and vice-versa make them employed as actuators and sensors. Bonded piezoelectric patches in a structure act as sensor to monitor

or as actuator to control the response of the structure. In addition to these properties piezoelectric materials have several other characteristics such as quick response, lower power consumption, high efficiency and compactness, easily mounted on the structures and low weight etc. Piezoelectric patches are available in two forms: multi layered active materials and multi phase active materials [61]. Multi layered active materials are stack of active materials in which large fields are obtained with the moderate level of input voltage. It is manufactured by tape casting technology and electrodes are embedded in several different ways. The multi layered composite system is also amenable to miniaturization in order to decrease the thickness of active multi layers.

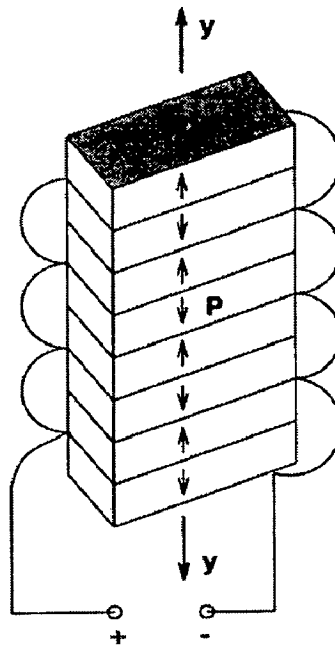


Figure 1.1: A multi-layer actuator [61]

Multi-phase composite systems consist of an active phase embedded in a passive matrix (e.g. PZT rods in a polymer matrix). Different connectivity schemes are possible in a two-phase system. The multi-phase composites are most often useful when there are conflicting requirements on the active material system. This type of active-passive phase combinations helps in achieving multifunctionality.

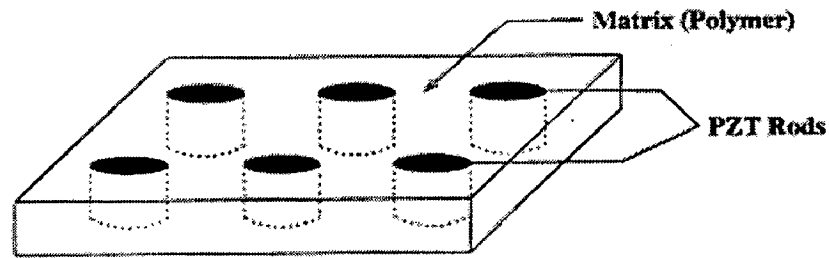


Figure 1.2: A schematic of a 1-3 connectivity composite [61]

The piezoelectric materials are very much frequently used as the sensor/ actuator in the smart structure for vibration suppression because sensing and actuation mechanism becomes parts of the structure itself. But, for the complex structure, it is very much costly to implement smart materials over the entire surface. Hence sensor and actuator are distributed discretely over the entire structure. One of the main limitations of the piezoelectric actuator is the amount of force it exerts. Hence, actuator should be placed on the optimal location in order to minimize the control effort. Hence, optimization of the placement of the sensor and actuator over the structure is one of the challenging tasks in the suppression of the vibration of structure. The problem becomes so much critical if the no of sensor/actuator increases and the mode shape becomes complicated. Due to these problems optimization technique has to be used in order to investigate the good set of sensor/actuator position. There are several optimization techniques such as Genetic Algorithms, Tabu Search, Simulated Annealing and Hill Climbing etc.

1.2 Preamble

The main focus of this study is to develop simple finite element of isotropic plate for active vibration control. This work contents modeling of plate using finite element method using classical plate theory. The dynamic characteristics of the structure are studied and piezoelectric patches are used to control the vibration. The vibration of the plate is controlled by proportional control method experimentally. Piezo sensing and actuation system are used in order to sense and control the vibration using proportional control method. Mode shapes and natural frequencies for the different aspect ratio of the composite plates are presented.

1.3 Organization of the Thesis

Chapter 2 addresses some background of smart structures and materials. Piezoelectric materials are explained in details. Piezoelectric constitutive relations and its manufacturing processes are also discussed. The strategies in active vibration control are also presented.

Chapter 3 contains brief description regarding the previous study of this field. Summarized details of work carried out by different authors, their objectives and conclusions are explained.

Chapter 4 details the development of the finite element model using classical laminated plate theory. Natural frequency equations are derived with PZT patches. The governing equation of motion, sensor voltage relations and actuator forces relations are explained in details. Two different control strategies are discussed.

Chapter 5 presents descriptions about experimental setup for active vibration control and its specifications. Procedure for active vibration control is also explained.

Chapter 6 presents the results and discussion of the present work. The optimal placement of sensor/actuator pairs is also discussed. The controlled and uncontrolled responses are compared in the normalized form.

Chapter 7 presents the conclusion of the present work and scope for future work.

This chapter contains the theoretical background of smart structures and smart materials, mainly piezoelectric materials and a brief description of active vibration control strategy.

2.1 Perspectives in smart Structure

A structure is an assembly that performs engineering function e.g. building, bridge, power plant, ship, Jet engine and space craft etc. It is reasonable to expect that all engineering design should be smart and not dumb. But one can still make a distinction between smartly designed structures and smart structures. The latter term has acquired a specific technical meaning over the last few decades. Smart structures are structures that are capable of sensing and reacting to their environment in a predictable and desired manner through the integration of various elements, such as sensors, actuators, power sources, signal processors and communications network etc. The integrated structure is called smart structure because it has ability to sense, measure, process and diagnoses at critical locations for any change in selected variables and to command suitable action to restore structural integrity and continue to perform the required function. The variable may be deformation, change in temperature and pressure, and change in state and phase and may be optical, electrical, magnetic, chemical or biological. In addition to carrying mechanical loads, smart structures may alleviate vibration, reduce acoustic noise, and monitor their own condition and environment, automatically perform precision alignments, or change their shape or mechanical properties [71]. The development in the field of smart structures are totally depends on the development of material science and the control logic. In the field of material science, various new smart materials are developed that allow them to be used for sensing and actuation in an efficient and controlled manner. Smart materials, similar to living beings, have the ability to perform both sensing and actuating functions and are capable of adapting to changes in the environment. In other words, smart materials can change themselves in response to an outside stimulus or respond to the stimulus by producing a signal of some sort. By utilizing these materials, a complicated part in a system consisting of individual structural,

sensing, and actuating components can now exist in a single component, thereby reducing overall size and complexity of the system.

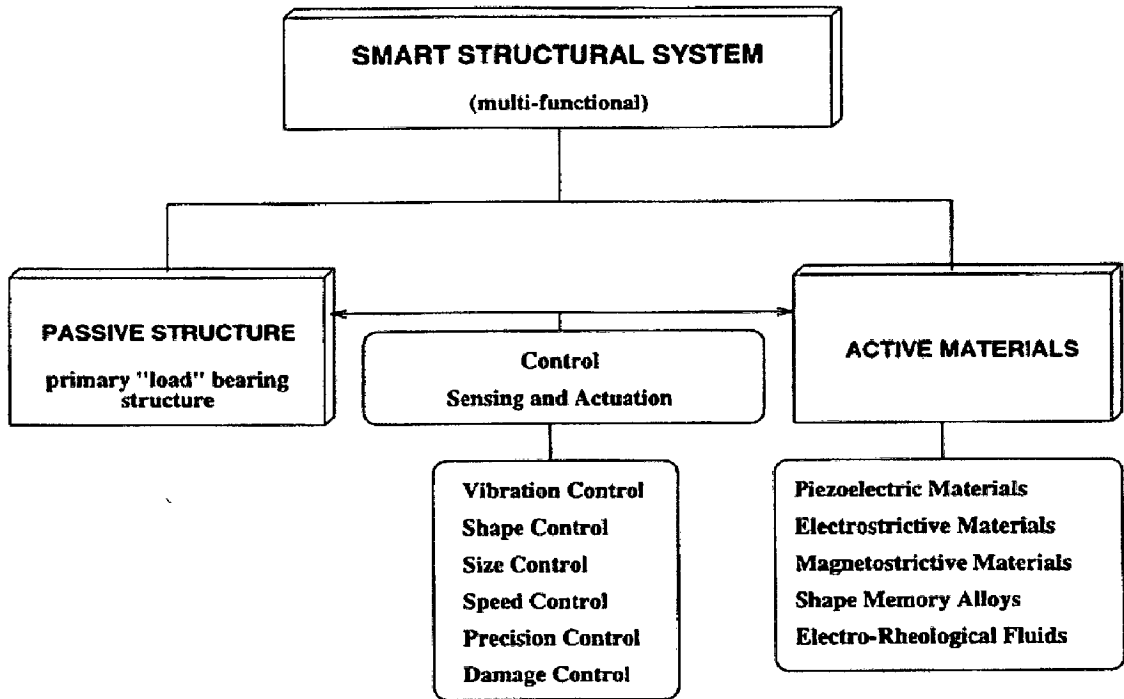


Figure 2.1 (a): Components of a smart structural system [61]

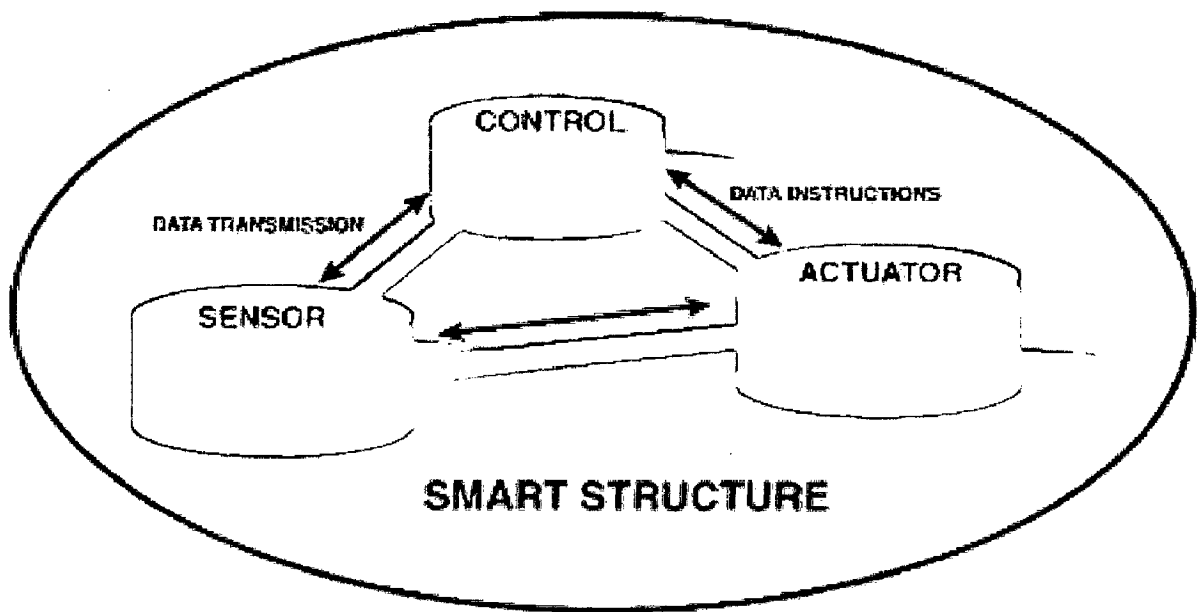


Figure 2.1 (b): Components of a smart structural system [4]

Smart materials can be conveniently subdivided into passively and actively smart materials. A passively smart material responds to an external change without thought or signal processing while an actively smart material analyzes the sensed signal, perhaps for its frequency components, and then makes a choice as to what type of response to make.

A variety of smart material already exists, and is being researched extensively. These includes shape memory alloy, piezoelectric material, magnetostrictive material, electrostrictive material, ferromagnetic shape memory alloy, electrorheological and magnetorehological fluids and fiber optics etc.

2.1.1 Shape memory alloy (SMA)

Shape memory alloys (SMAs) are the most common group of metallic materials that can be deformed and can revert back to their original (undeformed) shapes when heated above their transformation temperatures. The first developed SMA was an alloy of nickel and titanium called Nitinol, which was discovered by scientists at the U.S. Naval Ordnance Laboratory in 1965. This alloy can deform up to 10 % and still regain its original form. Beyond this limit, it deforms plastically and does not regain its original shape. The newest types of SMAs are combinations of copper and zinc that are alloyed with other metals such as aluminum. The shape memory effect is shown in Figure.2.2 Basically, shape recovery is due to solid-to-solid phase transformation from martensite to austenite [88].

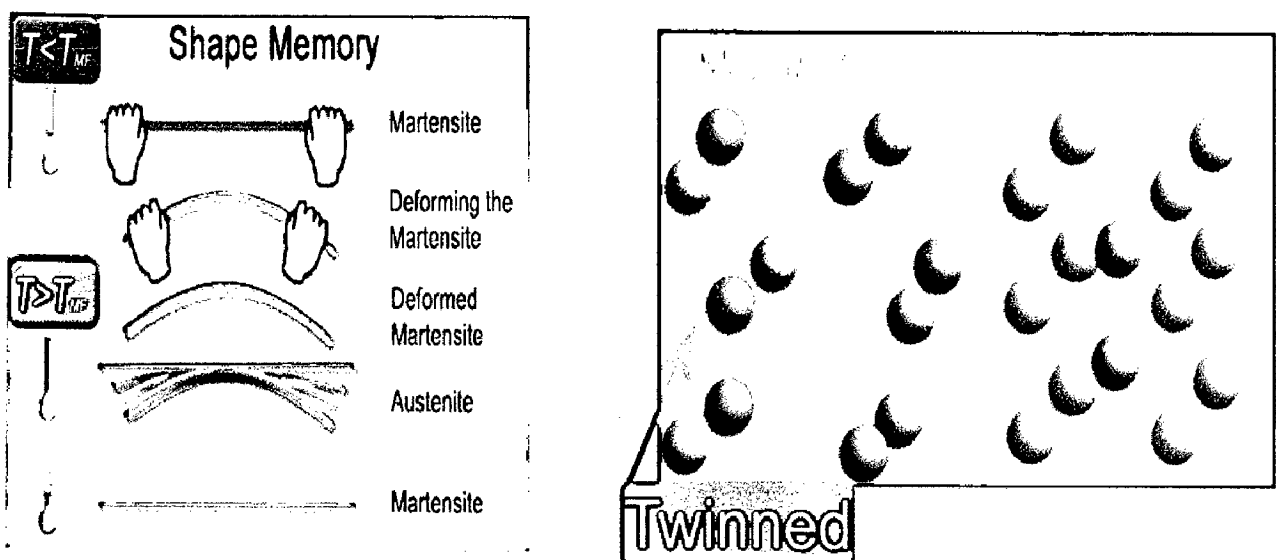


Figure 2.2: The shape memory effect [89]

Martensite is the relatively soft and easily deformed phase of shape memory alloys, which exists at lower temperature. The molecular structure in this phase is twinned which is shown in the Figure 2.3. Upon deformation, this phase takes the second form as shown in Figure 2.3. Austenite, the stronger phase of shape memory alloys, occurs at higher temperatures. The shape of the Austenite structure is cubic, as shown in Figure 2.3. The un-deformed Martensite phase has the same size and shape as the cubic Austenite phase on a macroscopic scale, so that no change in size or shape is visible in shape memory alloys until the Martensite is deformed [90].

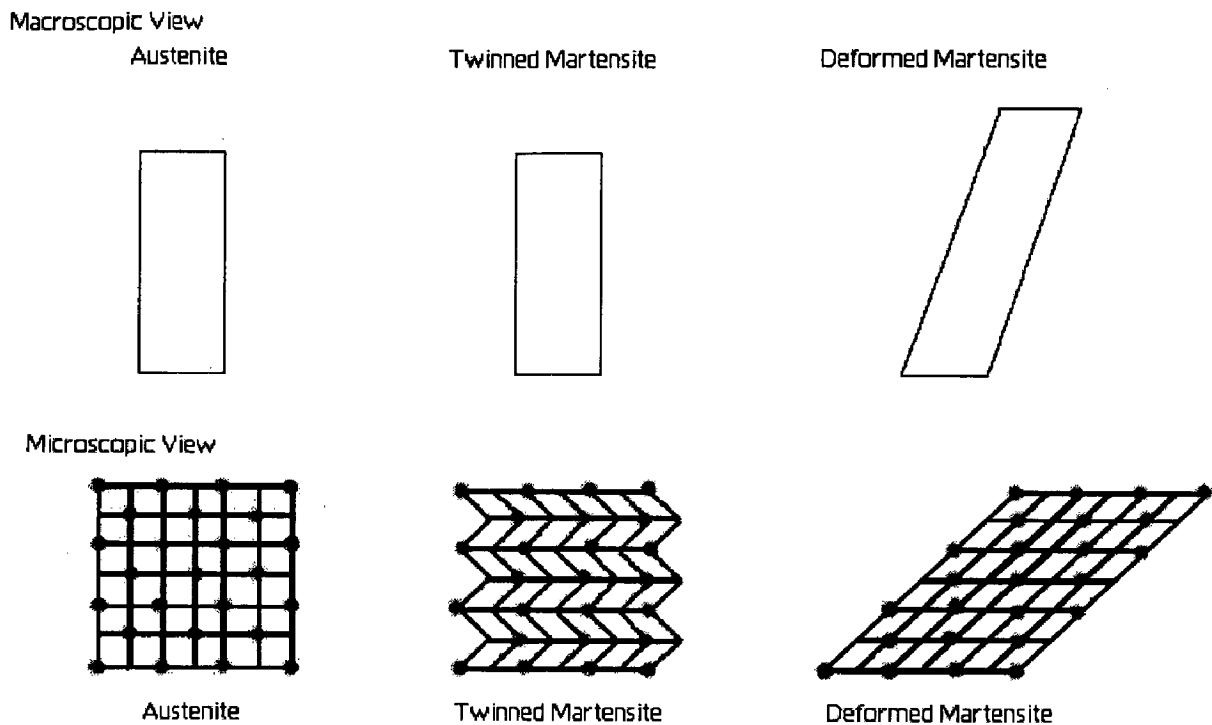


Figure 2.3: Microscopic and Macroscopic Views of the Two Phases of SMA

The temperatures at which each of these phases begin and finish forming are represented by M_s , M_f , A_s and A_f respectively. The amount of loading placed on a piece of shape memory alloy increases the values of these four variables as shown in Figure 2.4.

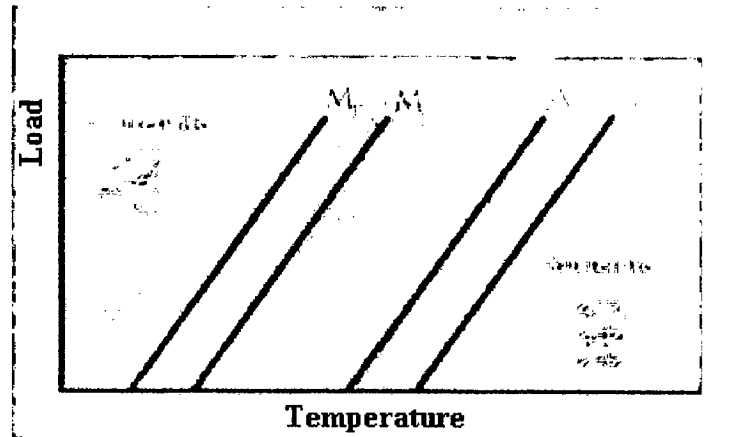


Figure 2.4: The Dependency of Phase Change Temperature on Loading [89]

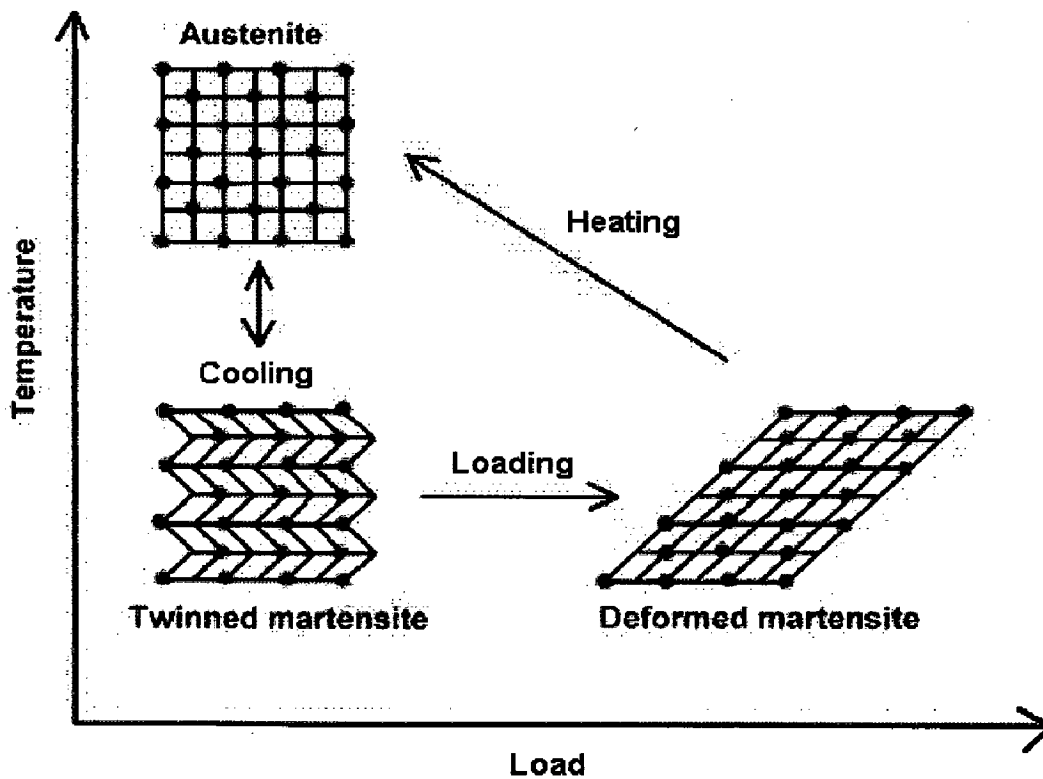


Figure 2.5: Microscopic Diagram of the Shape Memory Effect [89]

The shape memory effect is observed when the temperature of a piece of shape memory alloy is cooled below the temperature M_f . At this stage the alloy is completely composed of Martensite which can be easily deformed. After distorting the SMA the original shape can be recovered simply by heating the wire above the temperature A_f . The heat transferred to the wire is the power driving the molecular rearrangement of the alloy.

The deformed Martensite is now transformed to the cubic Austenite phase, which is configured in the original shape of the wire.

The main use of SMA is especially as actuators but it has little use in vibration control. Following materials shows the SMA characteristics.

Commercially available shape memory alloys:

- Nickel/Titanium alloys such as Nitinol and Tinel
- Copper/Zinc/Aluminum Alloys
- Copper/Aluminum/Nickel Alloys

Other alloys that are known to display shape memory properties are:

- Silver/Cadmium Alloys
- Gold / Cadmium alloys
- Copper / Tin alloys
- Copper / Zinc alloys
- Indium / Titanium alloys
- Nickel / Aluminium alloys
- Iron / Platinum alloys
- Manganese / copper alloys
- Iron / Manganese / Silicon alloys

2.1.2 Piezoelectric Materials

Piezoelectric materials produce an electric field when exposed to a change in dimension caused by an imposed mechanical force (piezoelectric or generator effect). Conversely, an applied electric field will produce a mechanical stress (electrostrictive or motor effect). Piezoelectric materials transform energy from mechanical to electrical and vice-versa. The stress is very small, 0.1-0.3%. They are used for sensing purposes (e.g.

microphone, transducer), and for actuating applications. They are often used to measure fluid composition, fluid density, fluid viscosity and the force of impact. Piezoelectric materials can be broadly classified into two groups i.e. crystalline and ceramics. In the category of crystalline, Quartz (SiO_2), Aluminum orthophosphate - Berlinite (AlPO_4), Gallium orthophosphate (GaPO_4), Tourmaline etc are available. In the field of ceramics, Barium Titanate (BaTiO_3) and Lead Zirconate Titanate (PZT) are available. Except these several other materials also shows piezoelectric effect in certain extent, such as Zinc oxide ZnO, Aluminum nitride AlN, Polyvinylidene fluoride PVDF, Lithium tantalite, Lanthanum gallium silicate, Potassium sodium tartrate etc [90].

2.1.3 Electrostrictive Materials

These materials are very similar to the piezoelectric materials with better strain capability, but very much sensitive to temperature. The major difference between them is that piezoelectric materials will elongate or get compressed, whereas electrostrictive material will elongate only, irrespective to the direction of the applied electric field. Generally this property is found in all materials in very small quantity (approximately $10\text{E}-5$ to $10\text{E}-7$ % strain) [91].

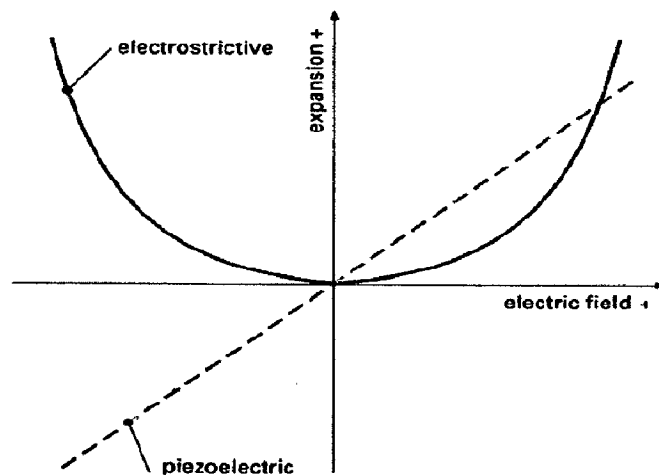


Figure 2.6: Displacement Vs Voltage behavior of piezoelectric and electrostrictive materials [91].

2.1.4 Magnetostrictive Materials

Magnetostrictive materials transduce or convert magnetic energy to mechanical energy and vice versa. As a magnetostrictive material is magnetized, it strains; that is it exhibits a change in length per unit length. Conversely, if an external force produces a strain in a magnetostrictive material, the material's magnetic state will change. This bi-directional coupling between the magnetic and mechanical states of a magnetostrictive material, provides a transduction capability that is used for both actuation and sensing devices. Magnetostrictive Materials were discovered in the 1840s by James Prescott Joule, when he noticed that iron changed length in response to changes in magnetism and named the phenomenon the Joule Effect.

Magnetostrictive materials can operate at higher temperatures than piezoelectric and electrostrictive actuators. They can also undergo higher strains and lower input voltages than most piezoelectric and electrostrictive materials can. However, magnetostrictive materials are not easily embedded in control structures. Some kinds of magnetostrictive materials are cobalt, iron, nickel, ferrite, terbium Alloys (Terfenol-D) and metglass etc [92].

2.1.5 Electro-rheostatic and Magneto-rheostatic fluids

Electro-rheostatic (ER) and magneto-rheostatic (MR) materials are such types of fluids upon which when external electric field is applied, the viscosity of fluid increases, and when the electric field is taken away, the viscosity of fluid goes back to original state. This characteristic is called ER effect. These fluids can change from a thick fluid (similar to motor oil) to nearly a solid substance within the span of a millisecond when exposed to a magnetic or electric field. The effect can be completely reversed quickly when the field is removed. MR fluid changes viscosity when comes in the field of magnetic field but ER fluid shows same behavior in the electric field. MR fluids are mostly used in car shocks, machine vibration, exercise equipment and prosthetic limbs etc. and ER fluids are used to reduce noise and vibration in vehicles. Examples of MR fluids is tiny iron particles suspended in oil, while ER fluids can be as simple as milk chocolate or cornstarch and oil [93].

2.1.6 Fiber Optics

An optical fiber (or fibre) is a glass or plastic fiber that carries light along its length. Fiber optics is the overlap of applied science and engineering concerned, with the design and application of optical fibers. Optical fibers are widely used in fiber-optic communication, which permits transmission over longer distances and at higher data rates than other forms of communications. Fibers are used instead of metal wires because signals travel along them with low loss, and they are immune to electromagnetic interference. Optical fibers are also used to form sensors and in a variety of other applications. The fiber optic sensors (FOSs) provide several advantages over their electrical counterparts, viz high bandwidth, small size, low weight, corrosion resistance, geometrical flexibility and an inherent immunity to electromagnetic interference (EMI). FOSs can be embedded in composite materials in a non-obtrusive manner that does not degrade structural integrity. In general, the embedded fiber optic sensors can monitor the health of the structures in service condition.

- ❖ For the vibration suppression of thin structures, piezoelectric materials are widely used due to large amount of characteristics:
 - ✓ Low weight
 - ✓ Easily mounted on the structures
 - ✓ Quick response
 - ✓ Low power consumption
 - ✓ High efficiency and compactness
 - ✓ Dual nature (sensing and actuation both)
 - ✓ Lower prices

2.2 Piezoelectric Materials

Piezoelectricity ("Piezo" is a Greek term which means "to squeeze.") was discovered by Pierre and Jacques Curie in the 1880s. The Curies noticed two things: Firstly, applying mechanical stress on certain natural non-symmetrical crystals changes

their internal electric polarization in proportion to that stress. Secondly, the same crystals deform when they are subjected to an electric field. These unique properties are known as the direct and converse piezoelectric effects respectively. The piezoelectric effect is practically linear and direction-dependent. As shown in Figure. 2.7, compressive and tensile stresses applied along the polarization direction of the material, will generate electric fields and hence voltages of opposite polarity. The phenomenon is also reciprocal so that upon application of electric fields of opposite polarity, the material will expand and contract in accordance with the applied fields. While these direct and converse effects are mostly used in sensors/generators and actuators/motors respectively, this dual functional ability enables piezoelectric to be employed as transducers, converting electrical energy into mechanical energy and vice-versa [88].

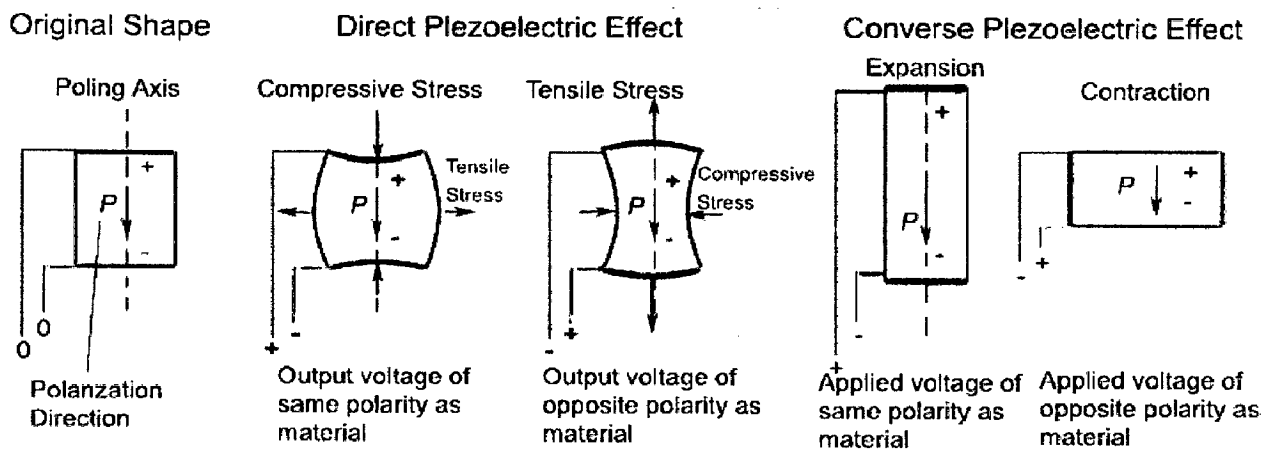


Figure 2.7: Piezoelectric effect [88].

For a material to exhibit the piezoelectric effect, its structure should have no center of symmetry (non Centro-symmetric). That is, the material has anisotropic characteristics, i.e. its properties differ according to the direction of measurement. Consequently, piezoelectricity is an anisotropic characteristic. Figure 2.8 shows the change in crystal structures of a PZT upon temperature change. Above the Curie temperature (T_c), the ceramic has a cubic (Centro-symmetric) structure with no electric dipole moment within its unit cell. Below T_c , however, the positively charged Ti/Zr ion shifted from its central location along one of the several allowed directions, thereby distorting the crystal lattice

into perovskite (non Centro-symmetric) structure and producing an electric dipole with a single axis of symmetry.

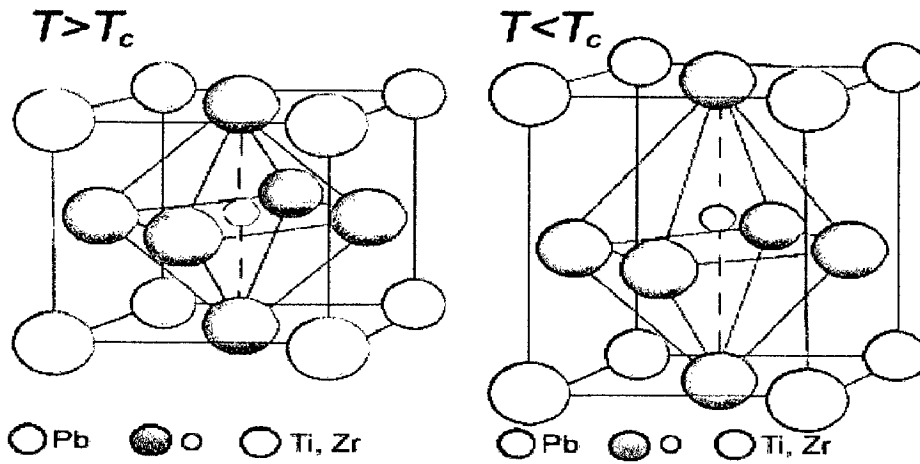


Figure 2.8: Crystal structures of PZT ceramics above and below their T_c [91]

This dipole form regions of local alignment called domains. The alignment gives a net dipole moment to the domain, and thus a net polarization. The direction of polarization among neighboring domains is random, so the ceramic element has no overall polarization (Figure 2.9).

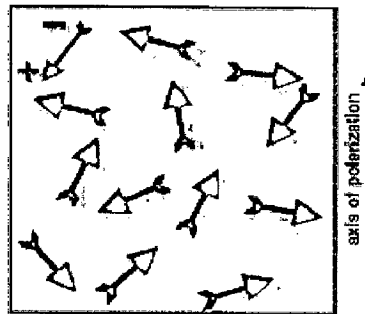


Figure 2.9: Random orientation of polar domain prior to polarization [91]

The domains in a ceramic element are aligned by exposing the element to a strong direct current electric field (more than 1KV/mm), usually at a temperature slightly below the Curie point (Figure 2.10). Through this polarizing (poling) treatment, domains most nearly aligned with the electric field expand at the expense of domains that are not aligned with the field, and the element lengthens in the direction of the field. When the electric field is removed most of the dipoles are locked into a configuration of near

alignment (Figure 2.11). The element now has a permanent polarization, the remanent polarization, and is permanently elongated [91].

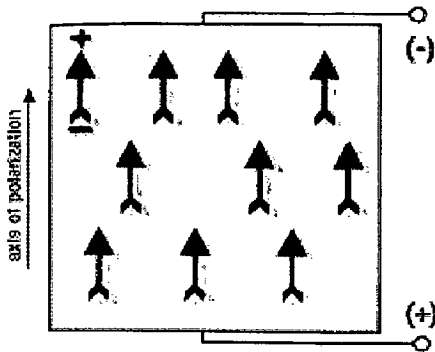


Figure 2.10: Polarization in DC electric field

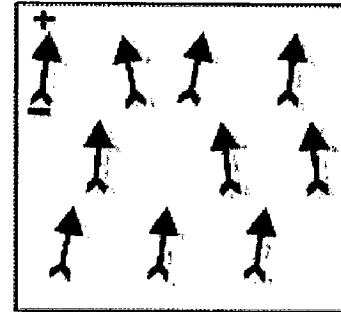


Figure 2.11: Remanent polarization after electric field is removed

The ability of piezoelectric materials to exchange electrical and mechanical properties vice-versa draw attention to employ them as sensor and actuator. If piezoelectric material is bonded properly to the structure, deformation of the structure will be sensed properly, because deformation of the structure would cause the deformed piezoelectric material to produce an electric voltage. This characteristic shows it as the sensor. On the other side structural deformation can be induced by applying a voltage to the material, which is termed as the actuator. The extent of electrical deformation is observed by measuring the electrical voltage produced by the material. But the natural crystal shows very much weak piezoelectric effect, so it is not directly used as the sensor and actuator. But exponential developments in the field of material science have provided piezoelectric material, which shows very good inter-relation in between electrical and mechanical domain. There are various piezoelectric materials in which Polyvinylidene fluoride (PVDF) (semi crystalline polymer film) and lead zirconate titanate (PZT) [$\text{Pb}(\text{Zr}, \text{Ti})\text{O}_3$] (piezoelectric ceramic material) are commonly used in practice. PZT apply larger forces or moments on structure as compared to PVDF because it has larger value of electromechanical coupling coefficient. But, PZT is relatively brittle in nature while PVDF is flexible and can be cut into any desired shape. PVDF shows excellent sensing

properties so it is mostly used as sensor. Piezoelectric materials are mostly used as actuators, for large range of frequency including ultrasonic application.

❖ But there are several limitations to use the piezoelectric materials:

- **Electrical Limitations** - Exposure to a strong electric field, having polarity opposite to that of the polarizing field will depolarize a piezoelectric material. The degree of depolarization depends on the grade of material, the exposure time, the temperature, and other factors, but fields of 200-500 V / mm or more typically have a significant depolarizing effect. An alternating current will have a depolarizing effect during each half cycle in which polarity is opposite to that of the polarizing field. Piezoelectric materials shows linear relationship in electric field and strain for low field values (max up to 100V/mm) but it shows non linear behavior for large field values and shows hysteresis characteristics. It shows drift from zero state of strain under cyclic electric field, hence it is unable to reproduce strain.
- **Mechanical Limitations-** Mechanical stress sufficient to disturb the orientation of the domains in a piezoelectric material can destroy the alignment of the dipoles. Like susceptibility to electrical depolarization, the ability to withstand mechanical stress differs among the various grades and brands of piezoelectric materials.
- **Thermal Limitations** - If a piezoelectric ceramic material is heated to its Curie point, the domains will become disordered and the material will be depolarized. The recommended upper operating temperature for a ceramic usually is approximately half-way between 0°C and the Curie point. Within the recommended operating temperature range, temperature-associated changes in the orientation of the domains are reversible. On the other hand, these changes can create charge displacements and electric fields. Also, sudden temperature fluctuations can generate relatively high voltages, capable of depolarizing the ceramic element.

- **Stability** - Most properties of a piezoelectric ceramic element erode gradually, in a logarithmic relationship with time after polarization. Exact rates of aging depend on the composition of the ceramic element and the manufacturing process used to prepare it. Mishandling the element by exceeding its electrical, mechanical, or thermal limitations can accelerate this inherent process.

2.2.1 Classification of Piezoelectric Materials

Ferroelastic: Materials in which spontaneous polarization is induced by mechanical load.

Ferroelectrics: Materials in which spontaneous polarization is induced by electric field.

Their polarization is changed by reversing the electric field.

Pyroelectrics: Materials in which the electric field is generated as a result of application of heat and degree of polarization depends on the temperature range.

2.2.2 Piezoelectric constitutive relations

The equations which describe the electromechanical behavior of piezoelectric materials are called piezoelectric constitutive relations. Piezoceramic is considered as the orthotropic materials such as unidirectional laminated composite. The relations are derived by considering several assumptions:

- Piezoelectric material is linear and actuation strain is modeled like thermal strain.
- Total strain in the actuator is the sum of the mechanical strain induced by the stress, the thermal strain due to temperature and the controllable actuation strain due to electric voltage.

The axes are expressed in numeral forms as 1-corresponding x-axis, 2- corresponding y-axis and 3-corresponding z-axis. The z-axis is generally referred as the poling direction in the monolithic-type material. A piezoelectric material produces electric displacement when it is strained along the poling direction conversely; it produces strain when electric field is applied along the poling direction. Hence, the former property is used as the sensing and latter is used as the actuation.

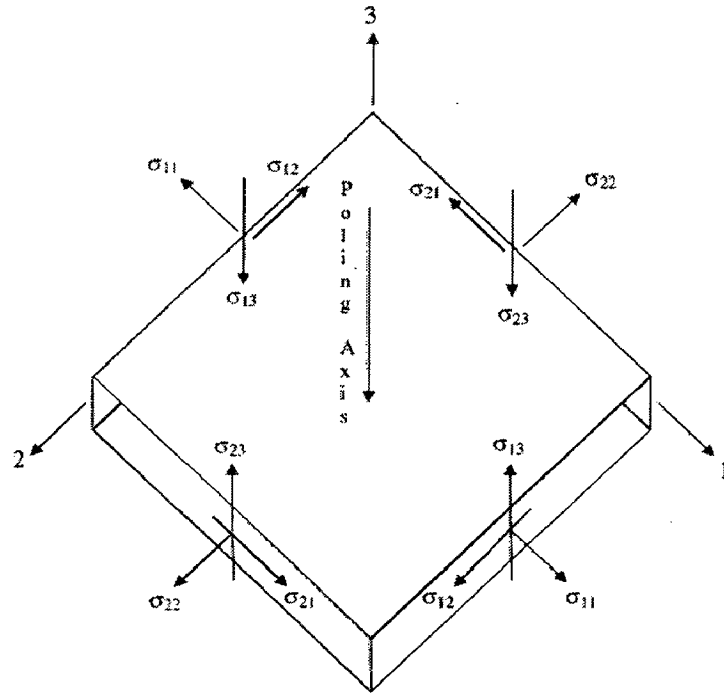


Figure 2.12: Axis configuration of piezoelectric patch

Coupled electromechanical constitutive relations are:

$$\begin{bmatrix} D_1 \\ D_2 \\ D_3 \end{bmatrix} = \begin{bmatrix} e_{11} & e_{12} & e_{13} & e_{14} & e_{15} & e_{16} \\ e_{21} & e_{22} & e_{23} & e_{24} & e_{25} & e_{26} \\ e_{31} & e_{32} & e_{33} & e_{34} & e_{35} & e_{36} \end{bmatrix} \begin{bmatrix} S_{11} \\ S_{22} \\ S_{33} \\ S_{23} \\ S_{13} \\ S_{12} \end{bmatrix} + \begin{bmatrix} \epsilon_{11} & \epsilon_{12} & \epsilon_{13} \\ \epsilon_{21} & \epsilon_{22} & \epsilon_{23} \\ \epsilon_{31} & \epsilon_{32} & \epsilon_{33} \end{bmatrix} \begin{bmatrix} E_1 \\ E_2 \\ E_3 \end{bmatrix} \quad (2.1)$$

$$\begin{bmatrix} \sigma_{11} \\ \sigma_{22} \\ \sigma_{33} \\ \sigma_{23} \\ \sigma_{13} \\ \sigma_{12} \end{bmatrix} = \begin{bmatrix} c_{11} & c_{12} & c_{13} & c_{14} & c_{15} & c_{16} \\ c_{12} & c_{22} & c_{23} & c_{24} & c_{25} & c_{26} \\ c_{13} & c_{23} & c_{33} & c_{34} & c_{35} & c_{36} \\ c_{14} & c_{24} & c_{34} & c_{44} & c_{45} & c_{46} \\ c_{15} & c_{25} & c_{35} & c_{45} & c_{55} & c_{56} \\ c_{16} & c_{26} & c_{36} & c_{46} & c_{56} & c_{66} \end{bmatrix} \begin{bmatrix} S_{11} \\ S_{22} \\ S_{33} \\ S_{23} \\ S_{13} \\ S_{12} \end{bmatrix} - \begin{bmatrix} e_{11} & e_{21} & e_{31} \\ e_{12} & e_{22} & e_{32} \\ e_{13} & e_{23} & e_{33} \\ e_{14} & e_{24} & e_{34} \\ e_{15} & e_{25} & e_{35} \\ e_{16} & e_{26} & e_{36} \end{bmatrix} \begin{bmatrix} E_1 \\ E_2 \\ E_3 \end{bmatrix} \quad (2.2)$$

Equation (2.1) describes direct effects and equation (2.2) the converse effects. Equation (2.1) and (2.2) can be written simply as:

$$\{D\} = [e]^t \{S\} + [\varepsilon^s] \{E\} \quad (2.3)$$

$$\{\sigma\} = [c^E] \{S\} - [e] \{E\} \quad (2.4)$$

Where,

$\{D\}$ = Electric displacement vector

$[e]$ = Dielectric permittivity matrix

$\{S\}$ = Strain vector

$[\varepsilon^s]$ = Dielectric matrix at constant mechanical strain

$\{E\}$ = Electric field vector

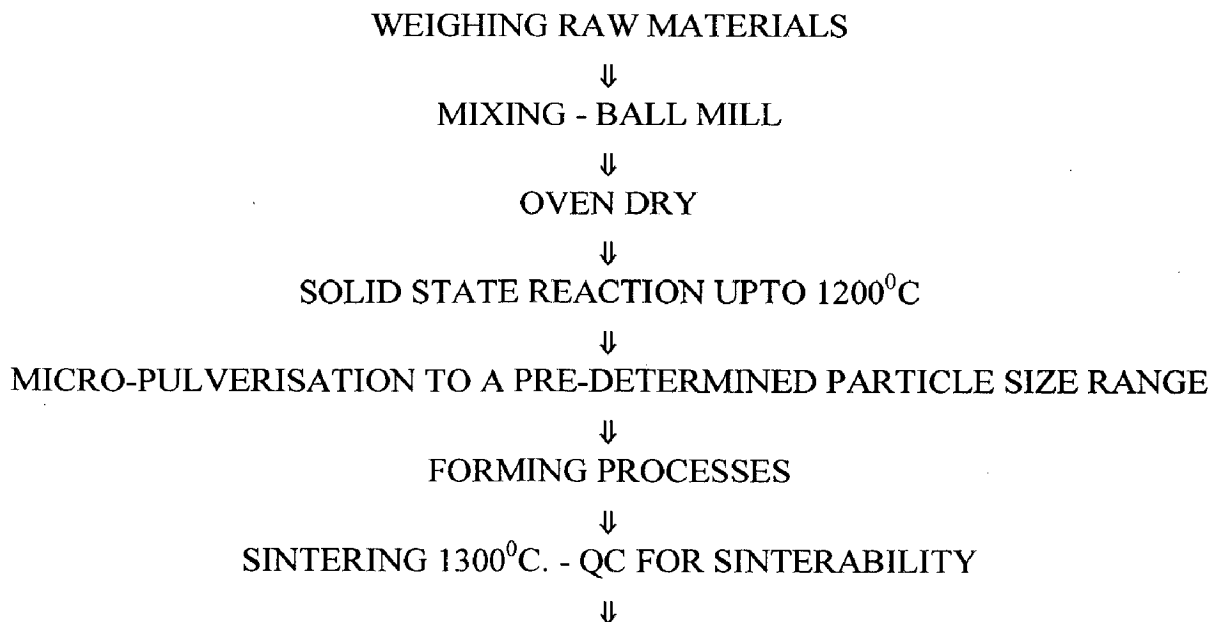
$\{\sigma\}$ = Stress vector

$[c^E]$ = elasticity matrix for a constant electric field.

t denotes transpose of the matrix.

2.2.3 PZT manufacturing processes

PZT are manufactured from their respective oxides/carbonates of Pb, Zr, Ti, rare earths, alkaline earths, transition metals etc. to the specified compositions, well tuned to the end properties, by mixing and solid state reactions. Typical production flowchart is given below :



GRINDING / LAPPING / SLICING TO THE REQUIRED DIMENSIONS



FIRED - ON SILVER ELECTRODES



POLING, HIGH DC FIELDS; TIME-TEMP PROFILE



TESTING

2.3 Active control strategy for vibration suppression

Active control methods use external active devices to generate a second set of disturbance waves of equal amplitude but opposite phase to cancel the targeted unwanted disturbance. Unlike passive control, active control needs an external power supply for its control system. A typical active control system is composed of three basic components; sensors, controller and actuators. A schematic for implementing active control is shown in Figure 2.13. Sensors sense the primary unwanted disturbance experienced (structural vibration or acoustic noise) and monitor how well the control system is performing. Based on the sensor inputs and some knowledge of how the plant responds to the actuators, the controller determines the signal that drives the control actuators. The calculated/determined control signal is eventually passed on to the control actuators to generate the second set of anti-disturbance waves to cancel the primary unwanted disturbance.

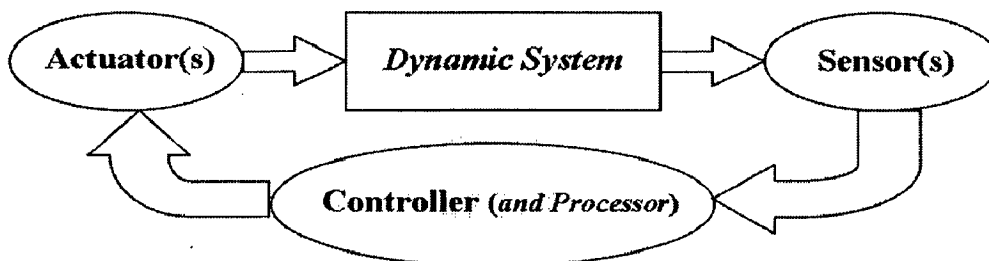


Figure 2.13: A schematic diagram of an active control system

The development of active control technology is supported by developments in the field of physics, control, signal processing and mechanical and electrical engineering. In contrast with passive control, active control works effectively over a wide bandwidth

where the working band does not depend on the characteristics of the structure, and is limited only by the bandwidth of the actuators. Furthermore, the actuators are less sensitive to the characteristics of the structures and the vibration sources. Therefore, the same actuators can be used even if the characteristics of the structures or the vibration sources are changed.

Interest in the use of smart-structure technology for noise and vibration reduction in several applications has been on the rise in recent years. It has been established that significant gains in structures performance can be achieved through active vibration control. Active vibration control came in existence in the early 1960's. This technology was re-introduced to seismic level vibration isolation problems in the early 1980's. It is currently being used in various research fields using electronics or modern DSP base system. Piezoelectric materials, offers an efficient means for implementing active vibration control technologies and as a consequence the topic has received considerable interest in the recent years. Piezoelectric materials have been widely used for sensors and actuators due to their excellent properties, such as low weight and quick response. A lot of numerical and experimental studies are available. A brief review of the available literatures is presented here.

Bhattacharya P. *et al.* [1998] developed a finite element model for the free vibration analysis of smart laminated composite beams and plates. The structure consists of a laminated composite substrate to which are surface bonded or embedded a set of piezoelectric layers, one of which is a sensor while the others are actuators. The linear piezoelectric constitutive relations and the first order shear deformations behavior was used for analysis. An eight noded quadratic isoparametric piezoelectric element is developed to discretize the analysis domain, and the same shape functions are used to describe the electric field, the charge density, the structural geometry as well as the structural displacement.

Yaman Yavuz *et al.* [2002] presented theoretical and experimental result of the modeling of a smart plate for active vibration control. The smart plate consists of a rectangular aluminum plate modeled in cantilever configuration with surface bonded piezoelectric patches. The patches are symmetrically bonded on the top and bottom surfaces. They have used *ANSYS* (v.5.6) software to derive the finite element model of the smart plate. By using this model, they have determined the influences of the actuator placement and size on the response of the smart plate and obtained the maximum

admissible piezoelectric actuation voltage. Based on this model, the optimal sensor locations are found and actual smart plate is produced. The experimental results of the smart plate are then used in the determination of a single-input, single-output system model. By using this model, a single-input/single-output H_∞ controller is designed to suppress the vibration of the first two flexural modes of the smart plate.

Taher H. Rokni Damavandi *et al.* [2006] computed the first nine frequency parameters of circular and annular plates with variable thickness and combined boundary conditions for different thickness to radius ratios. They have considered several combined boundary conditions for inner and outer edges. These boundary conditions are free, soft and hard simply supported and clamped boundary conditions. Three-dimensional elasticity theory is used. They have compared the results with works of other authors and the results of finite element method analysis which are in agreement.

3.1 Vibration Control

Hwang Woo-Seok *et al.* [1994] presented the vibration control of a laminated composite plate by passive and active control technique. In the passive control technique they have considered as the stiffness changes in composite structures by changes in laminate orientation but in active control technique negative velocity feed back control with the piezoelectric sensor/actuator is used. The effects of passive and active controls are investigated by changing the layer angles of a laminated composite plate or the location and number of the sensor/actuator pairs. Classical laminated theory with the induced strain actuation and Hamilton's principle are used to formulate the equation of motion of the system. The system equations are discretize by the finite element method. Finally they have suggested a design strategy for a laminated composite plate with piezoelectric sensor/actuator.

Peng X.Q. *et al.* [1998] developed a finite element model based on third order laminate theory for active position control and vibration control of composite beams with distributed piezoelectric sensor and actuators. They have used direct piezoelectric equation to calculate the total charge created by the strains on the sensor electrodes; and

the actuators provide a damping effect on the composite beam by coupling a negative velocity feedback control algorithm in a closed control loop. A modal superposition technique and the Newmark- β method are used in the numerical analysis to compute the dynamic response of the composite beams. Finally, the effect of the number and locations of the sensor/actuators on the control system are investigated.

Hu Yan-Ru *et al.* [2002] developed an approach for active vibration control of flexible structures with integrated piezoelectric actuators using control theory. First, dynamic models for a flexible circular plate with integrated piezoelectric actuators and sensors are derived using the Rayleigh-Ritz method. An active robust controller is designed to suppress vibration of the circular plate. They have discussed the Robustness of the control system of the circular plate for the model parameter uncertainty. This active robust vibration control method is tested via experimental implementation. The experimental results show that the proposed robust active control method is efficient for active vibration suppression.

Karagulle H. *et al.* [2004] presented the modeling of smart structure with piezoelectric materials using the product *ANSYS/Multiphysics*. They have realized the integration of control action into the *ANSYS* solution. First, the procedure is tested on the active vibration control problem with two-degree of freedom system. They have compared the analytical results obtained by the Laplace transformation method and by *ANSYS*. After that they have studied the smart structure by *ANSYS*. The input reference value is taken as zero in the closed loop vibration control. The instantaneous value of the strain at the sensor location at a time step is subtracted from zero to find the error signal value. The error value is multiplied by the control gain to calculate the voltage value which is used as the input of the actuator nodes. The process is continued with the selected time step until the steady-state value is approximately reached. The results obtained for the structure are compared with other studies.

Wang S.Y *et al.* [2004] investigated the dynamic stability of negative-velocity feedback control of piezoelectric composite plates using a finite element model.

Lyapunov's energy functional based on the derived general governing equations of motion with active damping is used in order to carry out the stability analysis. The active damping matrix must be positive semi-definite in order to guarantee the dynamic stability. It is found that the imperfect collocation of piezoelectric sensor/actuator pairs is not sufficient for dynamic stability in general and that ignoring the in-plane displacements of the midplane of the composite plate with imperfectly collocated piezoelectric sensor/actuator pairs may cause significant numerical errors, leading to incorrect stability. The numerical results based on a cantilevered piezoelectric composite plate shows that the feedback control system with an imperfectly collocated PZT sensor/actuator pair is unstable, but asymptotic stability can be achieved by either bonding the PZT sensor/actuator pair together or changing the ply stacking sequence of the composite substrate to be symmetric. This stability analysis is of practical importance for effective design of asymptotically stable control systems as well as for choosing an appropriate finite element model to accurately predict the dynamic response of smart piezoelectric composite plates.

Moita Jose M Simoes *et al.* [2005] presented a finite element formulation for active control of forced vibrations, including resonance of thin plate/shell laminated structures with integrated piezoelectric layers, acting as sensors and actuators, based on third-order shear deformation theory. The finite element model is a single layer triangular nonconforming plate/shell element with 24 degrees of freedom for the generalized displacements, and one electrical potential degree of freedom for each piezoelectric element layer, which are surface bonded or embedded in the laminate. They have used Newmark method to calculate the dynamic response of the laminated structures, forced to vibrate in the first natural frequency. In order to achieve a mechanism of active control of the structure dynamic response, a feedback control algorithm is used, which acts as a coupling in between sensor and active piezoelectric layers.

Sethi Vineet *et al.* [2005] presented results of multimodal vibration suppression of a smart flexible cantilever beam by using single piezoceramic actuator and a single sensor. Piezoceramic PZT (Lead Zirconate Titanate) patches are surface-bonded on the

beam and perform as actuator and sensor. They have employed System identification for the dynamics of the first three modes and model reduction techniques to assist in control system design. They have used the state space model from system identification for state estimation and development of control algorithm. A linear pole placement controller is designed and simulated using the identified model. Experimental results demonstrate the effectiveness of multimodal active vibration control of the structure using smart materials.

Fei Juntao *et al.* [2006] presented results on active control schemes for vibration suppression of flexible steel cantilever beam with bonded piezoelectric actuators. The PZT patches are surface-bonded near the fixed end of flexible steel cantilever beam. Active vibration control methods such as strain rate feedback control (SRF) and positive position feedback control (PPF) are investigated and implemented using xPC Target real time system. Experimental results demonstrate that the SRF control and PPF control achieve effective vibration suppression results of steel cantilever beam.

E. A. Kovalovs *et al.* [2007] have used macro-fiber composites (MFC) for vibration reduction of structures. The MFC consist of polyimide films with IDE-electrodes that are glued on the top and the bottom of rectangular piezoceramic fibers. The interdigitated electrodes deliver the electric field required to activate the piezoelectric effect in the fibers and allows invoking the stronger longitudinal piezoelectric effect along the length of the fibers. When this actuator embedded in a surface or attached to flexible structures, the MFC actuator provides distributed solid-state deflection and vibration control. The major advantages of the piezoelectric fiber composite actuators are their high performance, flexibility, and durability when compared with the traditional piezoceramic (PZT) actuators. The ability of MFC devices to couple the electrical and mechanical fields is larger than in monolithic PZT. They have experimentally showed that an MFC could be used as actuator to find modal parameters and reduce vibration for structures such as an aluminum beam and metal music plate. Two MFC actuators were attached to the surfaces of test subjects. First MFC actuator used to supply a signal as exciter of vibration and second MFC show his application for reduction of vibration in the range of resonance frequencies. They have compared experimental results of aluminum beam

with MFC actuators with finite element model which modeled in *ANSYS* software. The experimental and numerical results presented in this paper confirm the potential of MFC for use in the vibration control of structures.

3.2 Experimental Work

Lee Y. Y. *et al.* [2003] presented an experimental study for the active vibration control of structures subjected to external excitation using piezoelectric sensors and actuators. They have used a simply supported plate and a curved panel as the controlled structures in their experiment. They employed the independent model space control approach for the controller design. They also incorporated the time domain modal identification technique into the controller for real time update of the system parameter for increasing the adaptability. They have tested the adaptive effectiveness of the time domain modal identification technique by fixing an additional mass on the simply supported plate to change its structural properties.

Pankaj K. Langote *et al.* [2005] presented the hybrid damping design which contains active piezoelectric materials and passive viscoelastic materials (VEM) which achieve the advantage of both active and passive constrained layer damping. They have conducted experiment on nine systems viz., bare beam, active damping (AD), passive constrained layer damping (PCLD- three variants) and hybrid active/passive constrained layer damping (Hybrid AD/PCLD-four variants) .Based on the time domain analysis of these systems, it is shown that best performance is obtained by using a hybrid configuration where in the VEM and the piezoelectric layers are acting separately.

Qiu Jinhao *et al.* [2006] presented the active vibration control of a plate using a self-sensing actuator (SSA) and an adaptive control method. In self-sensing actuator, the same piezoelectric element functions as both a sensor and an actuator so that the total number of piezoelectric elements required can be reduced. A method to balance the bridge circuit of the SSA was proposed and its effectiveness was confirmed by using an extra piezoelectric sensor, which is not necessary for balancing bridge circuits of SSA in future applications. A control system including the SSA and an adaptive controller using

a finite impulse response (FIR) filter and the filtered $-X$ algorithm was established. The experimental result shows that the bridge circuit was well balanced and the vibration of the plate was successfully reduced at multiple resonance frequencies below 1.2 kHz.

Yan S.U. et al. [2007] analytically build the model of adaptive composite panels with surface-mounted/embedded piezoelectric patches by using the Lagrange-Rayleigh-Ritz method (LRRM), and verified through experiments and finite element method (FEM). They have considered two panels. A cantilevered adaptive composite beam (ACB) and an adaptive circular composite plate (ACCP) with complex boundaries. The inertia and stiffness of the surface-mounted/embedded piezoelectric patches are included in the developed models. To obtain the mode shapes of the ACCP, which are essential to the LRRM modeling, the method of separation of variables is employed and Bessel series and modified Bessel series are introduced. The built models are verified by experiments for the ACB and by the FEM for the ACCP. The actuation configurations of the piezoelectric patches in the panels are optimized based on the introduced analytical model. Finally, with the optimal locations of the piezoelectric patches, the vibration suppression of the ACB and the ACCP are experimentally and numerically carried out, and excellent vibration suppressions for both adaptive panels are obtained.

Malgaca Levent et al. [2007] studied experimentally and numerically analysis of actively controlled piezoelectric smart structure. They have considered two different configurations of smart structures for the control of the free and forced vibrations. Cantilevered smart structures consist of Aluminum beams with surface bonded Lead-Zirconate-Titanate (PZT) patches of Sensortech BM532. In the first case they have used a smart structure with single PZT patch for free vibration control under an initial displacement. In the second case, they have used a smart structure with two PZT patches for the vibration control. Harmonic excitation is applied to one of the PZT patches placed in the middle of the beam. The other patch is used as vibration controlling actuator. A non-contact laser displacement meter is used as a sensor. Natural frequency of the beams is found with chirp signals. Open loop and closed loop dynamic responses are obtained in the time domain to evaluate the effectiveness of the active control. Closed loop numerical

solutions are performed in the finite element environment. They have finally concluded that the experimental and numerical results are in good agreement.

3.3 FEM Formulation

Liu Chorng-Fuh *et al.* [1995] analyzed the axisymmetric vibration of annular and circular plates, isotropic or polar orthotropic by finite element. The main features of their studies are (i) the formulation of the finite element is based on elasticity theory and has no assumptions as in the conventional plate theory-based analyses, which is simple and ready for use, and (ii) the boundary conditions are satisfied exactly and the significant effect of boundary conditions on the vibration frequency is presented. They have finally shows the accuracy of their solution and the inadequacy of conventional methods in dealing with the vibration of annular and circular plates with simply supported boundary conditions.

Lam K. Y. *et al.* [1997] developed a finite-element model based on the classical laminated plate theory for the active vibration control of composite plate containing distributed piezoelectric sensors and actuators. The formulation is derived from the variational principle. The piezoelectric's mass and stiffness are taken into account in this model. A simple negative velocity feedback control algorithm coupling the direct and converse piezoelectric effects is used to actively control the dynamic response of an integrated structure through a closed control loop. The modal superposition technique and the Newmark- β method are used in the numerical simulation to calculate the dynamic response of the laminated composite plate.

Han J.-B *et al.* [1999] presented a numerical analysis of the axisymmetric free vibration of moderately thick annular plates using the differential quadrature method (DQM). The plates are described by Mindlin's first-order shear-deformation theory. The first five axisymmetric natural frequencies are presented for uniform annular plates, of various radii and thickness ratios, with nine possible combinations of free, clamped and simply supported boundary conditions at the inner and outer edges of the plates. The accuracy of the method is established by comparing the DQM results with some exact

and finite element numerical solutions. The convergence characteristics of the method for thick plate eigenvalues problems are investigated and the versatility and simplicity of the method is established.

Wang Q. *et al.* [2000] presented the vibration analysis of a circular plate surface bonded by two piezoelectric layers, based on the Kirchhoff plate model. The form of the electric potential field in the piezoelectric layer is assumed such that the Maxwell static electricity equation is satisfied. The validation of the theoretical model is done by comparing the resonant frequencies of the piezoelectric coupled circular plate obtained by the theoretical model and those obtained by finite-element analysis. The mode shape of the electric potential obtained from free vibration analysis is non-uniform in the radial direction. The piezoelectric layers have an effect on the frequencies of the host structure. The proposed model for the analysis of a coupled piezoelectric circular plate provides a means to obtain the distribution of electric potential in the piezoelectric layer.

Sekouri EI Mostafa *et al.* [2004] presented an analytical approach for modeling of circular plate containing distributed piezoelectric actuators under static as well as dynamic mechanical or electrical loadings. The analytical approach is based on the Kirchhoff plate model. The equations governing the dynamics of the plate, relating the strains in the piezoelectric elements to the strain induced in the system, are derived for circular plate using the partial differential equation. The natural frequencies and mode shapes of the structures were determined by modal analysis. The harmonic analysis is performed for analyzing the steady-state behavior of the structures subjected to cyclic sinusoidal loads. Numerical simulation results are obtained using finite element approach. They have verified the analysis and the computer simulations results by experiment using a thin circular aluminum plate structure with distributed piezoelectric actuators. They have found very good agreements between the results of these three approaches. Finally, the results show that the model can predict natural frequencies and modes shapes of the plate very accurately.

Moita Jose M. Simoes *et al.* [2006] presented a finite element formulation based on the classical laminated plate theory for laminated structures with integrated piezoelectric layers or patches, acting as sensors and actuators. The finite element model is a single layer triangular nonconforming plate/shell element with 18 degrees of freedom for the generalized displacements, and one additional electrical potential degree of freedom for each surface bonded piezoelectric element layer or patch. The control is initialized through a previous optimization of the core of the laminated structure, in order to minimize the vibration amplitude and maximize the first natural frequency. Also the optimization of the patches position is performed to maximize the piezoelectric actuators efficiency. In order to achieve the mechanism of active control of the structure dynamic response, a feedback control algorithm is used, coupling the sensor and active piezoelectric layers or patches. Newmark method is used to calculate the dynamic response of the laminated structure. They have also presented the influence of the position and number of piezoelectric patches, as well as the control gain.

Park Chan II [2008] derived the frequency equation for the in-plane vibration of the clamped circular plate of uniform thickness with an isotropic material in the elastic range. To derive the frequency equation for the clamped circular plate in the cylindrical coordinate, kinetic and potential energy for in-plane behavior were first obtained by using the stress-strain-displacement expressions and applying Hamilton's principle, which led to two sets of highly coupled differential equations for the equations of motion. Substitution of Helmholtz decomposition for the coupled differential equations produced uncoupled equations of motion. The assumption of a harmonic solution for the uncoupled equations led to wave equations. Using the separation of the variable, the general solutions for the wave equations were obtained. The solutions generated the in-plane displacements in the r and θ directions. Finally, the application of boundary conditions yielded the frequency equation for the clamped circular plate. The derived frequency equation was validated by finite element analysis and by comparison of previously reported results.

Yalcin Hasan Serter *et al.* [2009] analyzed the free vibrations of circular plates for simply supported, clamped and free conditions. The solution method is differential Quadrature transformation method (DTM), which is a semi-numerical-analytical solution technique that can be applied to various types of differential equations. By using DTM, the governing equations are reduced to recurrence relations and related boundary/regularity conditions are transformed into a set of algebraic equations. The frequency equations are obtained for the possible combinations of outer edge boundary conditions and the regularity conditions at the centre of the circular plate. Numerical results for the dimensionless natural frequencies have presented and compared to the Bessel function solution and other numerical solutions. It is observed that DTM is a robust and powerful tool for eigenvalues analysis of circular thin plates.

3.4 Optimal sensor/Actuator Placement

Han Jae-Hung *et al.* [1997] developed an analytical model of the laminated composite beam with piezoelectric sensors and actuators by using classical laminated beam theory and Ritz method. Smart composite beams and plates with surface-bonded piezoelectric sensors and actuators were manufactured and tested by them. It has been observed that the developed analytical model predicts the dynamic characteristics of composite plates very well. Utilizing a linear quadratic Gaussian (LQG) control algorithm as well as known classical control methods, a feedback control system was designed and implemented. A personal computer (PC) was used as a controller with an analogue-digital conversion card. For a cantilever beam the first and second bending modes are successfully controlled, and for cantilever plates the simultaneous control of the bending and twisting modes gives a significant reduction in the vibration level.

Halim Dunant *et al.* [2001] suggested a criterion for the optimal placement of collocated piezoelectric actuator–sensor pairs on a thin flexible plate using modal and spatial controllability measures. They have given consideration to the reduction of control spillover effect by adding an extra spatial controllability constraint in the optimization procedure. The spatial controllability is used to find the optimal placement of collocated

actuator–sensor pairs for effective average vibration reduction over the entire structure, while maintaining modal controllability and observability of selected vibration modes. It is found that the methodology for optimal actuator placement can be used for a collocated system without damaging the observability performance of the collocated sensors. Experimental validation of their optimal placement is done on a simply supported thin plate with a collocated piezoelectric actuator–sensor pair.

Yan Y.J. *et al.* [2002] presented the optimal design methodology for number and locations of actuators in active vibration control of a space truss using multiple piezoelectric ceramic stack actuators. They have applied eigenvalues distribution of the energy correlative matrix of the control input force, to determine the optimal number of actuator required, and genetic algorithms (GAs) were adopted to search for the optimal locations of actuators. They have finally concluded that the disturbance acting on a structure is a key factor in determining the optimal number and locations of actuators in active structural vibration control, and a global and efficient optimization solution of multiple actuator locations can be obtained using the GAs.

Quek S. T. *et al.* [2003] presented a simple optimal placement strategy of piezoelectric sensor/actuator (S/A) pairs for vibration control of laminated composite plate, where the active damping effect under a classical control framework is maximized using finite element approach. The classical direct pattern search method is employed to obtain the local optimum, where two optimization performance indices based on modal and system controllability are used. The start point for the pattern search is selected based on the maxima of integrated normal strain consistent with the size of the collocated piezoelectric patches used. This would maximize the virtual work done by the equivalent actuation forces along the strain field of an initial state. Numerical simulation using a cantilevered and a clamped composite square plate illustrate the effectiveness of the proposed strategy, where the results coincide with the global optimal layout from exhaustive search for both modal and system controllability indices. The number of trails to reach the optimal position is few compared to an initial blind discrete pattern search approach.

Peng F. *et al.* [2003] investigated the actuator placement on a plate structure and vibration control of the structure. They have optimized the location of actuators based on maximizing the controllability grammian. It was implemented using structural analysis in *ANSYS* and genetic algorithms. They have also used filtered-x LMS based multi-channel adaptive control to suppress the vibration. They have also done numerical simulations in suppressing tri sinusoidal response at three points of the plate. They have finally concluded that genetic algorithm is an effective method to reduce the energy required for achieving significant vibration reduction.

Wang S. Y. *et al.* [2006] presented the problem of topology optimization of collocated piezoelectric sensor/actuator (S/A) pairs for torsional vibration control of a laminated composite plate. Both isotropic and anisotropic PZT S/A pairs are considered and it is highlighted that the torsional vibration can be more effectively damped out by employing the topological optimal design of the S/A pairs than by using the conventional designs. To implement this topology optimization, a genetic algorithm (GA) based on a bit-array representation method is presented and a finite element (FE) simulation model based on the first-order shear theory and an output feedback control law is adopted. Numerical experiments are used to verify the present algorithm and show that the present optimal topology design can achieve significantly better active damping effect than the one using a continuously distributed PZT S/A pair.

Qiu Zhi-cheng *et al.* [2007] used piezoelectric ceramics patches as sensors and actuators to suppress the vibration of the smart flexible clamped plate. Firstly, modal equations and piezoelectric control equations of cantilever plate are derived. Secondly, an optimal placement method for the locations of piezoelectric actuators and sensors is developed based on the degree of observability and controllability indices for cantilever plate. The bending and torsional modes are decoupled by the proposed method using bandwidth Butterworth filter. Thirdly, an efficient control method by combining positive position feedback and proportional-derivative control is proposed for vibration reduction. The analytical results for modal frequencies, transient responses and control responses

are carried out. Finally, an experimental setup of piezoelectric smart plate is designed and built up. The modal frequencies and damping ratios of the plate setup are obtained by identification method. Also, the experimental studies on vibration control of the cantilever plate including bending modes and torsional modes are conducted. The analytical and experimental results demonstrate that the presented control method is feasible, and the optimal placement method is effective.

Kumar Ramesh K. *et al.* [2008] presented the optimal placement of collocated piezoelectric actuator–sensor pairs on flexible beams using a model-based linear quadratic regulator (LQR) controller. A finite element method based on Euler–Bernoulli beam theory is used. The contributions of piezoelectric sensor and actuator patches to the mass and stiffness of the beam are considered. The LQR performance is taken as the objective for finding the optimal location of sensor–actuator pairs. The problem is formulated as a multi-input, multi-output (MIMO) model control. The discrete optimal sensor and actuator location problem is formulated in the framework of a zero–one optimization problem which is solved using genetic algorithms (GAs). Classical control strategies like direct proportional feedback, constant gain negative velocity feedback and the LQR optimal control scheme are applied to study the control effectiveness. They have studied the optimal location of actuators and sensors for different boundary conditions of beams like cantilever, simply supported and clamped boundary conditions.

Al-Hazmi Mohammed W. [2008] presented a 3-D finite element analysis for cantilever plate structure excited by patches of piezoelectric actuators. He has investigated the influence of actuator location and configuration of piezoelectric actuators attached to the plate structure in order to identify the optimal configuration of the actuators for selective excitation of the mode shapes of the cantilever plate structure. The FEM modeling based on *ANSYS* package using harmonic analysis is used in his study for cantilever plate structure excited by patch type of piezoelectric actuators. The results clearly indicate that effective active damping of structural vibration of the cantilever plate can be achieved by proper positioning of the piezoelectric actuator patches.

CHAPTER 4 BASIC EQUATIONS AND FORMULATIONS

In this chapter, a finite element model of piezolaminated circular plate based on the classical laminated plate theory is presented. Brief relations of piezoelectric materials are described. The basic assumptions of classical plate theory are explained. The equations for calculating natural frequency with piezoelectric patches and without piezoelectric patches both are discussed. For piezoelectric material linear strain-displacement relations, relations for sensor voltage and actuator forces are also discussed. A brief description of proportional control is explained.

4.1 Classical Plate Theory

A plate is a structural element with plan form dimensions that are large compared to its thickness and is subjected to loads that cause bending deformation in addition to stretching. Plate theories are developed by assuming the form of the displacement or stress field as a linear combination of unknown functions and the thickness coordinate:

$$\varphi_i(x, y, z, t) = \sum_{j=0}^N (z)^j \varphi_i^j(x, y, t)$$

Where φ_i is the i th component of displacement or stress, (x, y) are the in-plane coordinate, z is the thickness coordinate, t denotes the time, and φ_i^j are the functions to be determined [60].

The classical plate theory is one in which displacement field is selected so as to satisfy the *Kirchhoff hypothesis*. The *Kirchhoff hypothesis* has the following three assumptions [60]:

- (1) Straight lines perpendicular to the mid-surface (i.e., transverse normal) before deformation remain straight after deformation.
- (2) The transverse normal do not experience elongation (i.e., they are in-extensible).

(3) The transverse normal rotates such that they remain perpendicular to the mid-surface after deformation.

4.2 Modeling of Circular Plate with Piezoelectric Patches

The structure under consideration consists of a thin circular plate with piezoelectric patches bonded on the surface of it. The plate is clamped around the inner boundary and free at the outside edge. The free patches generate strains in response to an applied voltage. When the plate is bonded to an underlying structure, these strains lead to the generation of in-plane forces and / or bending moments. The circular plate is also assumed to be made of linearly elastic, homogeneous and isotropic material. For wave propagation in this structure, the displacement field is according to Classical Plate Theory (CPT) is given as [60]:

$$u_r(r, \theta, z, t) = u_0(r, \theta, t) - z \frac{\partial w_0}{\partial r} \quad (4.1)$$

$$u_\theta(r, \theta, z, t) = v_0(r, \theta, t) - z \left(\frac{1}{r} \frac{\partial w_0}{\partial \theta} \right) \quad (4.2)$$

$$u_z(r, \theta, z, t) = w_0(r, \theta, t) \quad (4.3)$$

Where r -coordinate is taken radially outward from the centre of the plate, z -coordinate along the thickness (or height) of the plate and θ coordinate is taken along the circumference of the plate. The displacements (u_r, u_θ, u_z) are along the coordinate (r, θ, z) and functions of r, θ and z coordinates.

(u_0, v_0, w_0) are the radial, angular and transverse displacements respectively of a point on the midplane (i.e., $z = 0$) of the plate.

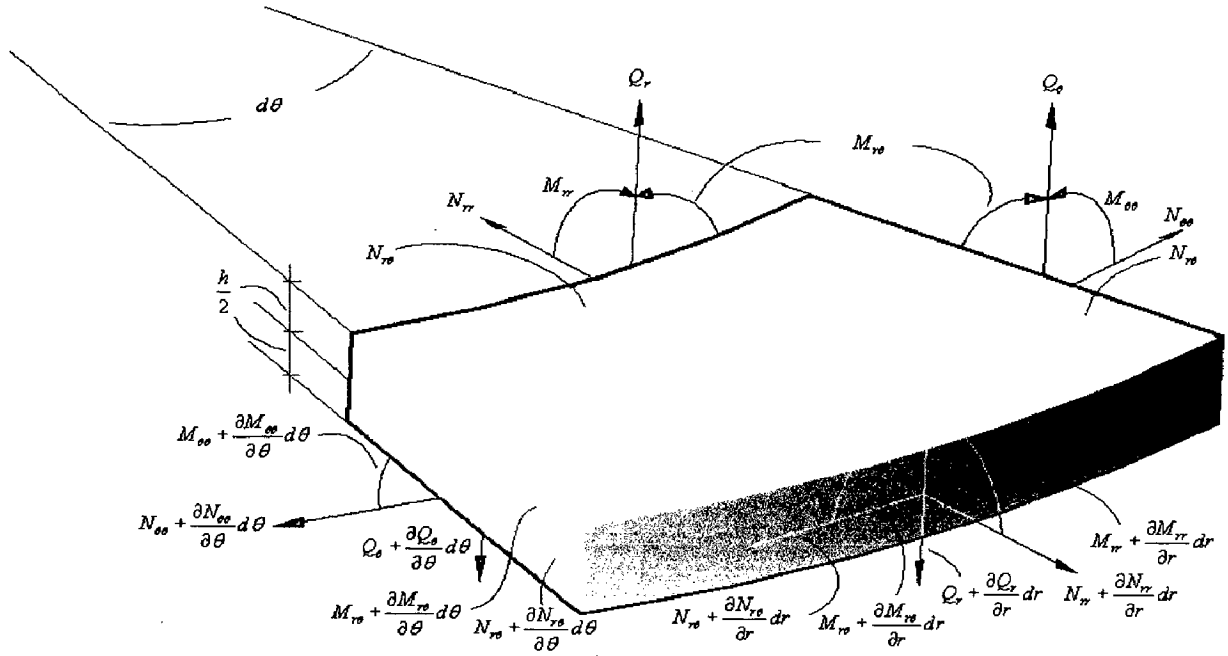


Figure 4.1: Moment and shear force resultant on an element of a circular plate

The nonlinear strains are given as (accounting only Von Karman non-linearity):

$$\varepsilon_{rr} = \frac{\partial u_r}{\partial r} + \frac{1}{2} \left(\frac{\partial u_z}{\partial r} \right)^2 \quad (4.4)$$

$$\varepsilon_{\theta\theta} = \frac{u_r}{r} + \frac{1}{r} \frac{\partial u_\theta}{\partial \theta} + \frac{1}{2} \left(\frac{1}{r} \frac{\partial u_z}{\partial \theta} \right)^2 \quad (4.5)$$

$$\varepsilon_{zz} = \frac{\partial u_z}{\partial z} \quad (4.6)$$

$$\varepsilon_{r\theta} = \frac{1}{2} \left(\frac{1}{r} \frac{\partial u_r}{\partial \theta} + \frac{\partial u_\theta}{\partial r} - \frac{u_\theta}{r} \right) \quad (4.7)$$

$$\varepsilon_{z\theta} = \frac{1}{2} \left(\frac{\partial u_\theta}{\partial z} + \frac{1}{r} \frac{\partial u_z}{\partial \theta} \right) \quad (4.8)$$

$$\varepsilon_{rz} = \frac{1}{2} \left(\frac{\partial u_r}{\partial z} + \frac{\partial u_z}{\partial r} \right) + \frac{1}{2} \frac{\partial u_z}{\partial r} \frac{\partial u_z}{\partial z} \quad (4.9)$$

Moment-displacement relations are given as:

$$M_{rr} = -D \left[\frac{\partial^2 w_0}{\partial r^2} + \nu \left(\frac{1}{r} \frac{\partial w_0}{\partial r} + \frac{1}{r^2} \frac{\partial^2 w_0}{\partial \theta^2} \right) \right] \quad (4.10)$$

$$M_{\theta\theta} = -D \left[\nu \frac{\partial^2 w_0}{\partial r^2} + \frac{1}{r} \frac{\partial w_0}{\partial r} + \frac{1}{r^2} \frac{\partial^2 w_0}{\partial \theta^2} \right] \quad (4.11)$$

$$M_{r\theta} = -(1-\nu)D \left(\frac{1}{r} \frac{\partial^2 w_0}{\partial r \partial \theta} - \frac{1}{r^2} \frac{\partial w_0}{\partial \theta} \right) \quad (4.12)$$

Shear force displacement are given as:

$$Q_r = -D \frac{\partial}{\partial r} (\nabla^2 w_0) \quad (4.13)$$

$$Q_\theta = -D \frac{1}{r} \frac{\partial}{\partial \theta} (\nabla^2 w_0) \quad (4.14)$$

$$\text{Where, } \nabla^2 = \frac{1}{r} \frac{\partial}{\partial r} \left(r \frac{\partial}{\partial r} \right) + \frac{1}{r^2} \frac{\partial^2}{\partial \theta^2}$$

Force resultants are given as:

$$N_{rr} = \int_{-\frac{h}{2}}^{\frac{h}{2}} \sigma_{rr} dz \quad (4.15)$$

$$N_{\theta\theta} = \int_{-\frac{h}{2}}^{\frac{h}{2}} \sigma_{\theta\theta} dz \quad (4.16)$$

$$N_{r\theta} = \int_{-\frac{h}{2}}^{\frac{h}{2}} \sigma_{r\theta} dz \quad (4.17)$$

The poling direction of the piezoelectric material is assumed to be in the z - direction. When external an electric potential is applied across the piezoelectric layer, a differential strain is induced that results in the bending of the plate. The strain in the plate and piezoelectric with respect to the radial and tangential directions and the shear components

are according to equations (4.4), (4.5), and (4.7). The piezoelectric ceramics equations are taken from the equations (4.3.1) and (4.3.2). For plate stress tensor equation are given as:

$$\{\sigma\} = [C]\{\varepsilon\} \quad (4.18)$$

Where $[C]$ is the elastic stiffness matrix of the plate.

In order to satisfy the assumptions, an electric field E is applied along the z - direction. (i.e. $E_1 = E_2 = 0$ and $E_3 = E(r, t)$) and thus the following conditions must be satisfied.

$d_{32} = d_{31}$, $d_{36} = 0$ and $d_{24} = d_{15}$ also for piezoelectric material, $e_{32} = e_{31}$, $e_{36} = 0$. The relationship in between electric field E and the applied voltage is given by

$$\{E\} = \{L_\phi\}\phi \quad (4.19)$$

Where,

$$\{L_\phi\} = \left\{ -\frac{\partial}{\partial x}, -\frac{\partial}{\partial y}, -\frac{\partial}{\partial z} \right\}$$

Hence, when a constant voltage is applied to the network along the Z -direction, the electric field generated is $\left\{ 0, 0, \frac{d\phi}{dz} \right\}^T$. The electric charge is obtained from electrical

displacement by following relation

$$\{Q\} = \int_S \{D\} ds \quad (4.20)$$

Where, $\{Q\}^T = [Q_1, Q_2, Q_3]$ and S denotes the surface area of the electrode.

The radial stresses in the Piezo-layers are assumed to be uniformly distributed in the direction perpendicular to the plate because of the plate's small thickness. The equations of each piezoelectric layer have the following form.

$$\sigma_r = \frac{E_p}{1-\nu_p^2} \left(\frac{\partial u_r}{\partial r} + \nu_p \left(\frac{u_r}{r} + \frac{1}{r} \frac{\partial u_\theta}{\partial \theta} \right) \right) - \frac{V d_{3r} E_p}{h_p (1-\nu_p)} \quad (4.21)$$

$$\sigma_\theta = \frac{E_p}{1-\nu_p^2} \left(\frac{u_r}{r} + \frac{1}{r} \frac{\partial u_\theta}{\partial \theta} + \nu_p \frac{\partial u_r}{\partial r} \right) - \frac{V d_{3\theta} E_p}{h_p (1-\nu_p)} \quad (4.22)$$

$$D_3 = d_{3r} \frac{du_r}{dr} + d_{3\theta} \frac{u_r}{r} - \varepsilon_{33} \frac{V}{h_p} \quad (4.23)$$

Where, σ_r, σ_θ and τ are respectively, radial stress, circumferential stress, and shear stress on the interface surface, d_{3r} and $d_{3\theta}$ are transverse piezoelectric constants in the radial and circumferential directions, respectively. V is the voltage acting in the direction perpendicular to plate. E_p and ν_p are the modulus and Poisson ratio of the actuator. D_3 is the electrical displacement and ϵ_{33} is a permittivity coefficient [65].

The constitutive equation of the plate

$$\sigma_r = \frac{E}{1-\nu^2} \left(\frac{\partial u_r}{\partial r} + \nu \left(\frac{u_r}{r} + \frac{1}{r} \frac{\partial u_\theta}{\partial \theta} \right) \right) \quad (4.24)$$

$$\sigma_\theta = \frac{E}{1-\nu^2} \left(\frac{u_r}{r} + \frac{1}{r} \frac{\partial u_\theta}{\partial \theta} + \nu \frac{\partial u_r}{\partial r} \right) \quad (4.25)$$

$$\tau_{r\theta} = \frac{E}{2(1+\nu)} \left(\frac{\partial u_\theta}{\partial r} + \frac{1}{r} \frac{\partial u_r}{\partial \theta} - \frac{u_\theta}{r} \right) \quad (4.26)$$

Where E and ν are the modulus and Poisson ratio of the material of the plate. For the radial actuator motion, the dynamics equation is expressed as

$$\left(r \frac{\partial \sigma_r}{\partial r} + \sigma_r - \sigma_\theta \right) h_p - \tau r = \rho_p h_p r \frac{\partial^2 u_r}{\partial^2 r} \quad (4.27)$$

The balance of the moment is expressed as:

$$\frac{\partial(rM_r)}{\partial r} - M_\theta - rT + hr\tau = 0 \quad (4.28)$$

Using Hooke's law the moment by the plate transverse displacement is given as

$$M_r = -D \left(\frac{\partial^2 w}{\partial r^2} + \nu \frac{\partial w}{r \partial r} \right) \quad M_\theta = -D \left(\frac{\partial w}{r \partial r} + \nu \frac{\partial^2 w}{r \partial^2 r} \right) \quad (4.29)$$

$$D = \frac{Eh^3}{12(1-\nu^2)}$$

Where, T is the shear force, M_r and M_θ are internal plate moments, D is the plate cylindrical stiffness, h_p is the thickness of the actuator, ρ_p is the modified density of the actuator and t is the time. Differentiating equation (4.28) with respect to r

$$r \frac{\partial^2 M_r}{\partial r^2} + 2 \frac{\partial M_r}{\partial r} - \frac{\partial M_\theta}{\partial r} - \frac{\partial(Tr)}{\partial r} + h \frac{\partial(r\tau)}{\partial r} = 0 \quad (4.30)$$

The equation of the transverse plate motion is

$$\frac{\partial(Tr)}{\partial r} = \rho h r \frac{\partial^2 w}{\partial r^2} \quad (4.31)$$

Where ρ is the density for combined structures given by $\rho = \rho_1 + n\rho_p\chi_i(r,\theta)$ in which ρ_1 , ρ_p and n are the density coefficient for the plate, the patches and the number of piezoelectric respectively. $\chi_i(r,\theta)$ is the characteristics function which has a value of 1 in the region covered by the i th and 0 elsewhere. Taking into account a perfect bonding the plate transverse displacement is related to the radial actuator displacement by

$$u_r = -\frac{h}{2} \frac{\partial w}{\partial r} \quad (4.32)$$

Substituting equation (4.31) into equation (4.30), differentiating equation (4.27) with respect to r , and replacing the term $\partial(r\tau)/\partial r$ finally, the equation for modeling the transverse motion is as follow

$$\nabla^4 w + \rho \frac{h}{D_p + D} \frac{\partial^2 w}{\partial t^2} - \frac{h^2 h_p \rho_p}{2(D_p + D)} \nabla^2 \frac{\partial^2 w}{\partial t^2} = \frac{P}{D_p + D} \quad (4.33)$$

$$D_p = n \frac{E_p h_p h^2}{2(1-\nu_p^2)} \chi_i(r,\theta) \quad (4.34)$$

Where $\nabla^4 = \frac{1}{r} \frac{\partial}{\partial r} \left(r \frac{\partial}{\partial r} \frac{1}{r} \left[\frac{\partial}{\partial r} \left(r \frac{\partial}{\partial r} \right) \right] \right)$ is the Laplacian operator in the polar coordinates r and θ , n is the number of actuators and P is the external surface force. The displacement in the transverse z - direction w of the circular plate integrated Piezo-ceramic actuators is governed by equation (4.33). To obtain the natural frequencies and modes, all external mechanical and electric excitations are assumed to be zero. For the case of axisymmetric boundary conditions the solutions is as follow

$$w(r,\theta,t) = \sum_{m=0}^{\infty} \sum_{n=0}^{\infty} g_{mn}(r) \cos(m\theta) f_{mn}(t) \quad (4.35)$$

Where, $g_{mn}(r) = A_{mn} J_m(\lambda_{mn} r r_0) + B_{mn} Y_m(\lambda_{mn} r r_0) + C_{mn} I_m(\lambda_{mn} r r_0) + D_{mn} K_m(\lambda_{mn} r r_0)$ in which m and n are the numbers of nodal diameters and circles, $f_{mn}(t) = e^{i\omega_{mn} t}$, A_{mn} , B_{mn} , C_{mn} and D_{mn} are the mode shape constants. J_m , Y_m are the Bessel functions of the first and second

kinds, I_m and K_m are the modified Bessel functions of the first and the second kind, and λ_{mn} is the frequency parameter. Hence, the frequency parameter, λ_{mn} is related to the circular frequency ω_{mn} of the plate with Piezo-ceramic

$$\omega_{mn} = \frac{\lambda_{mn}^2}{r_0^2} \sqrt{\frac{D + D_p}{\rho h}} \quad (4.36)$$

Where, r_i is the internal radius and r_o is the external radius of annular plate.

Similarly natural frequency of circular plate without piezoelectric patches is given as:

$$\omega_{mn} = \frac{\lambda_{mn}^2}{r_0^2} \sqrt{\frac{D}{\rho h}} \quad (4.37)$$

Where m indicates number of nodal diameters and n indicates number of nodal circles.

The frequency of circular plate doesn't depend on the Poisson's ratio.

4.3 Constitutive Equations of Piezoelectric Materials

The linear piezoelectric constitutive equations coupling the elastic field and the electric field can be expressed as the direct and the converse piezoelectric equations, respectively. It is assumed that thermal effect is not considered in the analysis. The piezoelectric sensor equations can be derived from the direct piezoelectric equation [69].

$$\{\sigma\} = [C_p] (\{\varepsilon\} - [d^T] \{E\}) \quad (4.3.1)$$

$$\{D_e\} = [e] \{\varepsilon\} + [\varepsilon^s] \{E\} = \{\sigma\} [d] + [\varepsilon^\sigma] \{E\} \quad (4.3.2)$$

Where,

σ = stress vector

C_p = electric stiffness matrix of piezoelectric ceramic

ε = strain vector

E = electric field vector

e = piezoelectric constant (piezoelectric stress/charge tensor)

D_e = electric displacement vector

ε^s = piezoelectric permittivity constant under constant strain condition

ε^σ = piezoelectric permittivity constant under constant stress condition

$$[e] = [d][C_p] \quad (4.3.3)$$

$$[\varepsilon^s] = [\varepsilon^\sigma] - [d][C_p][d]^T \quad (4.3.4)$$

The superscript "T" denotes the transpose of a vector or matrix.

4.3.1 Linear strain-displacement relations

Based on the first-order shear theory of small strain, the displacement components of a piezoelectric composite plate are as:

$$u(x, y, z, t) = u_0(x, y, t) + z\beta_x(x, y, t) \quad (4.3.5)$$

$$v(x, y, z, t) = v_0(x, y, t) + z\beta_y(x, y, t) \quad (4.3.6)$$

$$w(x, y, z, t) = w_0(x, y, t) \quad (4.3.7)$$

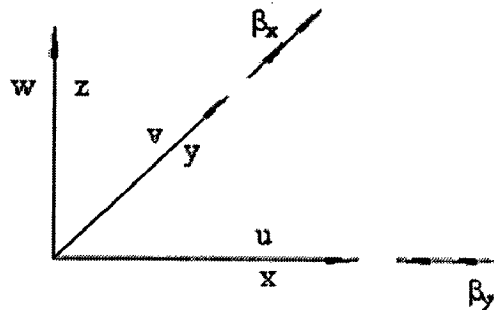


Figure 4.2: Definition of displacement and rotations

Where t denotes time, u, v and w are the displacement components in the piezoelectric composite plate space along the x, y and z axes, respectively. u_0, v_0 and w_0 are the displacement components of a reference point (x, y) on the midplane ($z=0$) and β_x and β_y are the slopes of the normal to the reference point $(x, y, 0)$ on the midplane in the yz and xz plane, respectively [77].

The reduced form of the strain vector at any point (x, y, z) with respect to the structural coordinate system can be expressed as

$$\{\tilde{\varepsilon}\} = [Z]\{\hat{\varepsilon}\} \quad (4.3.8)$$

Where,

$$[Z] = \begin{bmatrix} 1 & 0 & 0 & 0 & 0 & z & 0 & 0 \\ 0 & 1 & 0 & 0 & 0 & 0 & z & 0 \\ 0 & 0 & 1 & 0 & 0 & 0 & 0 & 0 \\ 0 & 0 & 0 & 1 & 0 & 0 & 0 & 0 \\ 0 & 0 & 0 & 0 & 1 & 0 & 0 & z \end{bmatrix} \quad (4.3.9)$$

$$\{\tilde{\varepsilon}\} = [\varepsilon_x \quad \varepsilon_y \quad \gamma_{yz} \quad \gamma_{zx} \quad \gamma_{xy}]^T \quad (4.3.10)$$

$$\{\hat{\varepsilon}\} = \left[\frac{\partial u_0}{\partial x} \quad \frac{\partial v_0}{\partial y} \quad \frac{\partial w_0}{\partial y} + \beta_y \quad \frac{\partial w_0}{\partial x} + \beta_x \quad \frac{\partial u_0}{\partial y} + \frac{\partial v_0}{\partial x} \quad \beta_{x,x} \quad \beta_{y,y} \quad \beta_{x,y} + \beta_{y,x} \right]^T \quad (4.3.11)$$

4.3.2 Isoparametric quadratic element

The eight-noded isoparametric quadratic element is adopted and the interpolation formulae for the spatial coordinates are:

$$x = \sum_{i=1}^8 N_i x_i \quad y = \sum_{i=1}^8 N_i y_i \quad (4.3.12)$$

Where N_i is the quadratic shape function.

The displacement vector $\{u\}$ at any point $(x, y, 0)$ on the midplane is defined in terms of nodal variables via the shape function matrix $[N_d]$ as

$$\{u\} = [N_d]\{u_i\} \quad (4.3.13)$$

Where,

$$\{u\} = [u_0 \quad v_0 \quad w_0 \quad \beta_x \quad \beta_y]^T$$

$$[N_d] = [[N_1 I] \quad [N_2 I] \quad \dots \quad [N_8 I]] \quad (4.3.14)$$

In which $[N_d]$ is the shape function matrix, $[I]$ is an identity matrix of size five and $\{u_i\}$ is the nodal displacement vector of element i

From equation (4.3.8), (4.3.11) and (4.3.13), the reduced strain vector $\{\tilde{\varepsilon}\}$ can be written as

$$\{\tilde{\varepsilon}\} = [Z][B_d]\{u_i\} \quad (4.3.15)$$

Where,

$$[B_d] = [[B_1] \quad [B_2] \quad \dots \quad [B_8]] \quad (4.3.16)$$

$$[B_i] = \begin{bmatrix} \frac{\partial N_i}{\partial x} & 0 & 0 & 0 & 0 \\ 0 & \frac{\partial N_i}{\partial y} & 0 & 0 & 0 \\ 0 & 0 & \frac{\partial N_i}{\partial y} & 0 & N_i \\ 0 & 0 & \frac{\partial N_i}{\partial x} & N_i & 0 \\ \frac{\partial N_i}{\partial y} & \frac{\partial N_i}{\partial x} & 0 & 0 & 0 \\ 0 & 0 & 0 & \frac{\partial N_i}{\partial x} & 0 \\ 0 & 0 & 0 & 0 & \frac{\partial N_i}{\partial y} \\ 0 & 0 & 0 & \frac{\partial N_i}{\partial y} & \frac{\partial N_i}{\partial x} \end{bmatrix} \quad (4.3.17)$$

($i = 1, 2, \dots, 8$)

4.3.3 Electric field-electric voltage relations

The electric potential functions have linear variations across the thickness of the piezoelectric actuator and sensor layers. The electric voltage vector $\{\phi_i\}$ of the i th element can be expressed as

$$\{\phi_i\} = [\phi^{(1)} \quad \phi^{(2)} \quad \dots \quad \phi^{(N_p)}]^T \quad (4.3.18)$$

Where N_p the number of is piezoelectric layers and $\phi^{(k)}$ ($k = 1, 2, \dots, N_p$) is the electric voltage of the k th piezoelectric layer in the i th element.

The electric field vector $\{E_j\}$ in the j th piezoelectric layer is

$$\{E_j\} = \begin{bmatrix} 0 & 0 & \frac{\phi^{(j)}}{h_j} \end{bmatrix}^T \quad (j = 1, 2, \dots, N_p) \quad (4.3.19)$$

Where h_j ($j = 1, 2, \dots, N_p$) is the thickness of the j th piezoelectric layer in the i th element.

4.3.4 Governing equation of motion

Applying Hamilton's variational principal yields the following equation of motion:

$$[M]\{\ddot{X}\} + [C]\{\dot{X}\} + [K_0]\{X\} = \{F\} + [K_{da}]\{\phi_a\} \quad (4.3.20)$$

Where $\{X\}$, $\{\dot{X}\}$ and $\{\ddot{X}\}$ are the structural generalized displacement, velocity and acceleration vectors, respectively. $[M]$ and $[C]$ are the structural mass and linear damping matrices, respectively. $[K_0]$ is the structural generalized stiffness matrix, $\{F\}$ is the external force vector, $[K_{da}]$ is the structural electromechanical matrix, and $\{\phi_a\}$ is the actuator voltage vector.

The equivalent nodal force $\{F_a\}$ of the actuator voltage is given as:

$$\{F_a\} = [K_{da}]\{\phi_a\} \quad (4.3.21)$$

It can be expressed as a summation of the equivalent forces of each piezoelectric actuator element

$$\{F_a\} = \sum \{f_a\}^j = \sum \{k_{da}\}^{(j)} \phi_i \quad (4.3.22)$$

Where,

$$\{k_{da}\}^{(j)} = \int_{-1}^1 \int_{-1}^1 [B_a]^T [Z]_{z=z_0^a}^T [T_2]^T \{\bar{e}_3\} |J| d\xi d\eta \quad (4.3.23)$$

In which z_0^a is the coordinate of the mid-plane of the piezoelectric actuator layer along the thickness direction and the transformation matrix T_2 is

$$[T_2] = \begin{bmatrix} m^2 & n^2 & 0 & 0 & mn \\ n^2 & m^2 & 0 & 0 & -mn \\ 0 & 0 & m & -n & 0 \\ 0 & 0 & n & m & 0 \\ -2mn & 2mn & 0 & 0 & m^2 - n^2 \end{bmatrix} \quad (4.3.24)$$

$m = \cos \theta, n = \sin \theta$ and θ is the skew angle.

$$\{\bar{e}_3\} = [e_{31} \ e_{32} \ e_{34} \ e_{35} \ e_{36}]^T \quad (4.3.25)$$

4.3.5 Sensor Voltage

In the absence of the externally applied potential ($\{E\} = 0$), a strained sensor that is only poled in the z -direction will induce electric displacement D_z on the sensor surfaces given by

$$D_z = e_{31}\varepsilon_1 + e_{32}\varepsilon_2 + e_{34}\varepsilon_4 + e_{35}\varepsilon_5 + e_{36}\varepsilon_6 \quad (4.3.26)$$

Equation (4.3.26) in the matrix form

$$D_z = \{\bar{e}_3\}^T [T_2] \{\bar{\varepsilon}\} \quad (4.3.27)$$

From Gauss's law, the charge output $Q^i(t)$ of the i th electroplated sensor is expressed in terms of spatial integration of D_z over its surfaces as:

$$Q^i(t) = \sum Q^i_j(t) \quad (4.3.28)$$

Where,

$$Q^i_j(t) = \frac{1}{2} \left(\int_{A_j^+} D_z dA + \int_{A_j^-} D_z dA \right) \quad (4.3.29)$$

In which the subscript j denotes the element number of the i th sensor, and A_j^+ and A_j^- are the top and bottom surfaces of the sensor element.

Substituting equations (4.3.27) and (4.3.15) into (4.3.29) gives,

$$Q^i_j(t) = [k_{ds}]^{(j)} \{u_j\} \quad (4.3.30)$$

Where the mechano-electronic matrix of the j th piezoelectric element $[k_{ds}]^{(j)}$ is given as:

$$[k_j] = \int_{-1}^1 \int_{-1}^1 \{\bar{e}_3\}^T [T_2][Z]_{z=z_0^s} [B_d] |J| d\xi d\eta \quad (4.3.31)$$

$$\text{In which } z_0^s = \frac{1}{2}(z_i^+ + z_i^-) \quad (4.3.32)$$

Equation (4.3.31) can be given as:

$$[k_{ds}]^{(j)} = [A_1 \ A_2 \ A_3 \ A_4 \ A_5 \ z_0^s A_1 \ z_0^s A_2 \ z_0^s A_3] [\tilde{B}_d] \quad (4.3.33)$$

$$A_1 = m^2 e_{31} + n^2 e_{32} - 2nme_{36}$$

$$A_2 = n^2 e_{31} + m^2 e_{32} + 2nme_{36}$$

$$A_3 = me_{34} - ne_{35}$$

$$A_4 = -ne_{34} + me_{35}$$

$$A_5 = mne_{31} - mne_{32} \quad (4.3.34)$$

$$[\tilde{B}_d] = \int_{-1}^1 \int_{-1}^1 [B_d] |J| d\xi d\eta \quad (4.3.35)$$

For PZT sensor, normally the dielectric constant $e_{34} = e_{35} = e_{36} = 0$,

Hence, equation (4.3.34) becomes,

$$A_1 = m^2 e_{31} + n^2 e_{32}$$

$$A_2 = n^2 e_{31} + m^2 e_{32}$$

$$A_3 = A_4 = 0$$

$$A_5 = mne_{31} - mne_{32} \quad (4.3.36)$$

The PZT sensor is equally poled, $e_{31} = e_{32}$, then equation(4.3.36) can be given as:

$$A_1 = e_{31} \quad A_2 = e_{32} \quad A_3 = A_4 = A_5 = 0 \quad (4.3.37)$$

From equations (4.3.16), (4.3.17), (4.3.33), (4.3.35) and (4.3.37), mechano-electric matrix of the PZT sensor element is given as:

$$[k_{ds}]^{(j)} = [k_{1s} \ k_{2s} \ \dots \ k_{8s}] \quad (4.3.38)$$

Where,

$$[k_{ls}] = [e_{31} A_{lx} \ e_{32} A_{ly} \ 0 \ e_{31} z_0^s A_{lx} \ e_{32} z_0^s A_{ly}] \quad (4.3.39)$$

$(l = 1, 2, \dots, 8)$

Where,

$$A_{lx} = \int_{-1}^1 \int_{-1}^1 \frac{\partial N_1}{\partial x} d\xi d\eta$$

$$A_{ly} = \int_{-1}^1 \int_{-1}^1 \frac{\partial N_1}{\partial y} d\xi d\eta$$
(4.3.40)

By assembling the electric charge $Q_j^i(t)$ based on the equation (4.3.28) gives,

$$Q^i = [K_{ds}]^{(i)} \{X\}$$
(4.3.41)

Where $[K_{ds}]^{(i)}$ is the mechano-electronic matrix of the i th sensor. When piezoelectric sensors are used as strain rate sensors, the output charge Q^i can be transformed to sensor voltage Φ_s^i as:

$$\Phi_s^i = G_i^c \frac{dQ^i}{dt} = G_i^c [K_{ds}]^{(i)} \{\dot{X}\}$$
(4.3.42)

Where G_i^c is the constant gain of the charge amplifier of the i th electroplated sensor.

The sensor voltage vector $\{\Phi_s\}$ is expressed as:

$$\{\Phi_s\} = [\Phi_s^1 \quad \Phi_s^2 \quad \dots \quad \Phi_s^{N_s}]^T = [G_c][K_{ds}]\{\dot{X}\}$$
(4.3.43)

Where N_s is the total number of piezoelectric sensors and

$$[G_c] = \text{diag}\{G_1^c \quad G_2^c \quad \dots \quad G_{N_s}^c\}$$
(4.3.44)

$$[K_{ds}] = [K_1 \quad K_2 \quad \dots \quad K_{N_s}]^T$$

4.3.6 Actuator Forces

By comparing equation (4.3.23) with (4.3.31), the equivalent nodal force vector $\{f_a\}^{(j)}$ of an element j of the i th piezoelectric actuator induced by the input voltage ϕ_i can be given as:

$$\{k_{da}\}^{(j)} = [\tilde{B}_d]^T [A_1 \quad A_2 \quad A_3 \quad A_4 \quad A_5 \quad z_0^a A_1 \quad z_0^a A_2 \quad z_0^a A_3]^T$$
(4.3.45)

For PZT actuator, $e_{31} = e_{32}$, equation (4.3.45) becomes,

$$\{k_{da}^{(j)}\} = \{f_{1a} \quad f_{2a} \quad \cdots \quad f_{8a}\}^T \quad (4.3.46)$$

Where,

$$\{f_{ia}\} = \begin{bmatrix} e_{31}A_{ix} & e_{32}A_{iy} & 0 & e_{31}z_0^a A_{ix} & e_{32}z_0^a A_{iy} \end{bmatrix}^T \quad (4.3.47)$$

($i = 1, \dots, 8$).

Comparing equation (4.3.47) with (4.3.33), if the sensor/actuator pair is collocated, i.e.

$z_0^s = z_0^a$ Hence, the relationship between the mechano-electronic matrix and the electromechanical vector can be expressed as:

$$\left(\{k_{da}\}^{(j)}\right)^{(T)} = [k_{ds}]^{(j)} \quad (4.3.48)$$

The equivalent nodal force vector $\{F_a\}^{(i)}$ of the i th piezoelectric actuator is expressed as:

$$\{F_a\}^{(i)} = \{K_{da}\}^{(i)} \phi_i \quad (4.3.49)$$

Where $\{K_{da}\}^{(i)}$ is the expanded electromechanical vector of the same size as the system displacement vector $\{X\}$. The assembled equivalent actuator forces vector $\{F_a\}$ induced by the voltages $\{\Phi_a\}$ of all the N_a actuators is given as:

$$\{F_a\} = [K_{da}]\{\Phi_a\} \quad (4.3.50)$$

Where,

$$[K_{da}] = \begin{bmatrix} \{K_{da}\}^{(1)} & \{K_{da}\}^{(2)} & \cdots & \{K_{da}\}^{(N_a)} \end{bmatrix} \quad (4.3.51)$$

$$\{\Phi_a\} = \begin{bmatrix} \phi_1 & \phi_2 & \cdots & \phi_{N_a} \end{bmatrix}^T \quad (4.3.52)$$

4.4 The Control Law

The block diagram of the vibration control system is shown in the figure 3.2. It is single input single output feedback control system. The feedback signal is generated by the piezoelectric sensor. After that the signal is amplified with gain and applied to the piezoelectric actuator.

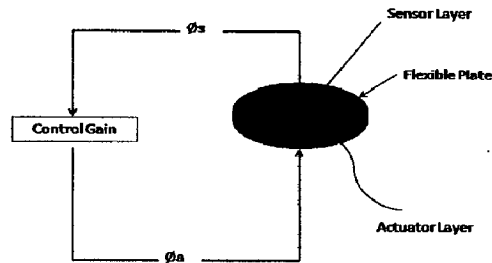


Figure 4.3: Circular plate with sensor and actuator

The vibration control can be realized in two different ways based on the signal conditioning:

- (1) Position or proportional control
- (2) Negative velocity control

In the proportional control, the actuation action is function of position like quantities, whereas in velocity control, the actuation depends on the time derivative of the same quantities.

(1) Proportional Control Method: In proportional control method, the feedback voltage ϕ_a is obtained by multiplying sensing voltage ϕ_s with gain G . Gain value for the vibration suppression is chosen arbitrarily, therefore the control equation is written as

$$\phi_a(t) = G\phi_s(t)$$

(2) Constant Gain Negative Velocity Feedback: Negative velocity control method involves differential terms of the sensor signal $\phi_s(t)$ i.e. $\dot{\phi}_s(t)$. The feedback voltage is obtained by multiplying the gain value G with the derivative of sensor signal and its sign is changed before injecting into the piezoelectric actuator.

$$\phi_a(t) = -G\dot{\phi}_s(t)$$

The velocity feed back enhances the system damping and therefore effectively controls the oscillation. But the velocity amplitude decays, the feedback voltage also decreases. This will reduces the effectiveness at low vibration levels for a given voltage limits.

The experimental setup used for the present work is explained in this chapter. Detailed specifications of the instruments used in the experiment are presented here. The procedure to conduct the experiment is also explained. The main focus of study is to monitor the real time vibration signal of the plate specimen, to keep in record of the signal file and to obtain the response of the plate using sensor voltage and finally implement the closed loop proportional feed back control logic in order to suppress the vibration.

5.1 Equipments

Following equipments are used in the experimental work

- (1) Aluminum Plate specimen
- (2) Vibration control unit (Piezo sensing and Piezo actuation unit)
- (3) Piezoelectric sensor and piezoelectric actuator (PZT patches)
- (4) USB based data acquisition card (National Instruments make)
- (5) Computer with LAB View software version 8.0
- (6) Connections BNC connector cables
- (7) Power supply 240V, 50HZ

Specifications of all equipments are given below:

Table 5.1: Material properties of plate specimen

Property Name	Value
Material	Aluminum
Dimension-Circular plate (annular)	Internal diameter: 15cm External diameter: 45cm Thickness: 0.26mm
Young's Modulus (N/m ²)	70E09
Density(Kg/m ³)	2700

Table 5.2: Properties of the piezoelectric sensor and actuator (PZT patches) by Sparkler Ceramics Ltd, Pune-411026, INDIA

Property Name	
Material	Lead Zirconate Titanate
Dimension(mm)	30 x 30 x 0.5
Young's Modulus (N/m ²)	63E09
Density(Kg/m ³)	7600
Dielectric constant (d ₃₁)(m/V)	254e-12
Stress constant (g ₃₁)(Vm/N)	9E-3

Table 5.3: USB based Data acquisition card by National Instrument Inc

Property Name	
Analog input	8 single ended, 4 differential software selectable
Max sampling rate	48 KS/sec
Input range	+/- 10 volt for single ended
Input resolution	13 bits
Analog output	2
Maximum update rate	150 Hz, software timed
Output range	0-5 Volt

Table 5.4: Properties of vibration control unit by Spranktronics Inc
Piezo Sensing System

It consists high quality charges to voltage converting signal-conditioning amplifier with variable gain, individual input/output connectors to cater for 2 channels displacement and velocity conditioner. The signal conditioners are biased with built in DC power supply.

Sensor	Piezoelectric crystal
Output	Sine/Random
No of channels	2
Frequency Range	10-2000Hz
Maximum input voltage	10 volt (RMS)
Maximum output voltage	200 volt (RMS)
Input / output connection	PT 10 terminals / B & C connectors
Input power	230 V, 50Hz AC

Piezo actuation system

It consists of a preamplifier circuit given as input and a power amplifier circuit. The output of the power amplifier is given to a step up transformer to boost the input Voltage of 0-5 Volts to 240 V RMS.

Actuator	Piezo electric crystal
Output	Sine / Random
No of channels	2
Frequency Range	10-2000Hz
Maximum output voltage	200 volt (RMS) –adjustable gain
Input / output connection	PT10 terminals / B & C connectors
Input power	230 V, 50 Hz AC

5.2 Experimental setup

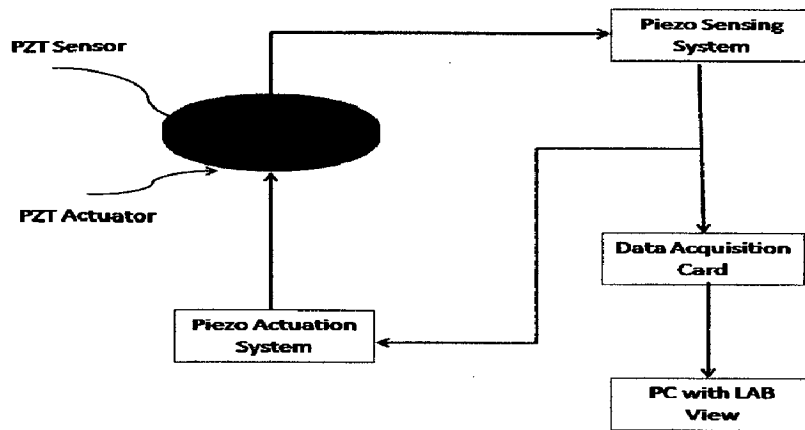


Figure 5.1: Block diagram of experimental setup of proportional feedback control

Figure 5.1 shows the schematic block diagram and Figure 5.2 shows the experimental setup of the proportional feedback control system. The PZT patch, Piezo sensing and actuation and National Instrument Inc DAQ card forms a closed loop system.

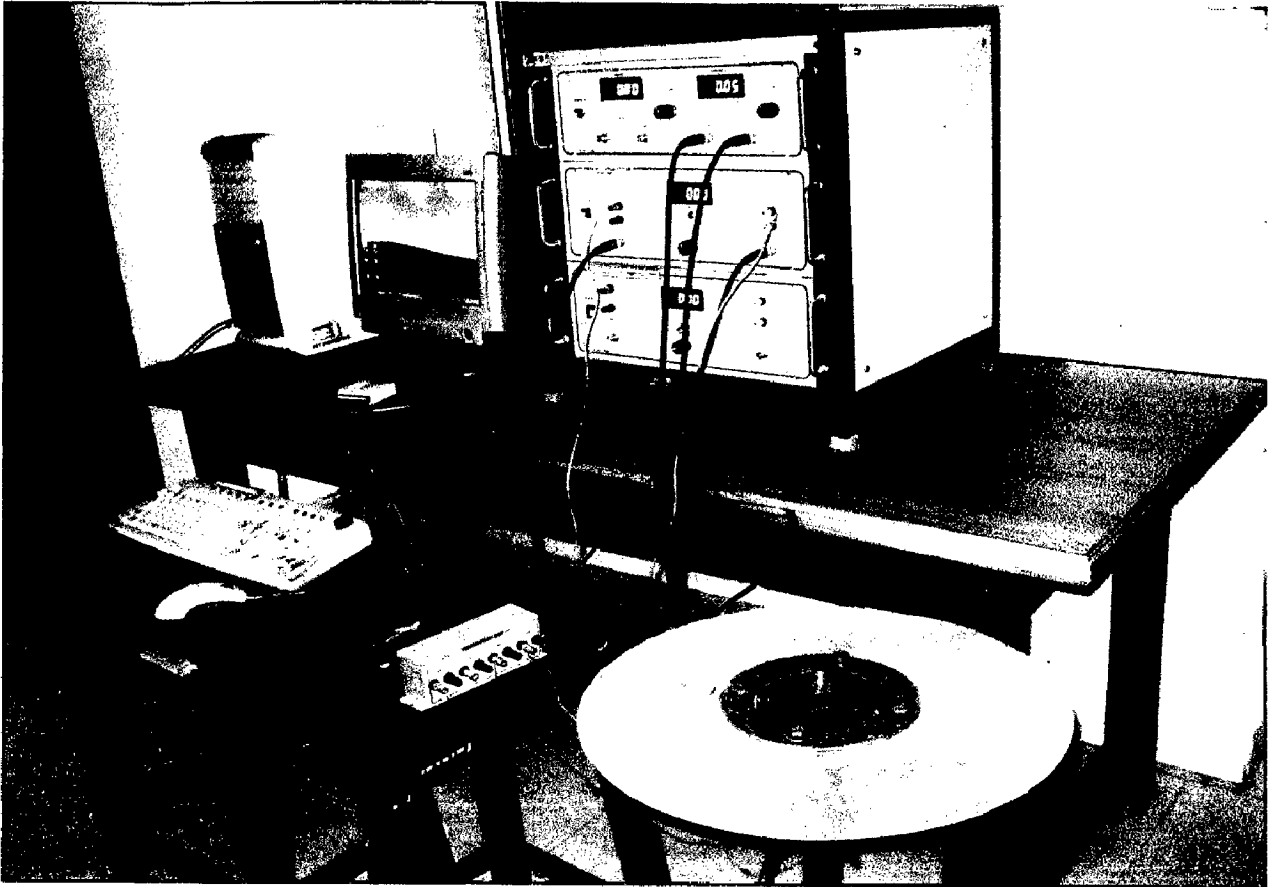


Figure 5.2: Experimental setup of the proportional control system

5.2.1 Piezoelectric material (PZT patch)

PZT patch is made by Sparkler Ceramics Pvt Ltd. It is Lead Zirconate Titanate (Material SP-5H plate) of dimension 30mm L x 30mm W x 0.5mm thickness, wrap round silver electrodes, poled across thickness polarity marked and soldered with lead wires approx 150mm length. For circular annular plate clamped at the inner boundary, one patch is bonded near the clamped edge, as the sensor and four patches are bonded on the opposite side in a symmetric fashion which acts as the actuators. Patches are bonded to the plate by graphite epoxy. Graphite epoxy is made by Resinova Chemie Ltd. When the plate is excited by impulse, it starts vibrating and the sensor when deformed mechanically develops the voltage across its terminal.



Figure 5.3: Aluminum plate clamped at the inner boundary with PZT patches.

5.2.2 USB based data acquisition

Data Acquisition system is National Instrument Inc, make card. This card is used for various purposes such as measuring and recording of several parameters like displacement, voltage, acceleration, strain, temperature etc. in machine equipments. PC based DAQ is used in real time signal to store the signal parameter which is used for further analysis in future. It consists of various internal devices for signal measurement and conversion. One of the prime applications is to analog to digital conversion and vice-versa. Multiplexer is used to combine several input signals into a vector form for the input/output port. Counter and timers are used to control the signal time and to store the data in the buffer for the specified amount of time. Counter clock runs with CPU clock and it is used to synchronize all elements.

Plate is excited at the outer boundary with unknown impulse and PZT sensor bounded to the plate send the sensed signal. This voltage is amplified by the Piezo sensing system and it is fed to the NI DAQ card and Piezo actuation system. PZT sensor is connected to the DAQ card through the signal sensing device. The voltage developed by the PZT sensor mounted by the plate surface is able to sense. The sensed voltage is scanned and stored in the computer with the help of LabVIEW software version 8. The stored data is used for further processing.

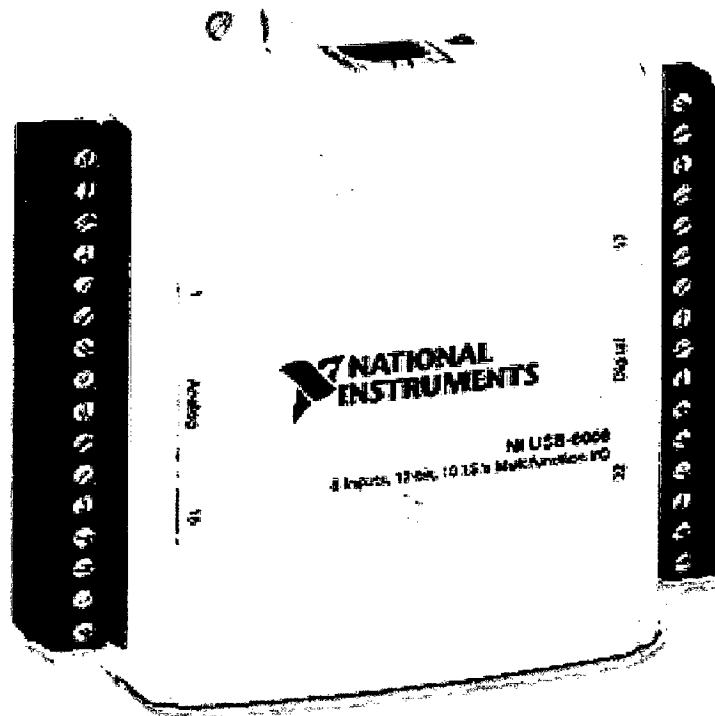


Figure 5.4 (a): NI make DAQ card-NI 6009

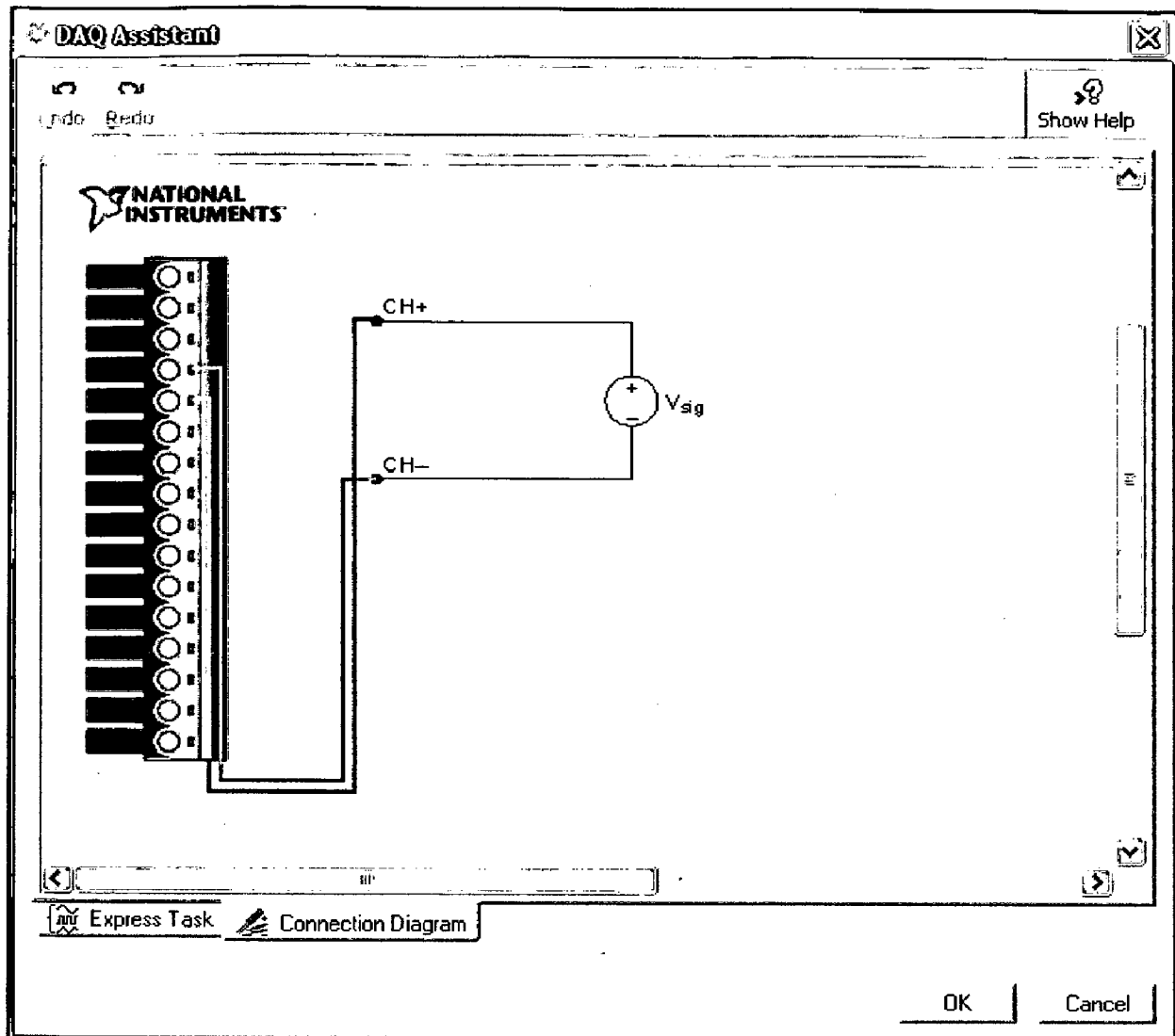


Figure 5.4(b): NI DAQ card connection unit

5.2.3 Piezo sensing and actuation system

The main function of Piezo sensing and actuation is used in the experiment for sensing the strain developed in the PZT patch and to amplify the signal so that it can be used for further processes. It has two channels for sensing and two channels for actuation. The output of the PZT sensor is connected to the Piezo sensing and Piezo actuation system by BNC cables and output of the sensing device is connected to the NI card and also connected to the actuation system. Piezo actuation system is similar to voltage amplifier which amplifies the voltage sensed by the sensing system so that it can be actuated by PZT for vibration suppression.

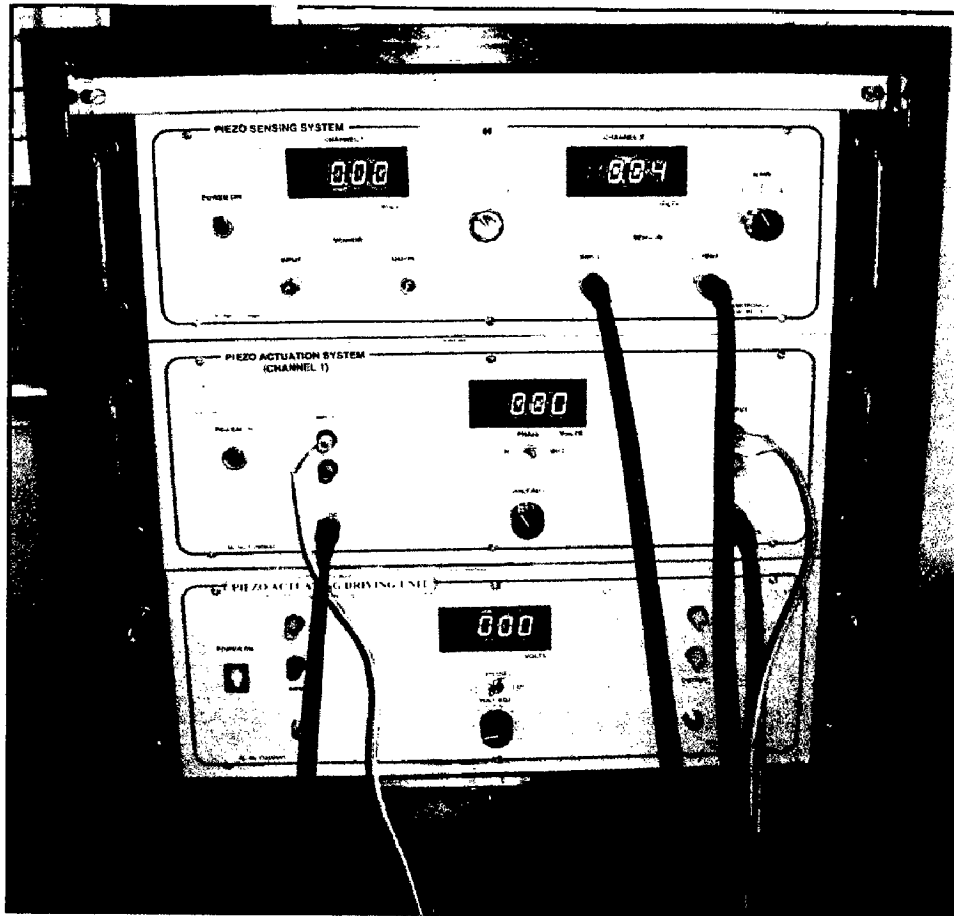


Figure 5.5: Piezo sensing and Piezo actuation system

The system is operated both IN and OUT of phase. First of all the signal is inverted and amplified by the system and then it is supplied by the PZT actuator. If the sensed signal is IN phase the output signal will be OUT of phase for suppression of vibration of plate. The output gain is adjusted by the knob on the actuation and sensing system. The vibration control is more effective by increasing the gain value.

5.2.4 Computer with LabVIEW software

Data acquisition card is connected to the USB port of computer by USB data cables. The outlook and appearance of the LABView is just like a physical instrument (e.g. Oscilloscope, Multimeter etc). Hence, it is also known as virtual instrument or VI. It contains various tools for acquiring, analyzing, displaying and storing data and so many tools for trouble shooting the code. LABView is built with control and indicators in which controls are in the form as knobs, buttons, dials and other input mechanics.

Indicators are in the form of graphs, LEDs and other output display unit [43, 44]. Various additional codes may be added using VIs and structures to control the front panel objects when building the user interface has been completed. The block diagram contents these codes. The front screen of the LabVIEW is shown in the figure 5.6 (a) and figure 5.6 (b). One VI has been built in the software in order to scan the data from the NI data acquisition card. The data can be displayed in the form of real time domain and through FFT it is also possible to display the frequency plot of the time base data. Figure 5.7(b) and figure 5.7(a) shows the block diagram of the LabVIEW programme and front panel of the LabVIEW programme respectively. Various parameters are setup as shown in the figure 5.8 in order to scan the voltage signal with the help of DAQ assistant block according to block diagram of the LabVIEW VI programme as shown in the figure 5.7(b). The wire is connected to the graph indicator block in order to see the real time signal from the sensor. Band pass filter is in between the graph indicator and DAQ assistant block and in between the FFT block and DAQ assistant block in order to remove the unwanted higher frequency components from the signal. By FFT block natural frequencies are displayed that is compared with theoretical frequency. Front panel of the VI shows only time domain signal graph and frequency domain signal graph. Both time domain file and FFT file are stored in the computer with the help of file to measurement block.

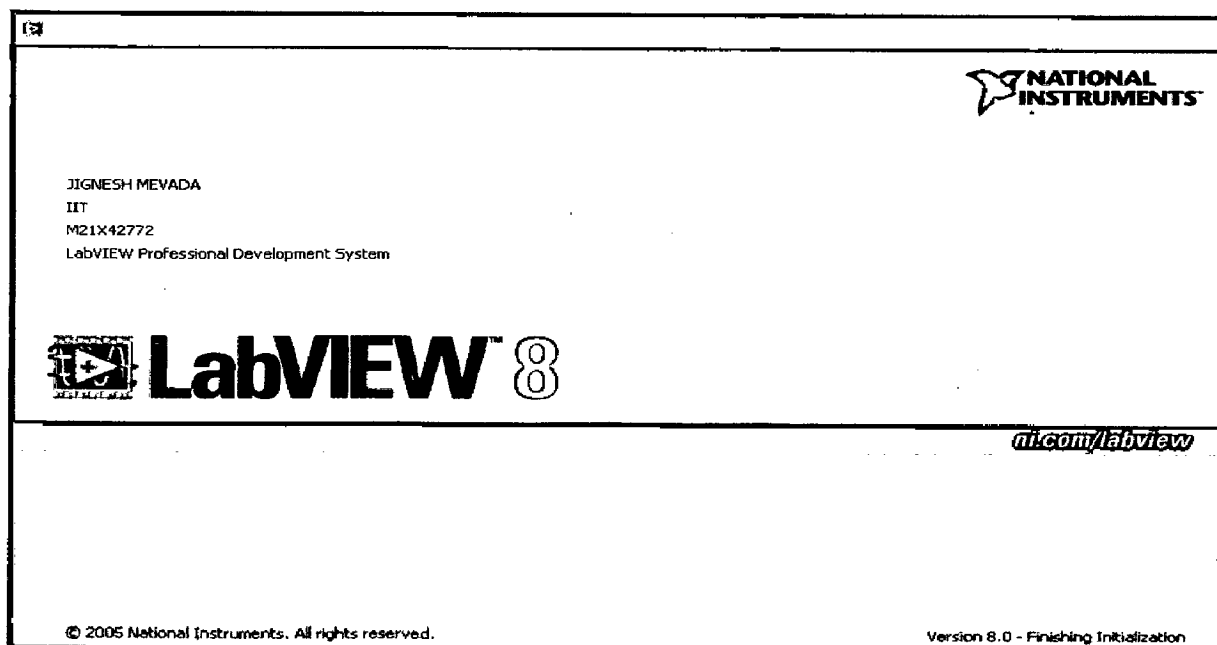


Figure 5.6 (a): LabVIEW main screen (at the time of starting)

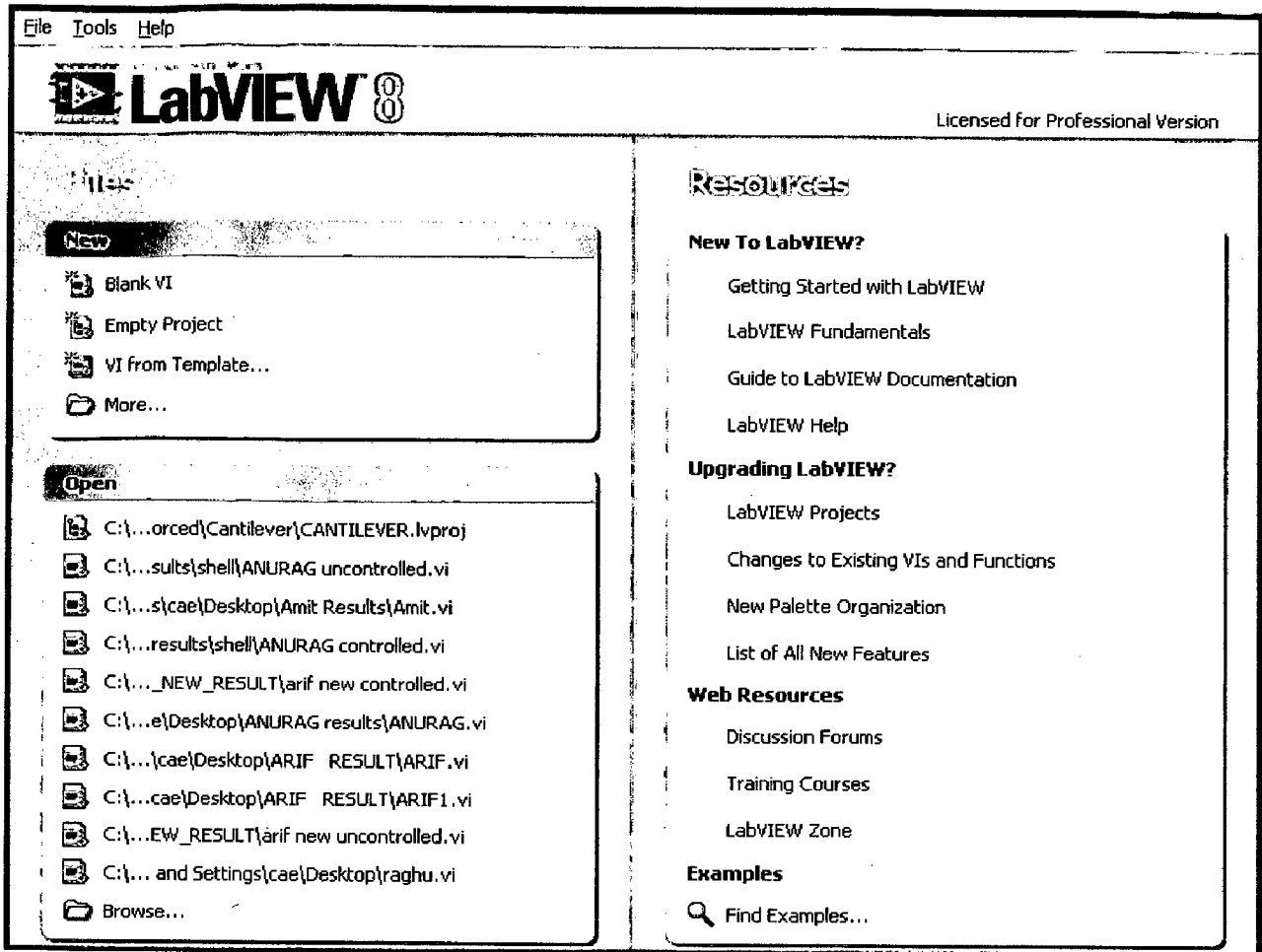


Figure 5.6 (b): LabVIEW main screen

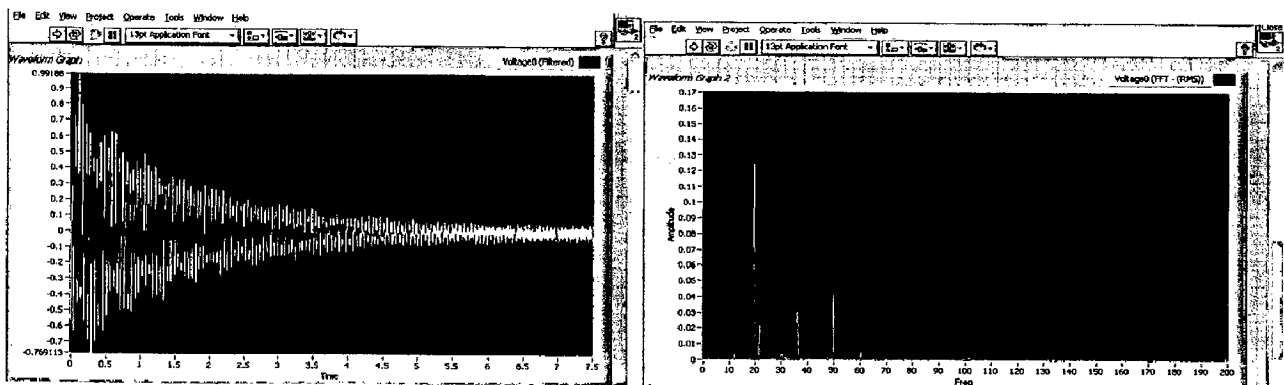


Figure 5.7 (a): Front panel of the LabVIEW VI programme.

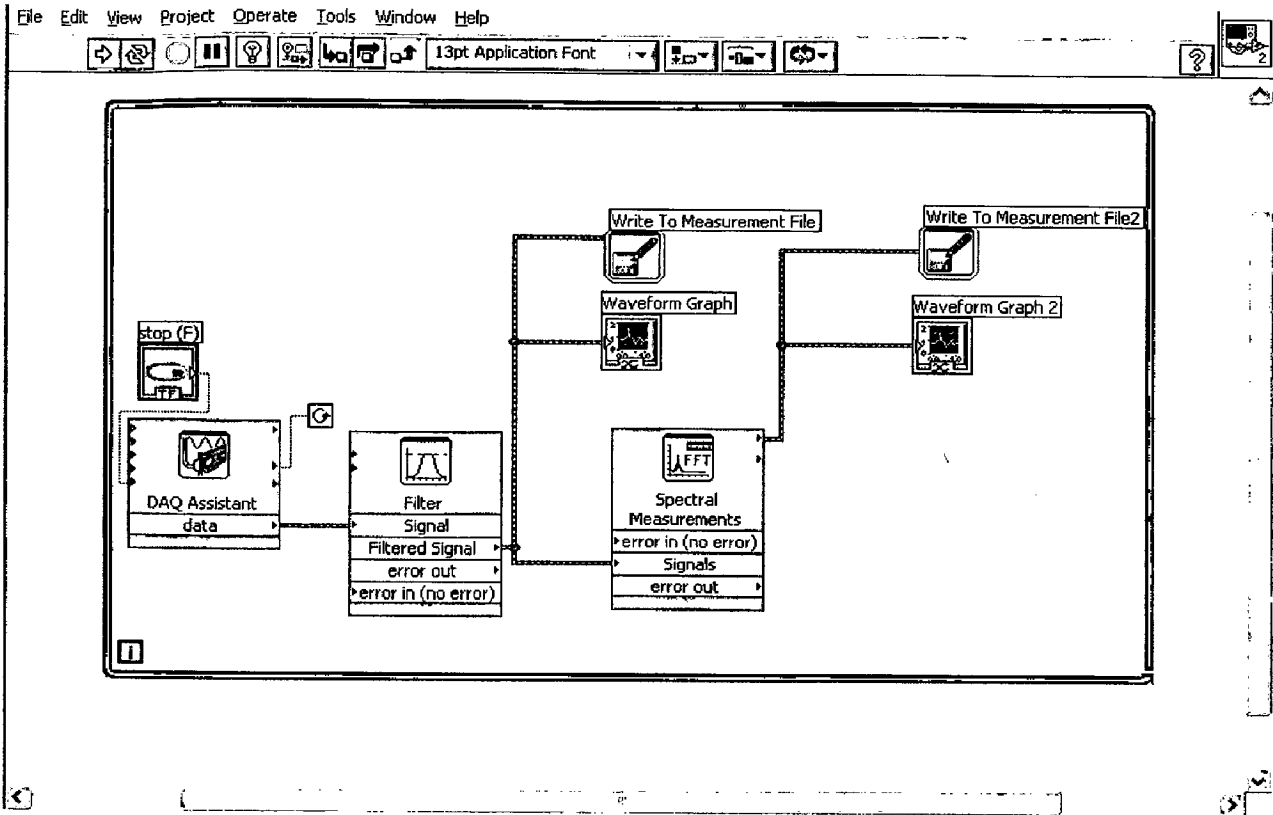


Figure 5.7(b): Block diagram of the LabVIEW VI programme

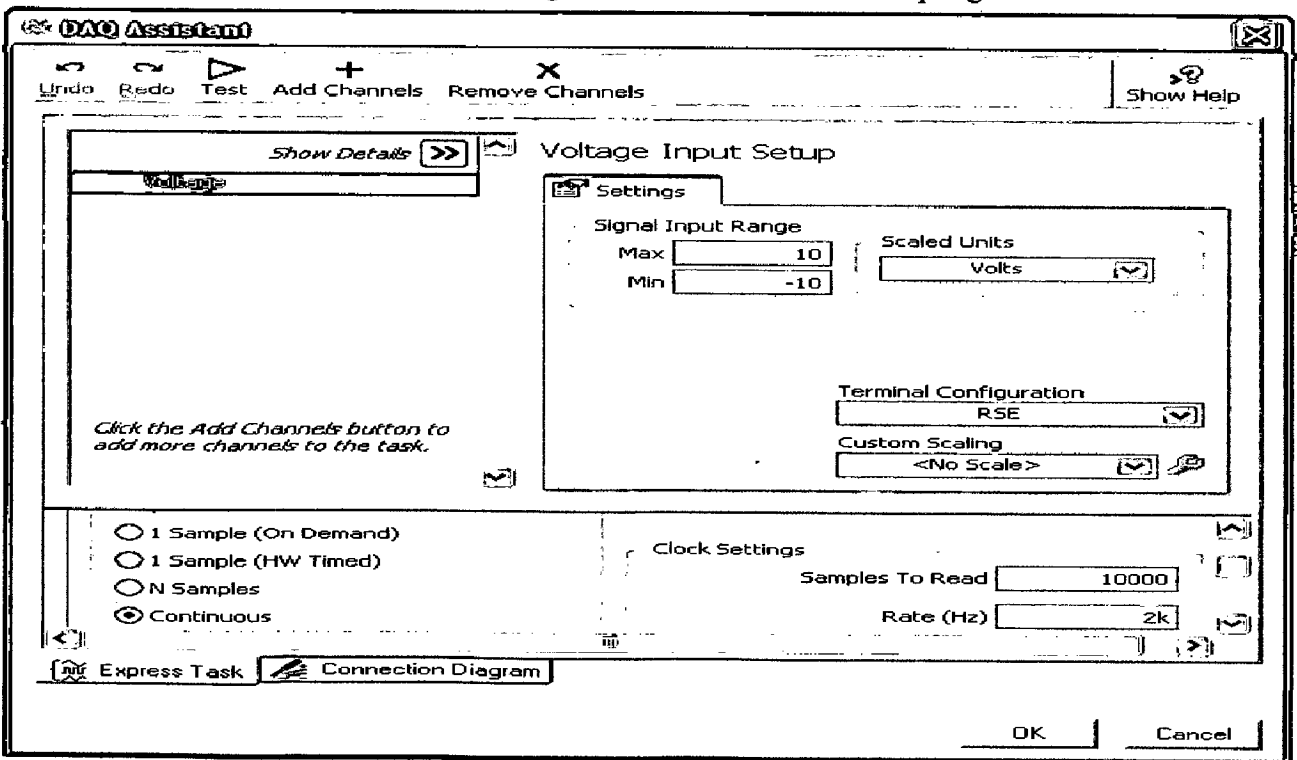


Figure 5.8: DAQ assistant parameter dialogue box

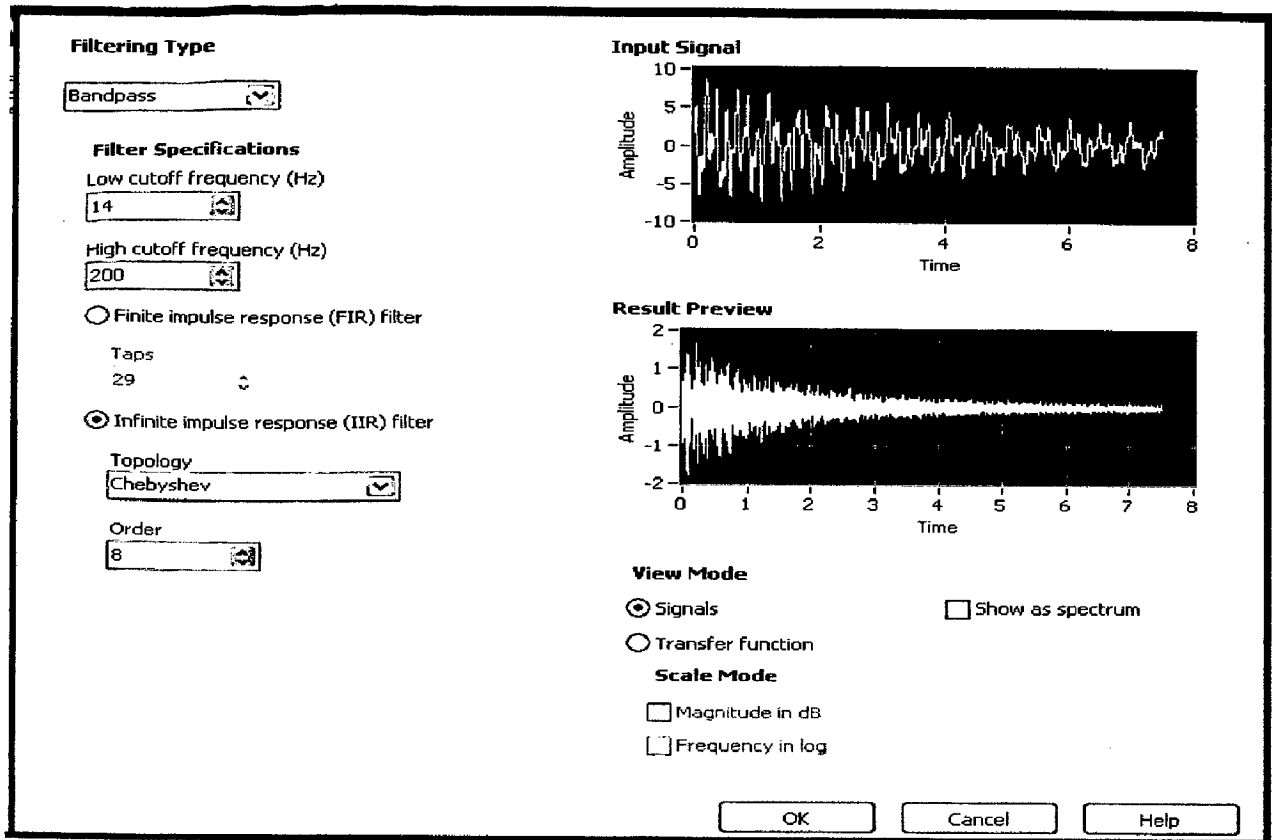


Figure 5.9: Band pass filter block

5.3 Procedure

Proportional control method is used for vibration control. Hence, the output of the sensing system is given to the actuation system by directly giving some gain (amplification). The plate is excited with unknown impulse at the outer boundary. Sensed voltage is recorded in the computer with gain and without gain by the actuation system. It means the data are stored without control action and with control action. The normalized data are compared with each other on the same scale with different gain values.

Following steps are taken during experiment:

- (1) Aluminum plate with PZT patches which are bonded near the fixed edge. The plate is annular circular plate clamped at the inner boundary.
- (2) PZT patches are connected to the Piezo sensing and actuation unit.

(3) DAQ NI card is connected to the computer through USB port. The output of the sensing system is connected to the analog input port of the NI card and input of the actuation system.

(4) BNC and coaxial wire connection is used for the interconnection of all the devices.

(5) Keeping the phase IN/OUT switch in PHASE position.

(6) Keeping the voltage adjusting switch below 50V

(7) Slowly increasing the actuation voltage till the Piezo sensing voltage is reached.

Free vibration analysis of an isotropic circular annular plate is carried out in order to obtain the natural frequencies and mode shapes.

Table 6.1: Properties of Piezoelectric patch and plate [55]

Property Name		PZT	Plate
Young's modulus of elasticity (GPa)	E11	63	70
	E22=E33	63	-
Poisson ratio	$\nu_{12} = \nu_{13}$	0.3	0.334
	ν_{23}	0.3	-
Shear modulus (GPa)	$G_{12}=G_{13}$	24.2	-
	G_{23}	24.2	-
Density, ρ (Kg/m ³)		7600	2700
Piezoelectric constant (m/V) $d_{31}=d_{32}$		254E-12	-
Electrical permittivity (F/m)	$\epsilon_{11} = \epsilon_{22}$	15.3E-9	-
	ϵ_{33}	15.0E-9	-

The circular annular plate is clamped at the inner boundary and free at the outer boundary. One PZT patch is bonded on the top surface near the clamped edge as the sensor and four patches are bonded just opposite side in the same location as the actuator, by graphite epoxy adhesive. The adhesive thickness layer is neglected for analysis. The natural frequencies of the annular plate are calculated without piezoelectric patches for different aspect ratio and the results are compared with the result available in the

literature [22]. Comparison of first five natural frequencies is shown in the table 6.2 and 6.3 and bar charts are drawn for comparison purpose.

$\frac{h}{r_0}$		Axisymmetric vibration mode number				
		1	2	3	4	5
0.001	Ref [22]	6.6604	42.614	123.46	244.18	405.23
	Present work	6.657	42.556	123.413	243.857	405.19
0.050	Ref [22]	6.6234	41.265	115.17	216.78	340.08
	Present Work	6.579	41.24	115.13	216.242	339.49
0.100	Ref [22]	6.5162	37.894	98.261	171.59	252.29
	Present work	6.49	37.79	97.74	171.58	251.799
0.150	Ref [22]	6.3494	33.766	82.172	136.07	192.56
	Present work	6.29	33.75	82.009	136.05	192.53
0.200	Ref [22]	6.1372	29.763	69.409	110.42	151.28
	Present work	6.136	29.63	68.93	110.168	151.232

Table 6.2: Comparison of natural frequency (Hz) of annular plate (clamped at inner boundary and free at outer boundary) for different $\frac{h}{r_0}$ ratio and $\frac{r_i}{r_o} = 0.3$

$\frac{r_i}{r_o}$		Axisymmetric vibration mode number				
		1	2	3	4	5
0.1	Ref [22]	4.2374	25.262	73.899	146.69	243.94
	Present work	4.234	24.87	73.71	146.1	243.01
0.2	Ref [22]	5.1811	32.291	94.082	186.42	309.68
	Present Work	5.179	32.08	93.44	185.9	308.65
0.3	Ref [22]	6.6604	42.614	123.46	244.18	405.23
	Present work	6.657	42.556	123.413	243.857	405.19
0.4	Ref [22]	9.0205	58.548	168.68	333.05	552.29
	Present work	9.013	58.52	168.32	332.17	552.109
0.5	Ref [22]	13.024	85.031	243.68	480.40	796.12
	Present work	12.987	84.687	243.675	480.34	796.07

Table 6.3: Comparison of natural frequency (Hz) of annular plate (clamped at inner boundary and free at outer boundary) for different aspect ratio and $\frac{h}{r_o} = 0.001$

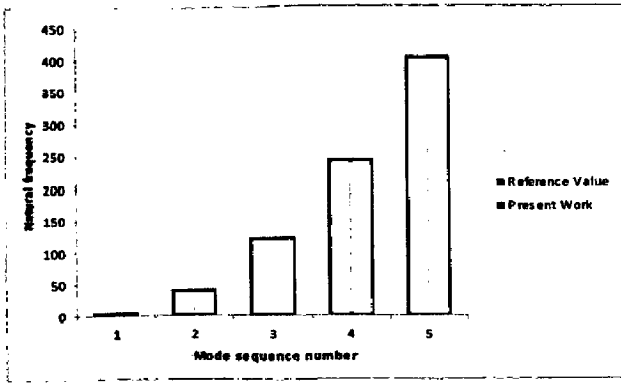


Figure 6.1: Natural frequency of annular plate for $\frac{r_i}{r_o} = 0.3$ and $\frac{h}{r_o} = 0.001$

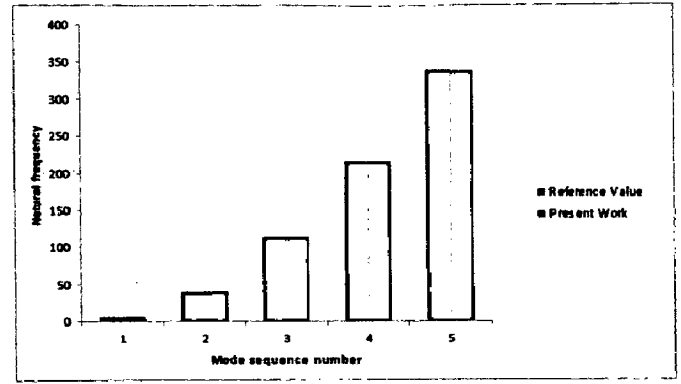


Figure 6.2: Natural frequency of annular plate for $\frac{r_i}{r_o} = 0.3$ and $\frac{h}{r_o} = 0.050$

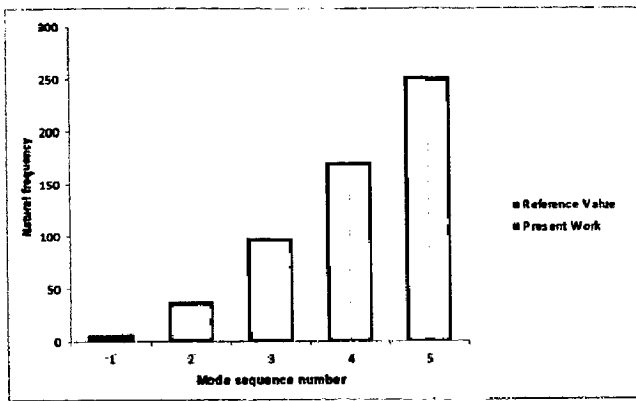


Figure 6.3: Natural frequency of annular plate for $\frac{r_i}{r_o} = 0.3$ and $\frac{h}{r_o} = 0.100$

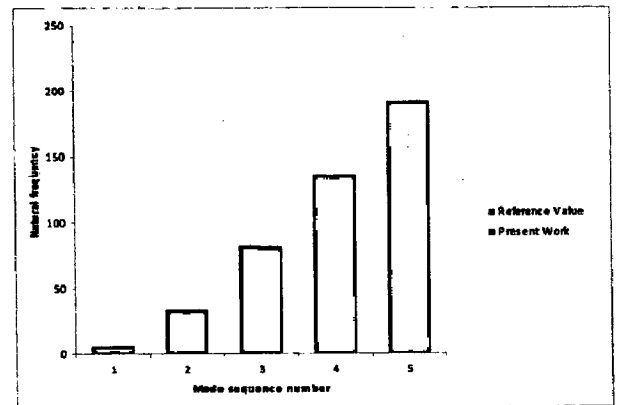


Figure 6.4: Natural frequency of annular plate for $\frac{r_i}{r_o} = 0.3$ and $\frac{h}{r_o} = 0.150$

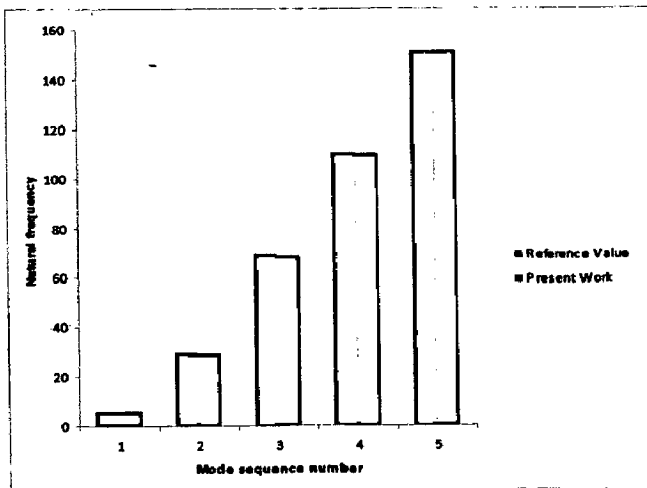


Figure 6.5: Natural frequency of annular plate for $\frac{r_i}{r_o} = 0.3$ and $\frac{h}{r_o} = 0.200$

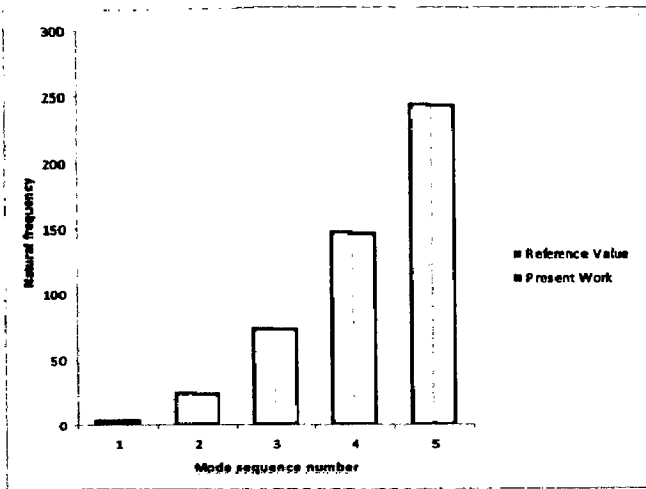


Figure 6.6: Natural frequency of annular plate for $\frac{h}{r_o} = 0.001$ and $\frac{r_i}{r_o} = 0.1$

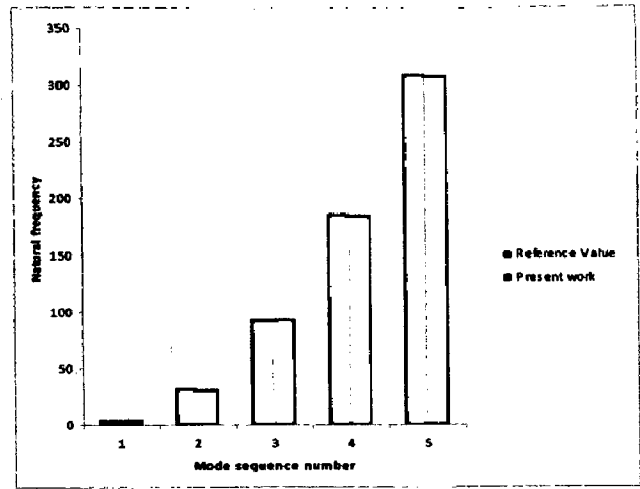


Figure 6.7: Natural frequency of annular plate for $\frac{h}{r_o} = 0.001$ and $\frac{r_i}{r_o} = 0.2$

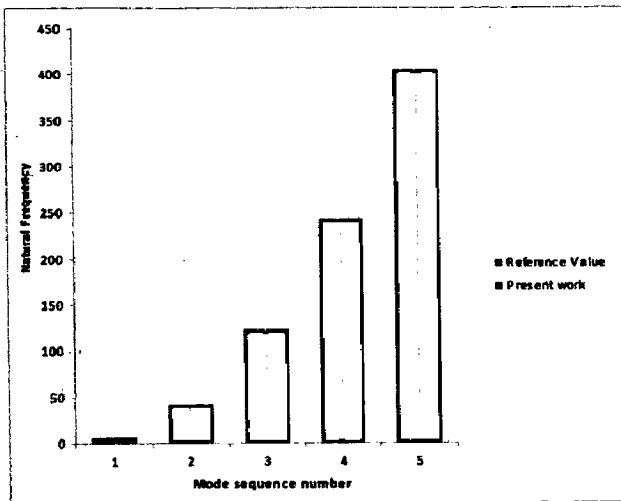


Figure 6.8: Natural frequency of annular plate $\frac{h}{r_o} = 0.001$ and $\frac{r_i}{r_o} = 0.3$

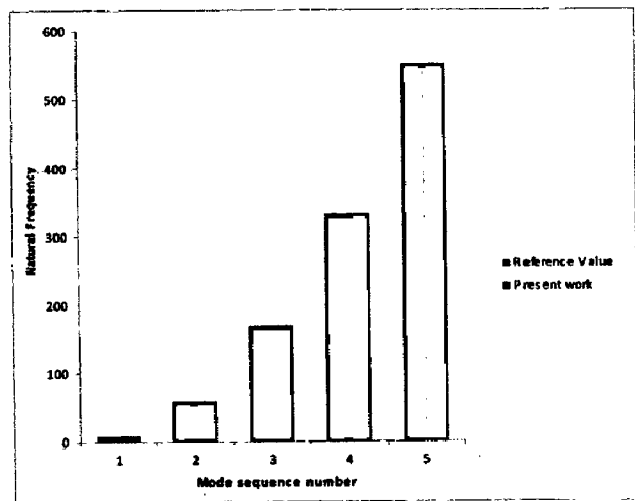


Figure 6.9: Natural frequency of annular plate for $\frac{h}{r_o} = 0.001$ and $\frac{r_i}{r_o} = 0.4$

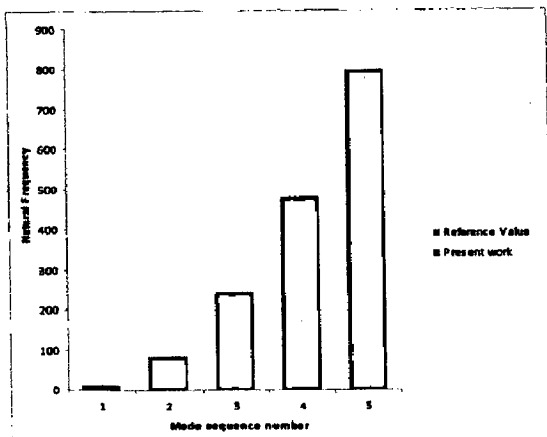


Figure 6.10: Natural frequency of annular plate for $\frac{h}{r_o} = 0.001$ and $\frac{r_i}{r_o} = 0.5$

6.1 Optimal placement of sensor/actuator pair

The problem of determining the optimal locations of actuators for the active vibration control of flexible structures is of considerable interest in engineering design where improved performance and efficiency of response is sought from each controller. In active vibration control of structures using piezoelectric materials, the locations of sensors and actuators have significant influence on the performance of the control system as well as the controlled response. Misplaced sensors and actuators lead to problems such as lack of observability and controllability. Hence it is very challenging problem in the field of active vibration control. Generally, the optimization problem is classified as continuous or discrete and the optimization methods would be either non-systematic (such as some intuitive “cut and try” placement techniques) or systematic optimization methods such as Simulated Annealing (SA), Tabu search (TS), and Genetic Algorithms (GAs) [57].

In this study, the placement of collocated piezoelectric S/A pairs in a laminated composite plate is determined by FE method. The equation of motion in the absence of structural damping with respect to the reduced modal space is given as [66, 77].

$$\{\ddot{\eta}\} + [\Omega]\{\eta\} = \{\bar{F}\} + [\bar{B}]\{\Phi^a\} \quad (6.1)$$

Where $\{\eta\} \in R^{r*1}$ is the modal coordinate vector, r the number of retained modes, $[\Omega] \in R^{r*r}$ the matrix of eigenvalues, $\{\bar{F}\} \in R^{r*1}$ the reduced force vector, $[\bar{B}] \in R^{r*p}$ the actuator influence matrix, $\{\Phi^a\} \in R^{p*1}$ the actuator voltage vector and p the total number of piezoelectric sensor and actuator pairs. If the effect of the mass and stiffness of the sensor and actuator pairs on the dynamic behavior of the composite plate is neglected, according to the pin force model [6], the equivalent actuators forces are the constant linear distributed moments along the edges for different placement. Hence, the values of non-zero elements of actuator influence matrix $[\bar{B}]$ remains constant for different placement, though the positions will change with the actual placement. According to equation (6.1), the equivalent actuator forces are maximized by maximizing the input voltages of the actuators $\{\Phi^a\}$. But for the classical constant gain negative velocity feed

back control system $\{\Phi^a\} = -[G]\{\Phi^s\}$ where $[G]$ is the constant gain matrix which is coupling in between input actuator voltage vector $\{\Phi^a\}$ and output sensor voltage $\{\Phi^s\}$ [77]. Hence, in order to maximizing the $\{\Phi^a\}$, the corresponding sensor voltage $\{\Phi^s\}$ should also be maximized.

$$\{\Phi^a\}_{\max} \rightarrow \{\Phi^s\}_{\max} \quad (6.2)$$

In order to maximize the sensor voltage $\{\Phi^s\}$ for actively damped free vibration, with the help of equation (4.3.42) and equation (4.3.28) it is concluded that these strain-rate piezoelectric sensors should be placed in regions where more electric charges and high electric current are obtained.

$$(\Phi_i^s)_{\max} \rightarrow (Q^i)_{\max} \quad (6.3)$$

To maximize the induced electric charge, the integration of electric displacement D_z according to equation (4.3.26) should be maximized. But for the PZT $e_{34} = e_{35} = e_{36} = 0$. Hence, equation (4.3.26) becomes,

$$\begin{aligned} D_z &= e_{31}\varepsilon_1 + e_{32}\varepsilon_2 \\ &= (m^2e_{31} + n^2e_{31})\varepsilon_x + (m^2e_{32} + n^2e_{31})\varepsilon_y \end{aligned} \quad (6.4)$$

Where, $m = C \cos \theta$, $n = \text{Sin} \theta$ and θ is the skew angle of the sensor, which is constant.

$$Q^i = (m^2e_{31} + n^2e_{32}) \int_{\bar{\psi}} \varepsilon_x d\psi + (m^2e_{32} + n^2e_{31}) \int_{\bar{\psi}} \varepsilon_y d\psi \quad (6.5)$$

Where $\bar{\psi}$ represents the top and bottom surfaces of the sensor. Hence, in order to obtain the maximum input voltages, equations (6.2), (6.3) and (6.5) shows that the surface bonded sensors should be placed in regions where high integrated values of the normal strain over the bonding surface are located. For PZT ($e_{31} = e_{32}$) equation (6.5) is given as

$$(Q^i)_{\max} \rightarrow \left(\int_{\bar{\psi}} (\varepsilon_x + \varepsilon_y) d\psi \right)_{\max} \quad (6.6)$$

Hence, to maximize the input voltage of actuators $\{\Phi^a\}$, the isotropic PZT pairs should be placed in the regions where the sum of the normal strain integrated over the actuator patch is high. The actuators are assumed to be perfectly bonded to the structure,

with negligible mass compared to the mass of the host structure. Generally the sizes of the piezoelectric patches are small compared to the host laminated composite plate. Therefore, it does not add significantly to the bending stiffness [10]. But for the specified applied voltage and constant electric field along the thickness direction of a surface-bonded PZT actuator, distributed shear forces are induced at the bonding surfaces. Based on linear variation in potential and first-order plate theory, the equivalent surface shear forces for the i^{th} PZT actuator is expressed as [77]

$$\begin{aligned} T_1 &= -e_{31}E_3t_i = -e_{31}\Phi_i^a \\ T_2 &= -e_{32}E_3t_i = -e_{32}\Phi_i^a \end{aligned} \quad (6.7)$$

Where, T_1 and T_2 are the equivalent surface shear forces under the applied voltage Φ_i^a , E_3 the electric field along the thickness direction and t_i the thickness of the i^{th} actuator. Both T_1 and T_2 actively damp out the vibration energy of the dynamic system and these are proportional to Φ_i^a . To maximize the active damping effect, the actuator should be located where the virtual work \tilde{W} done by T_1 and T_2 along the surface strain field is maximum with the given initial state. The virtual work is given as

$$\tilde{W} = \int_{\tilde{\psi}} (T_1\varepsilon_1 + T_2\varepsilon_2) d\psi \quad (6.8)$$

Substituting equations (6.7) and (6.4) into equation (6.8) gives,

$$\tilde{W} = -\Phi_i^a \left[(m^2e_{31} + n^2e_{32}) \int_{\tilde{\psi}} \varepsilon_x d\psi + (m^2e_{32} + n^2e_{31}) \int_{\tilde{\psi}} \varepsilon_y d\psi \right] \quad (6.9)$$

Comparing equation (6.9) with equation (6.5) shows that to maximize the virtual work for a given S/A pair, the actuator should be placed at the location where the electric charge of the sensor is also maximum. Because it is already assumed that PZT S/A pair is collocated. Therefore, the collocated S/A pairs should be located in regions where the normal strains integrated over the bonding surfaces is high, resulting in maximum virtual work done by the actuators.

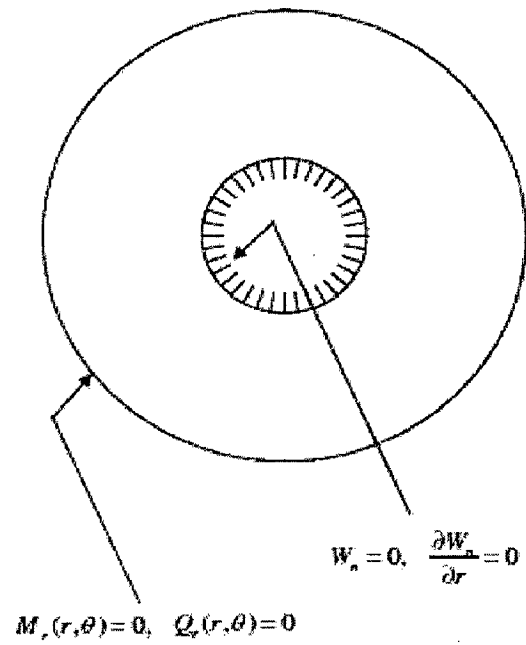


Figure 6.11: Boundary condition imposed on the plate

Where,

W_n = Transverse deflection

$\frac{\partial W_n}{\partial r}$ = Slope

$M_r(r, \theta)$ = Bending moment

$Q_r(r, \theta)$ = Shear Force

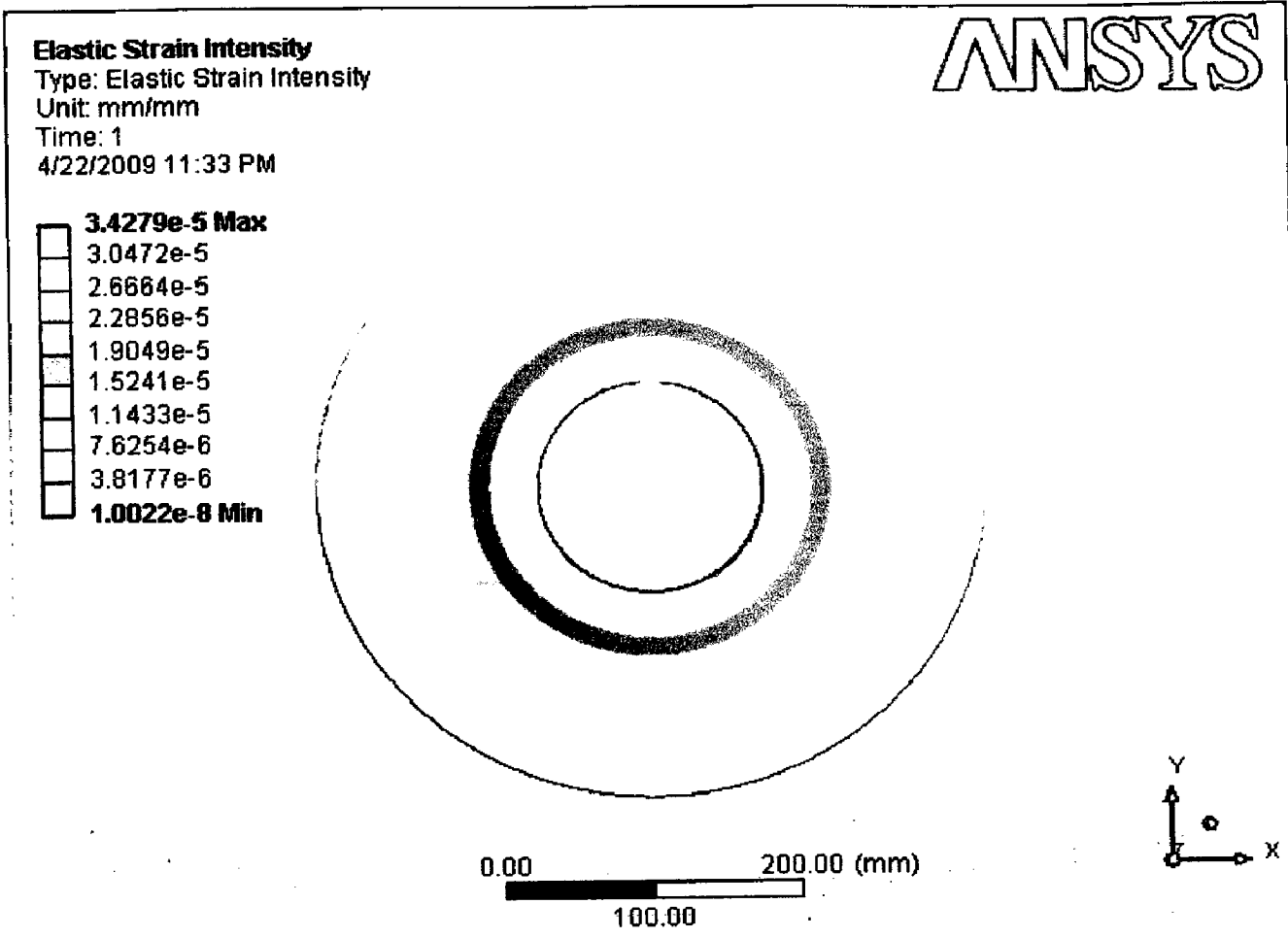


Figure 6.12: Normal elastic strain of circular annular plate

6.2 Experimental work

For the experimental work the excitation force (an impulsive load) is applied at the free end. The sensor readings are recorded in the computer with the help of data acquisition card and rate of decay are calculated for comparison purpose.

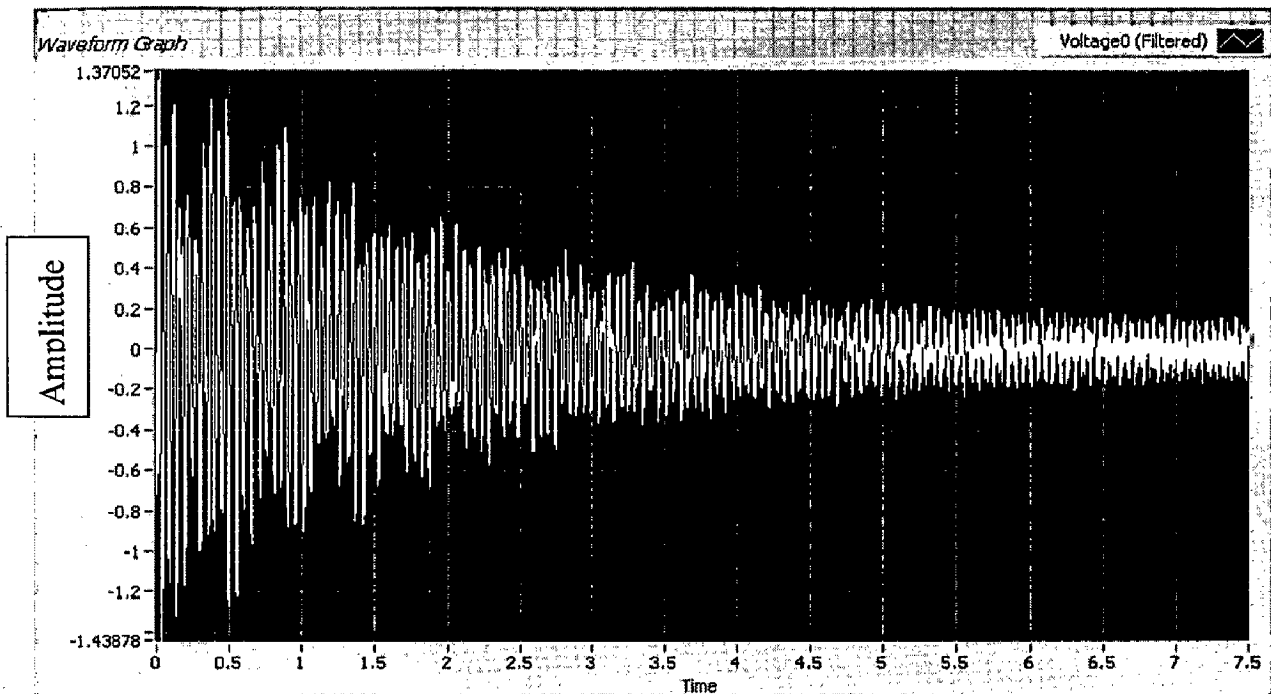


Figure 6.13: Uncontrolled response of amplitude of vibration with respect to time

Figure 6.13 shows the uncontrolled response of amplitude of vibration with respect to time. In figure 6.14 best fit curve crossing the peak level of amplitude of vibration are drawn in order to calculate the rate of decay. Similar procedure is adopted for the controlled response and rate of decay are compared. It is shown that rate of decay are increasing with the gain.

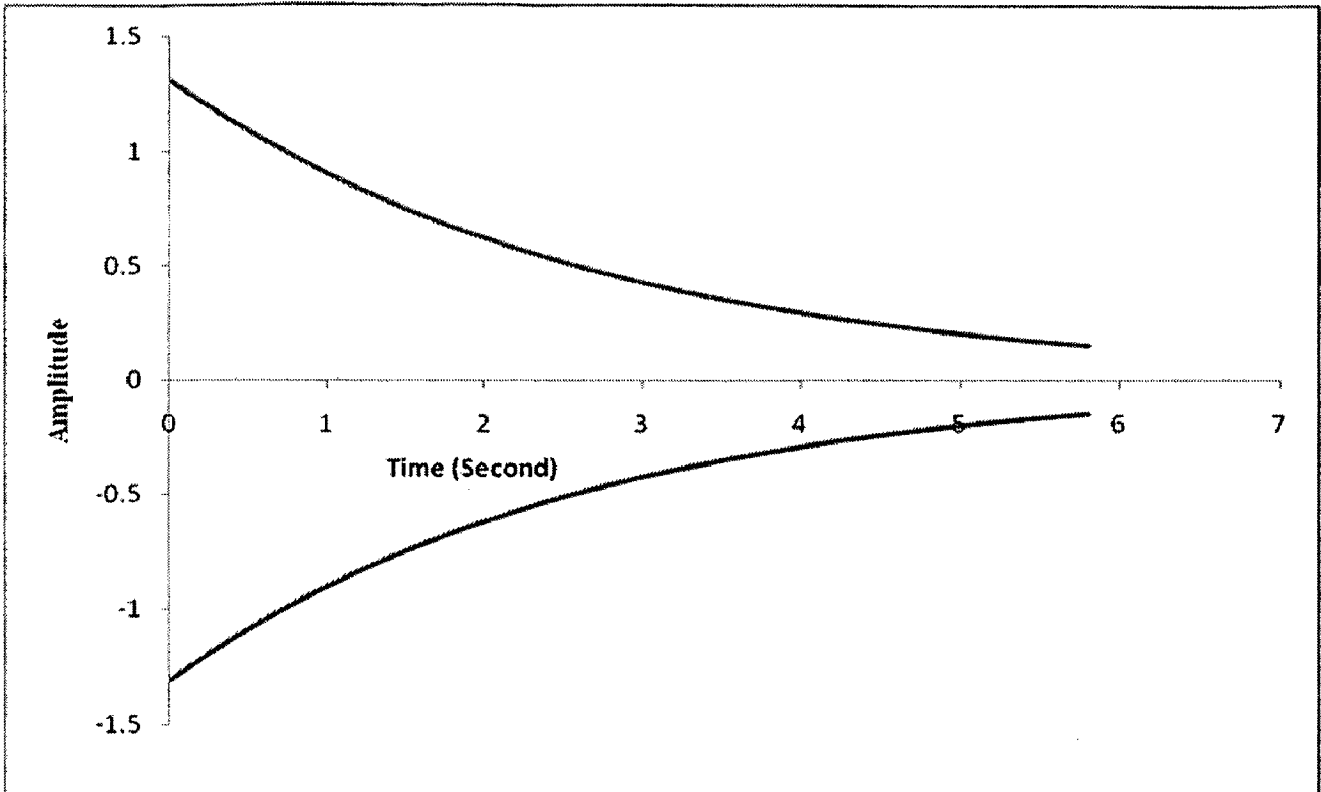


Figure 6.14: Best fit curve (Uncontrolled response) crossing the peak level of amplitude for figure6.2

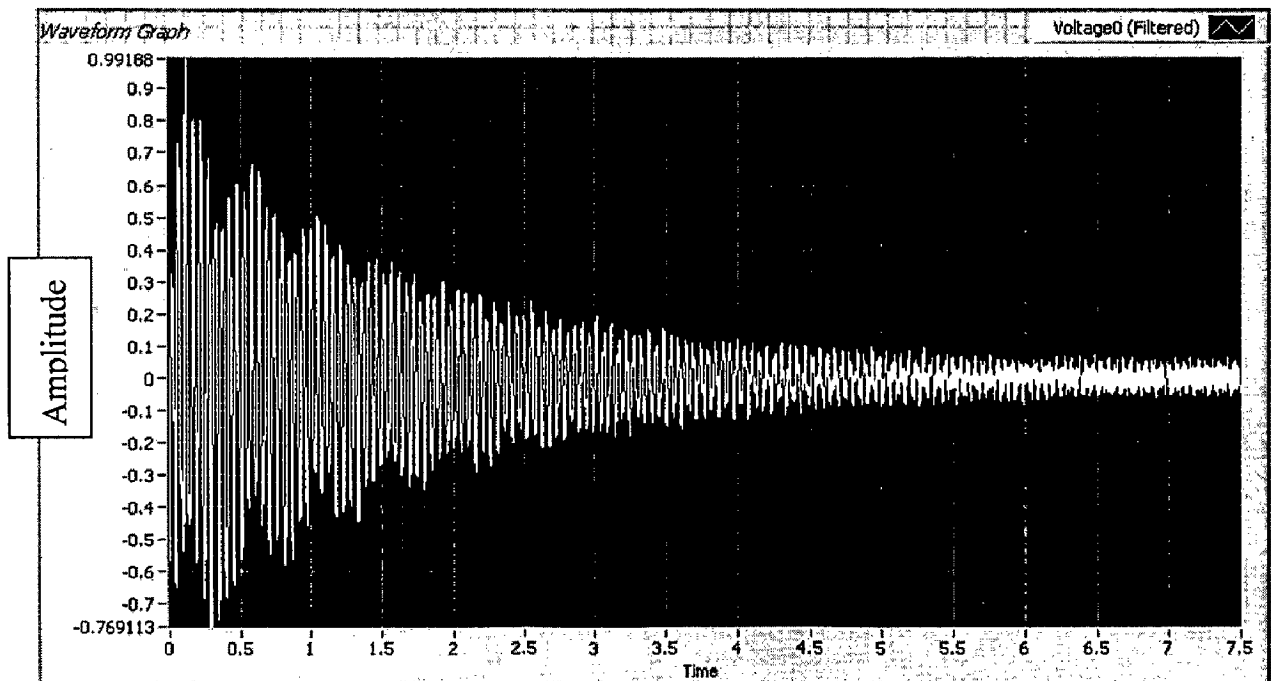


Figure 6.15: Controlled response (Gain-1) of amplitude of vibration with respect to time

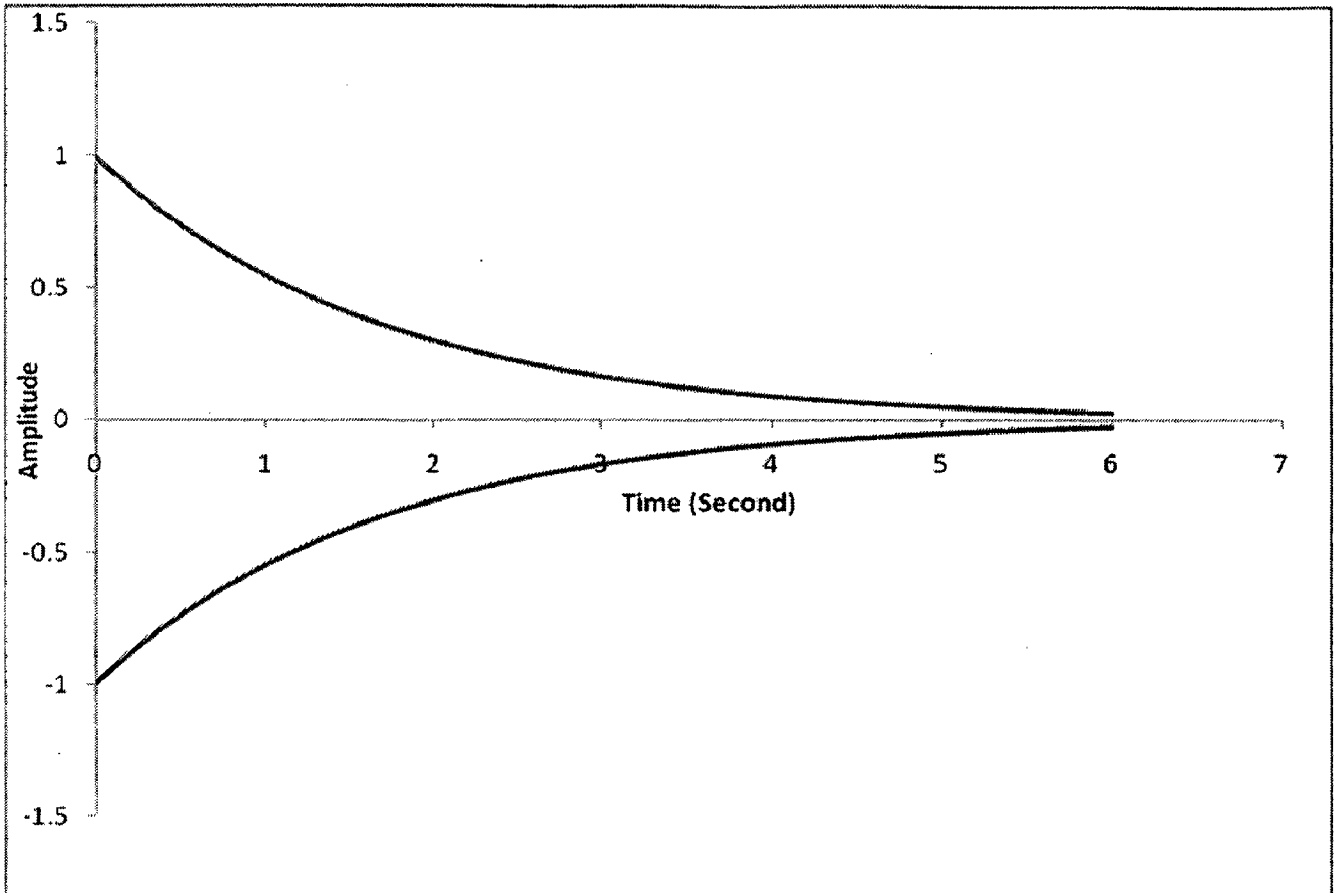


Figure 6.16: Best fit curve crossing the peak level of amplitude for Gain-1

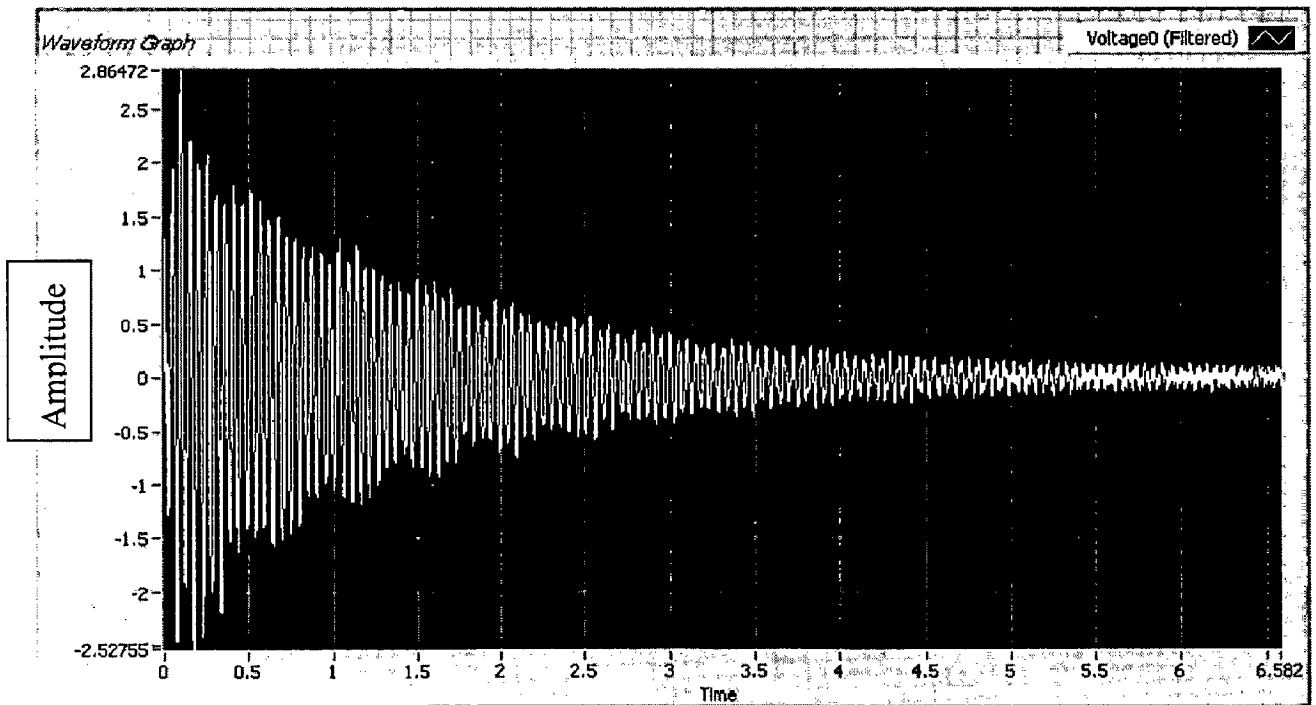


Figure 6.17: Controlled response (Gain-2) of amplitude of vibration with respect to time

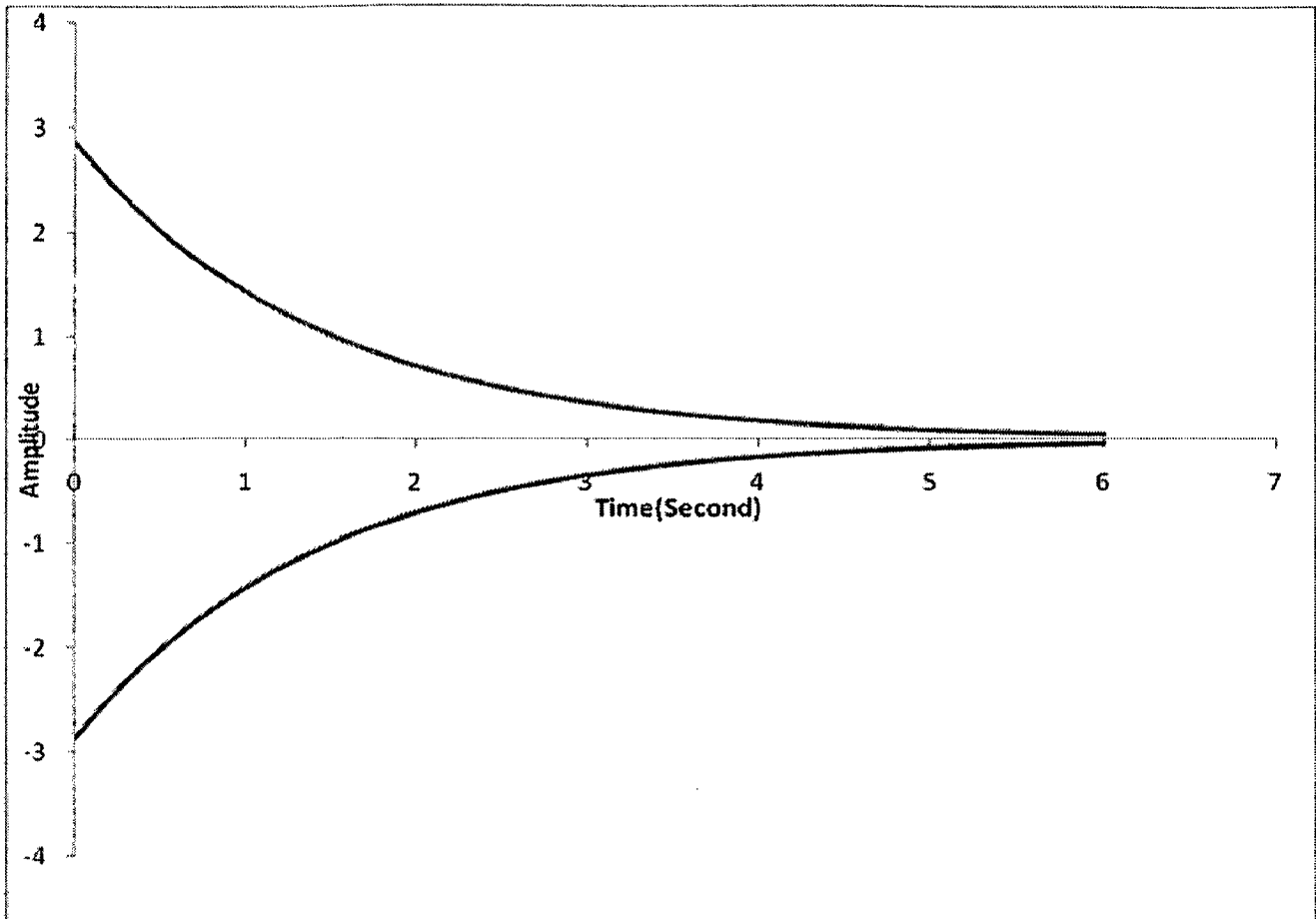


Figure 6.18: Best fit curve crossing the peak level of amplitude for Gain-2

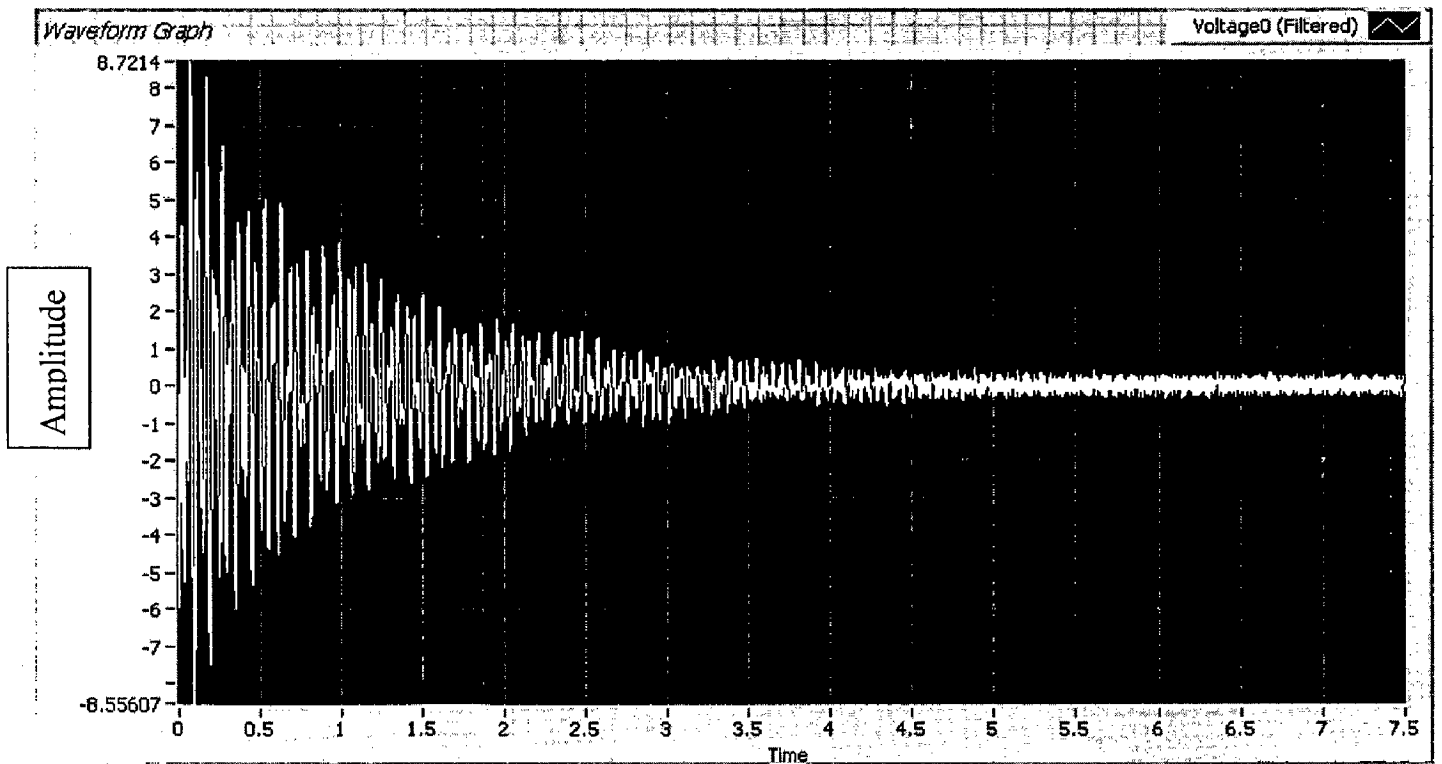


Figure 6.19: Controlled response (Gain-3) of amplitude of vibration with respect to time

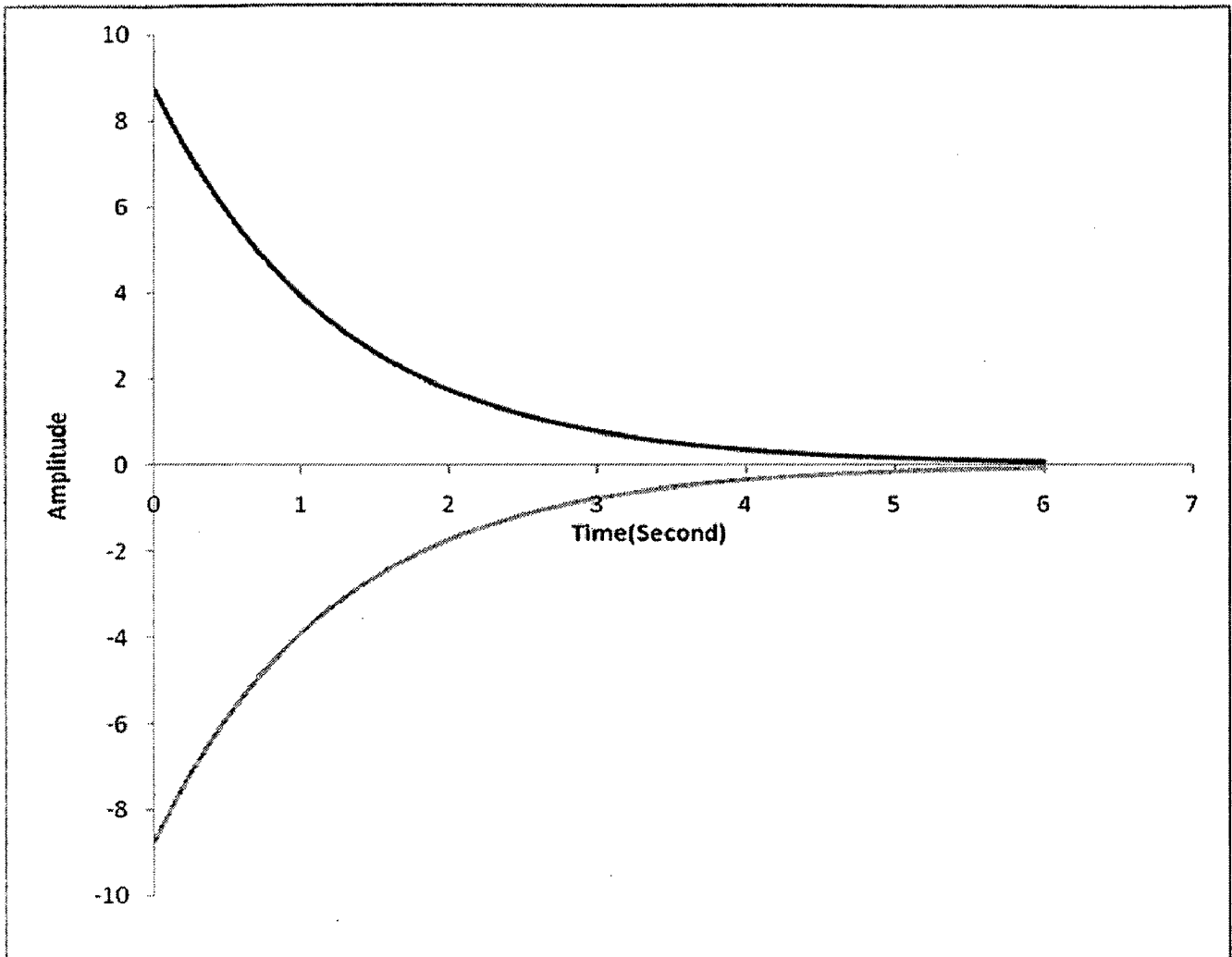


Figure 6.20: Best fit curve crossing the peak level of amplitude for Gain-3

Response	δ (Logarithmic Decrement Index)
Uncontrolled	0.375945
Controlled (Gain-1)	0.5953740
Controlled (Gain-2)	0.7042063
Controlled (Gain-3)	0.807432

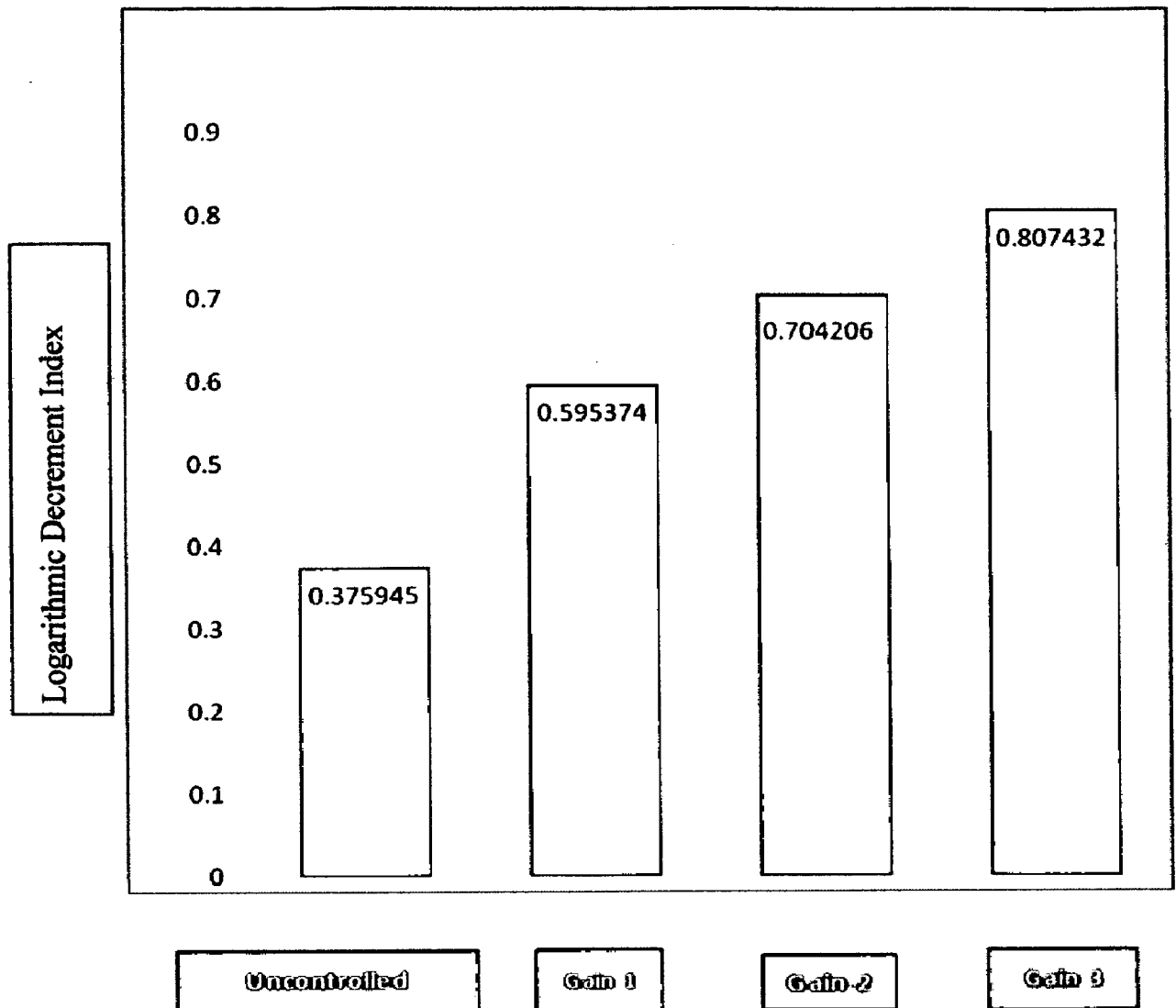


Figure 6.21: Bar chart to show the logarithmic decrement

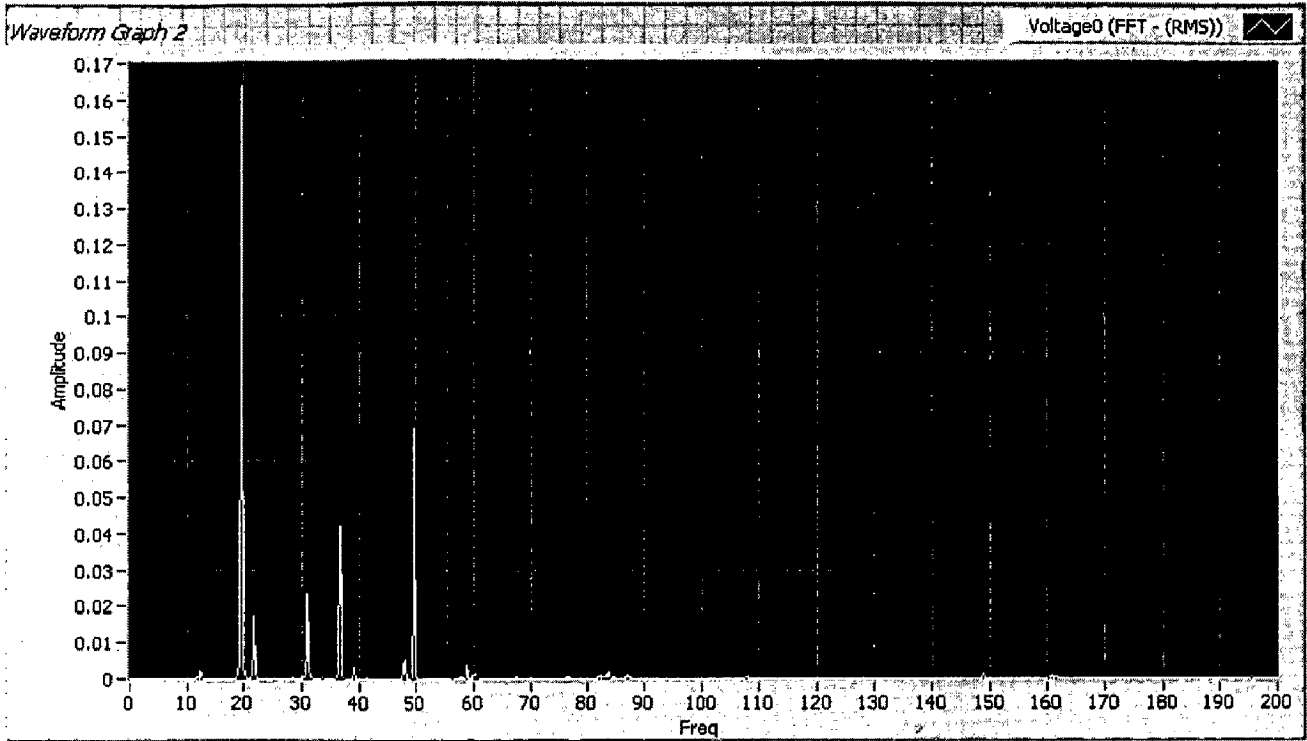


Figure 6.22: Uncontrolled response of amplitude of vibration with respect to frequency

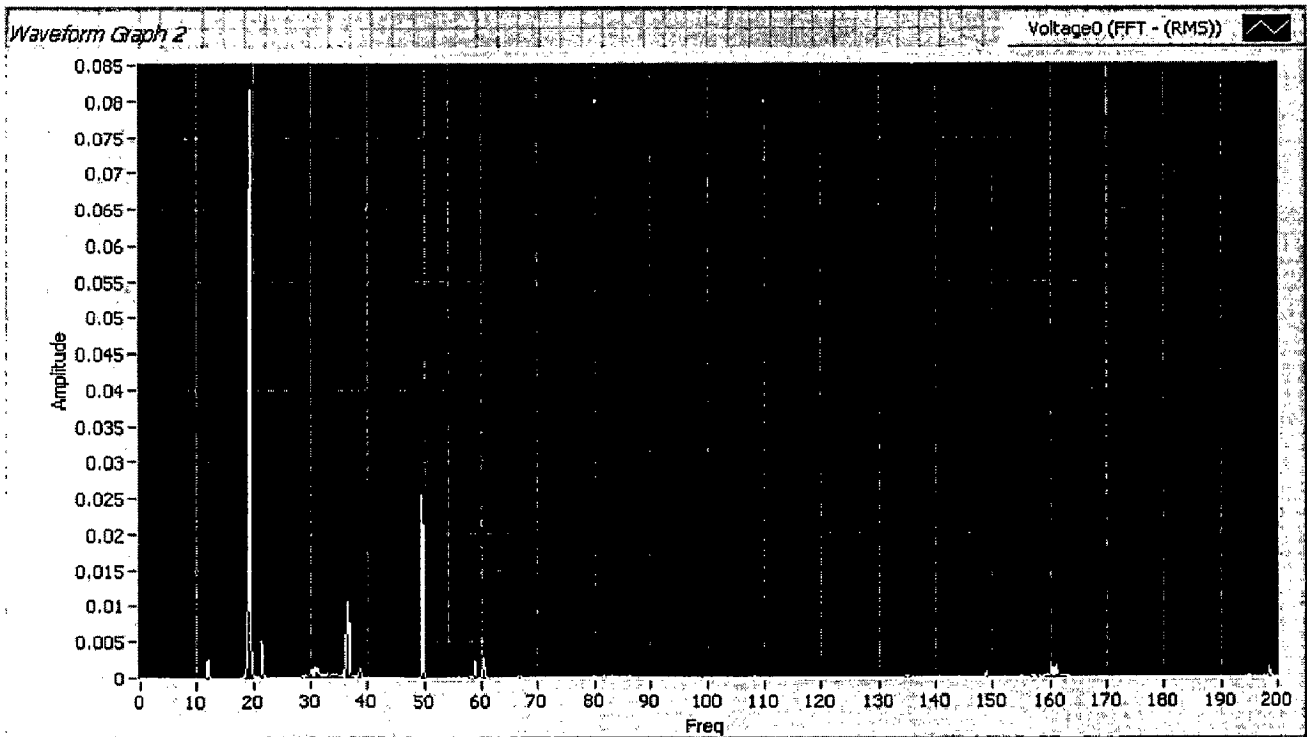


Figure 6.23: Controlled response (Gain-1) of amplitude of vibration with respect to frequency

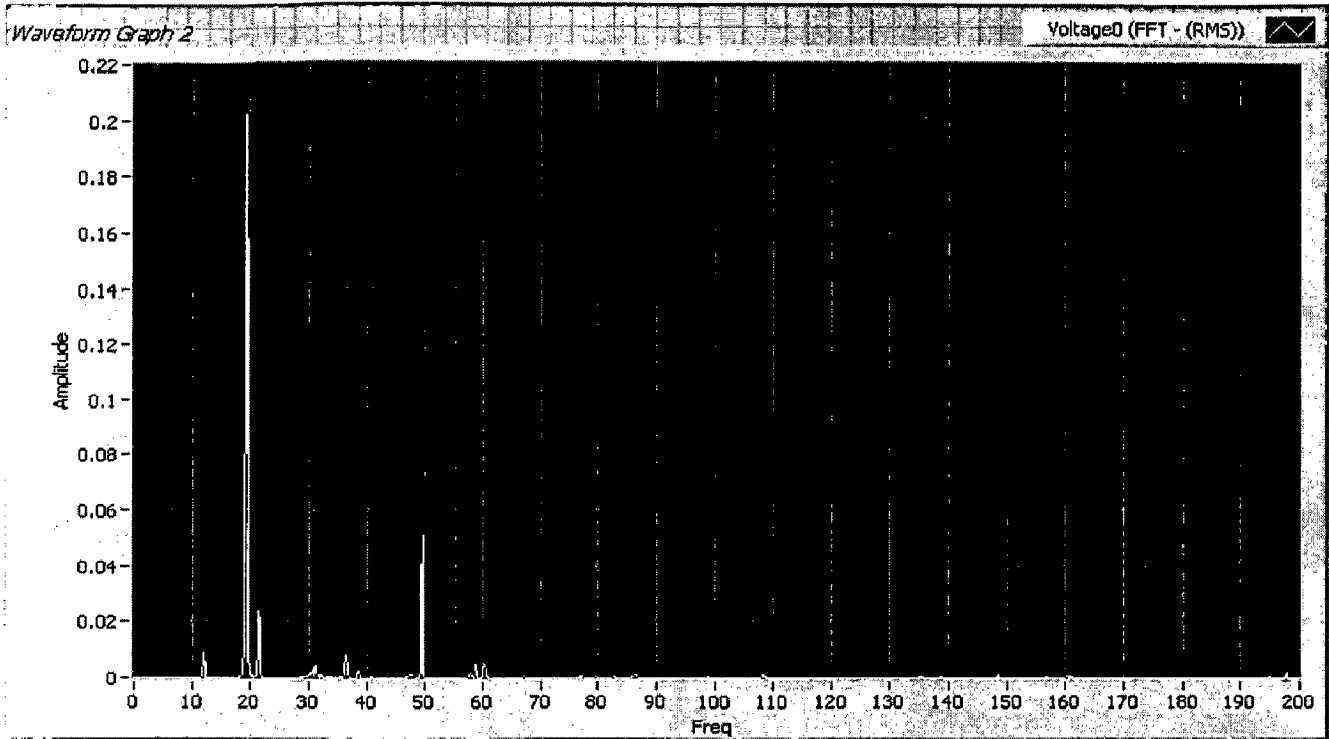


Figure 6.24: Controlled response (Gain-2) of amplitude of vibration with respect to frequency

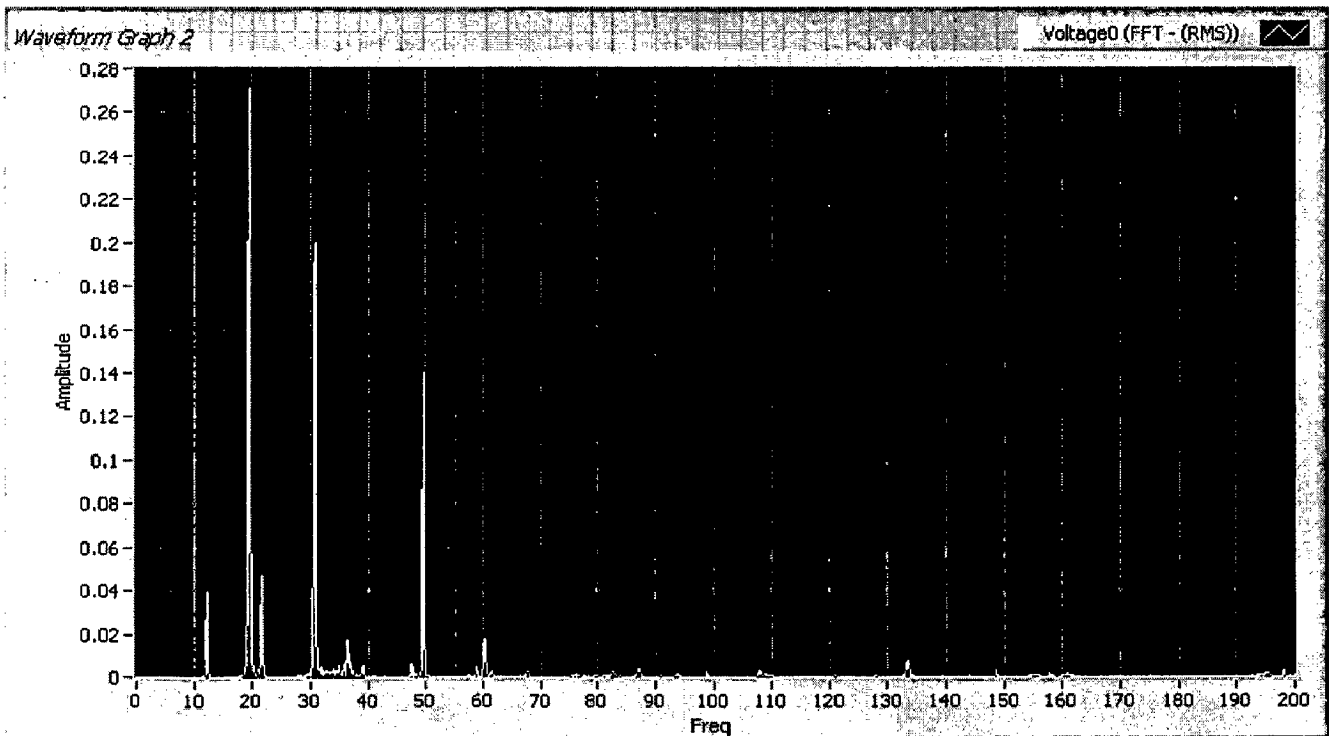


Figure 6.25: Controlled response (Gain-3) of amplitude of vibration with respect to frequency

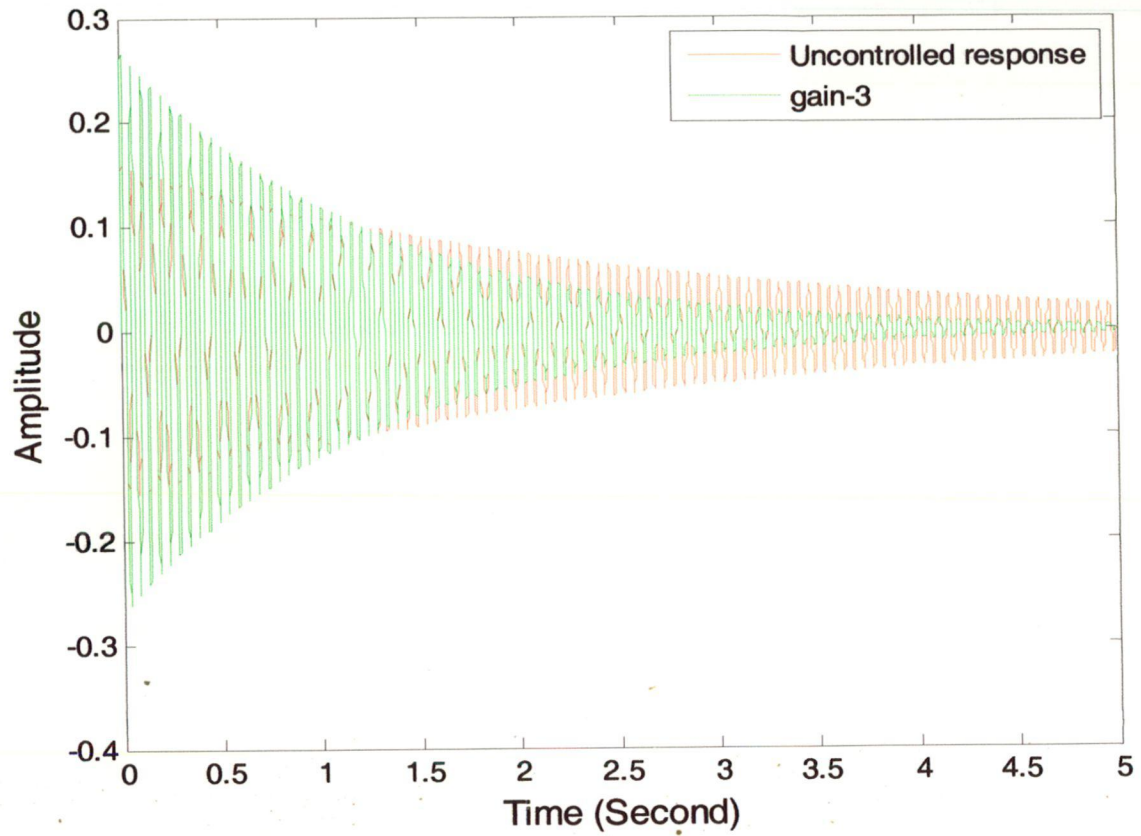
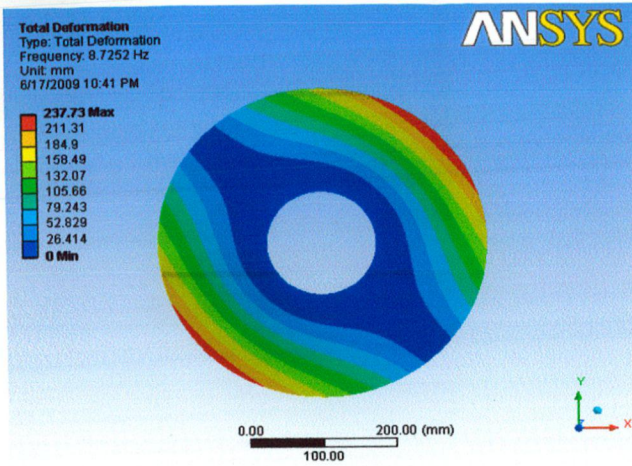


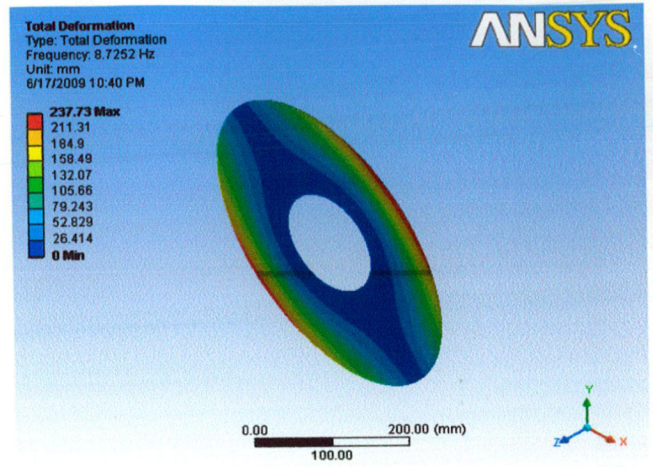
Figure 6.26: Combined plot in between uncontrolled response and controlled response (Gain-3)

6.3.1 Mode Shapes without piezoelectric patches

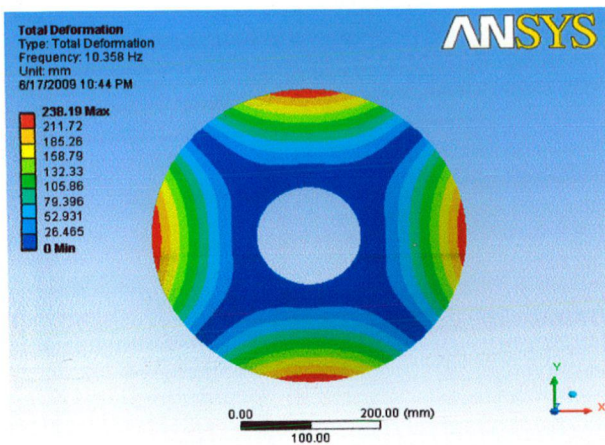
In this section, first six mode shapes of annular plate are presented without considering piezoelectric patches.



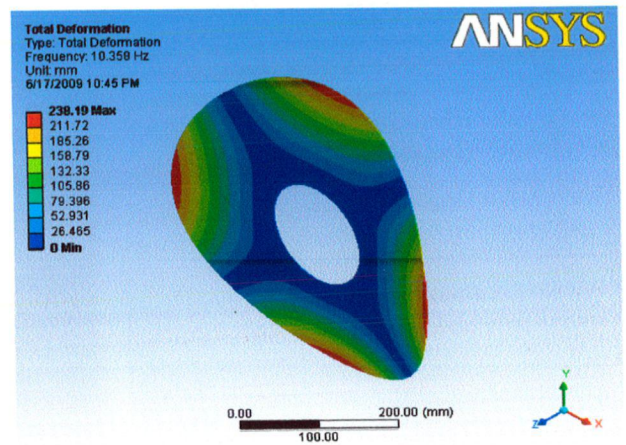
I Mode: $f_n = 8.7252$ Hz
(Front view)



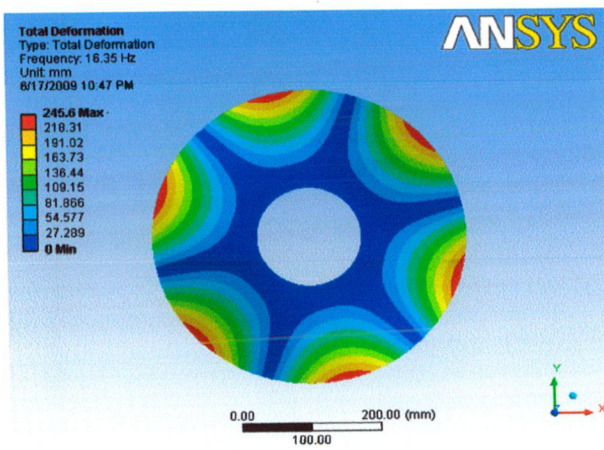
I Mode: $f_n = 8.7252$ Hz
(Isometric view)



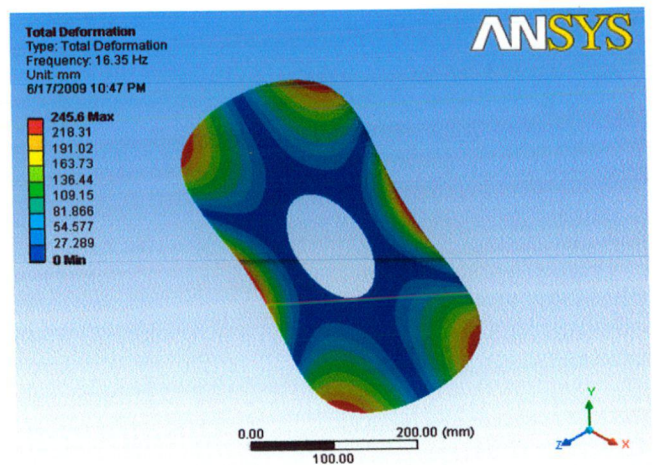
II Mode: $f_n = 10.358$ Hz
(Front view)



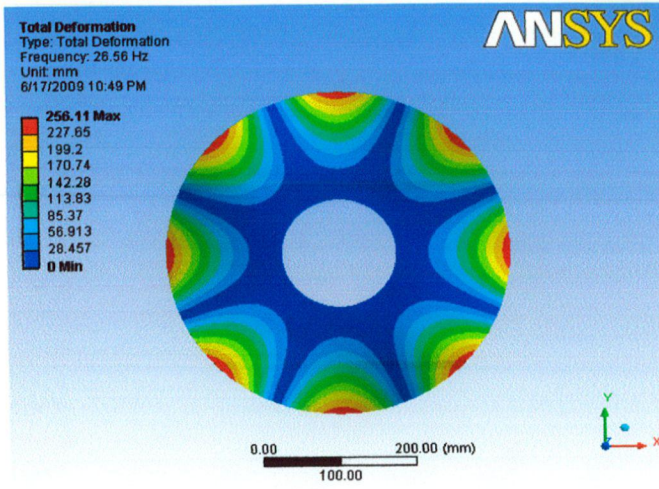
II Mode: $f_n = 10.358$ Hz
(Isometric view)



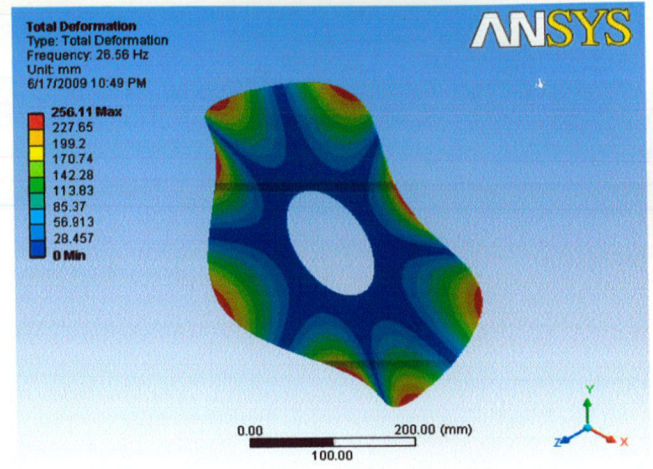
III Mode: $f_n = 16.35$ Hz
(Front view)



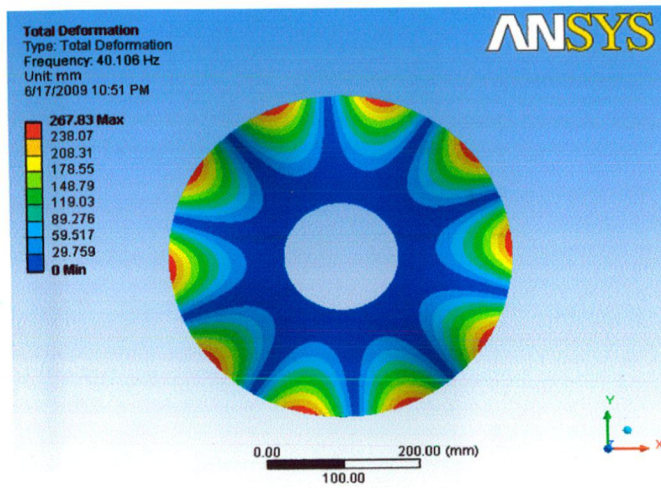
III Mode: $f_n = 16.35$ Hz
(Isometric view)



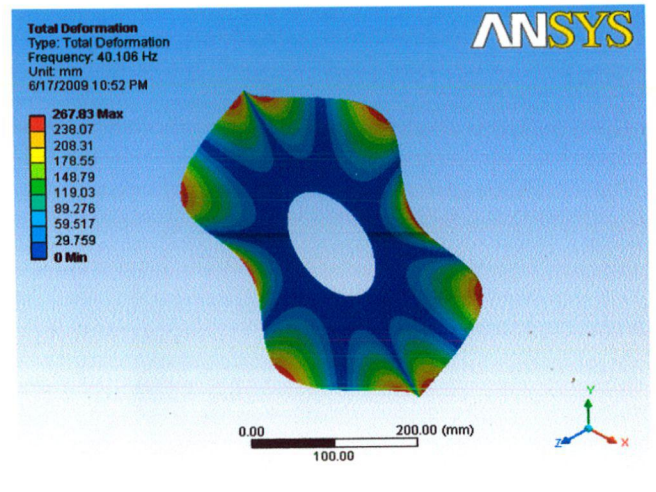
IV Mode: $f_n = 26.56$ Hz
(Front view)



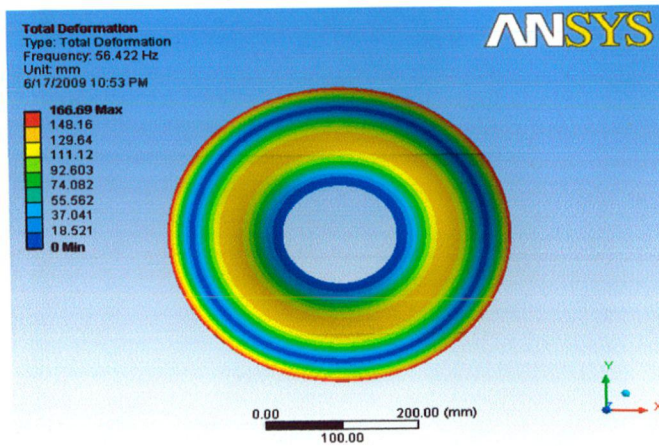
IV Mode: $f_n = 26.56$ Hz
(Isometric view)



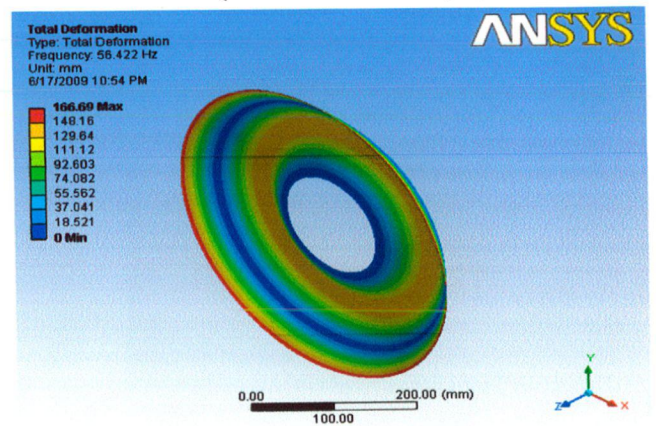
V Mode: $f_n = 40.106$ Hz
(Front view)



V Mode: $f_n = 40.106$ Hz
(Isometric view)



VI Mode: $f_n = 56.422$ Hz
(Front view)

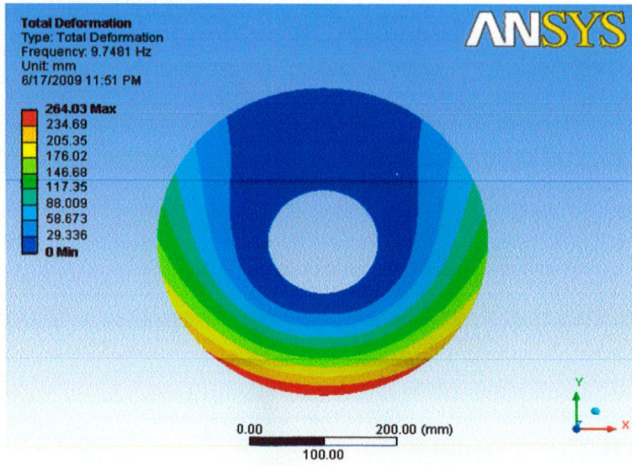


VI Mode: $f_n = 56.422$ Hz
(Isometric view)

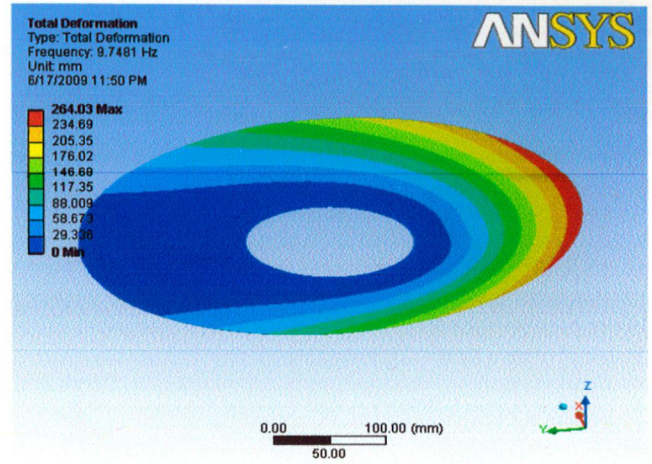
Figure 6.27: Six mode shape of circular annular plate without PZT patches

6.3.2 Mode Shapes with piezoelectric patches

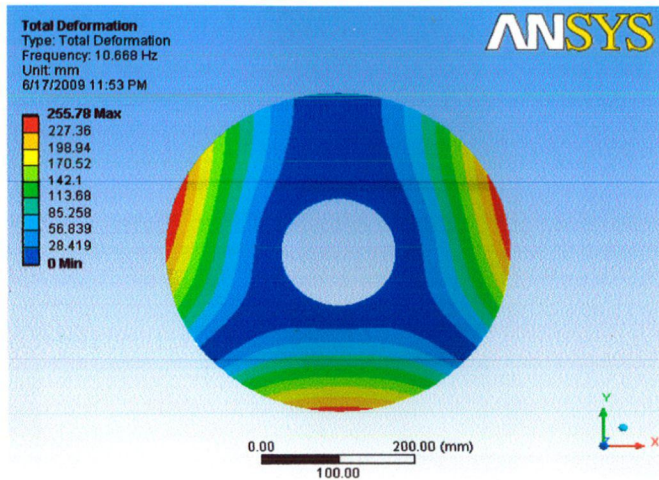
In this section, mode shapes of the annular plate are presented considering the mass and stiffness of piezoelectric patches.



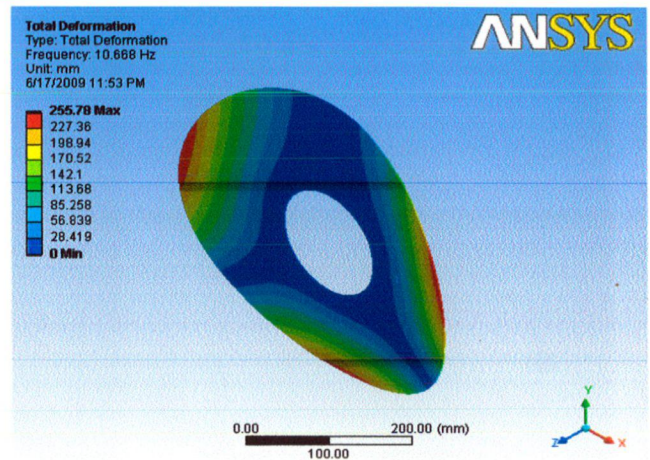
I Mode: $f_n = 9.7481$ Hz
(Front view)



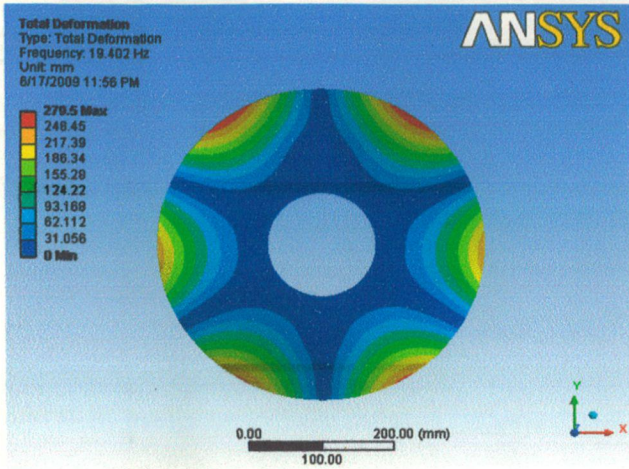
I Mode: $f_n = 9.7481$ Hz
(Isometric view)



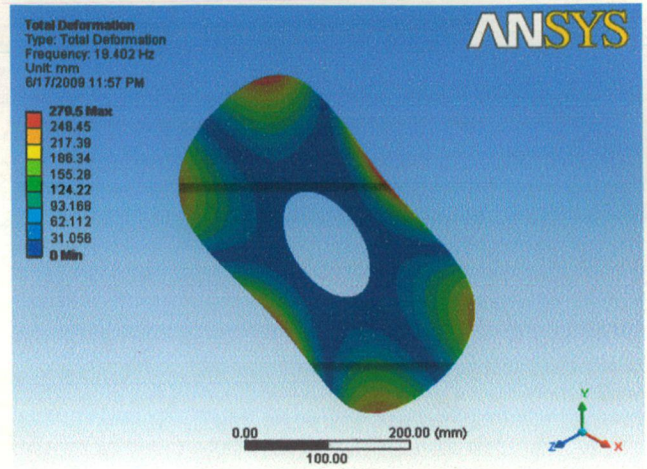
II Mode: $f_n = 10.668$ Hz
(Front view)



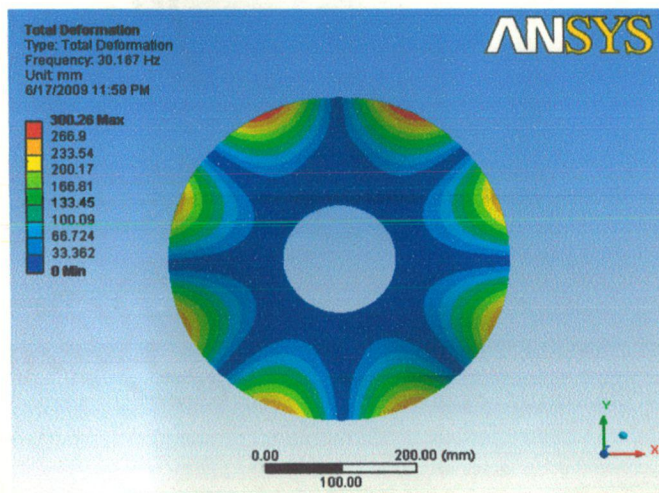
II Mode: $f_n = 10.668$ Hz
(Isometric view)



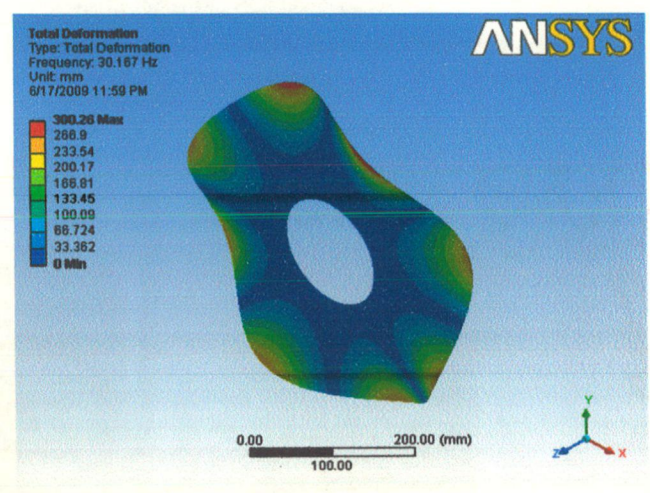
III Mode: $f_n = 19.402$ Hz
(Front view)



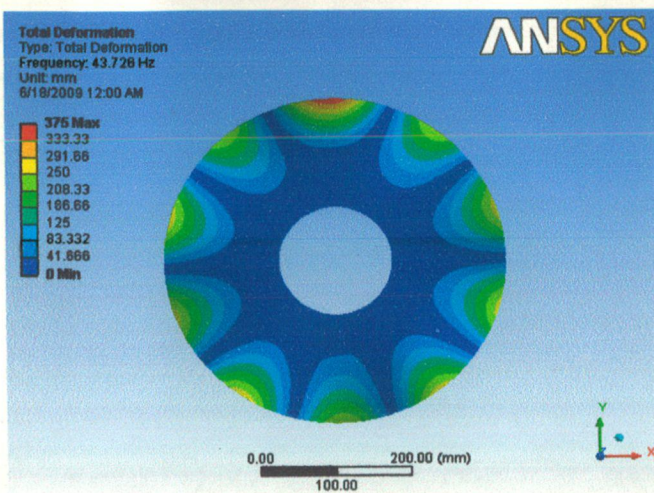
III Mode: $f_n = 19.402$ Hz
(Isometric view)



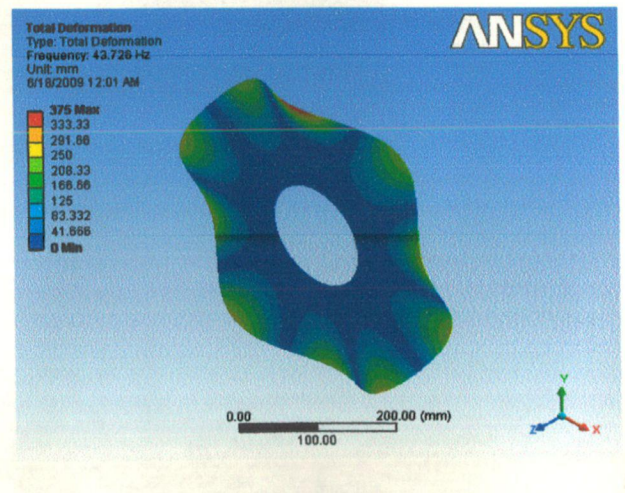
IV Mode: $f_n = 30.167$ Hz
(Front view)



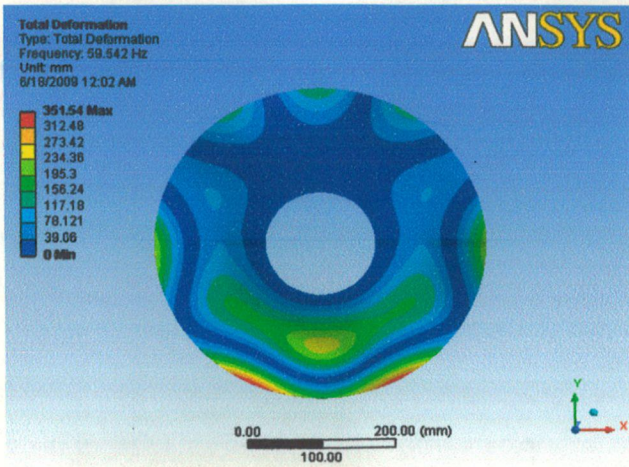
IV Mode: $f_n = 30.167$ Hz
(Isometric view)



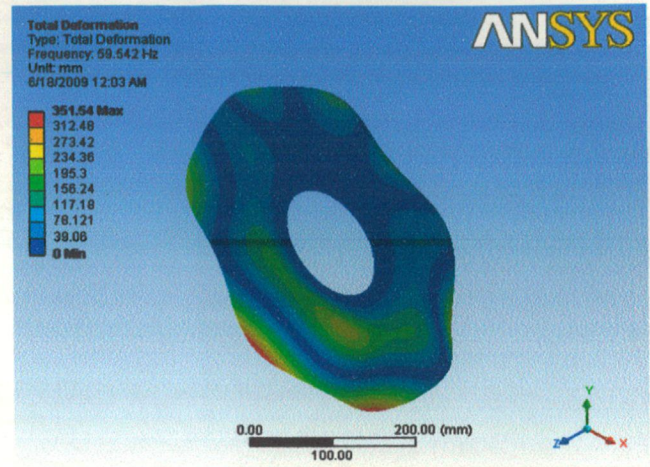
V Mode: $f_n = 43.726$ Hz
(Front view)



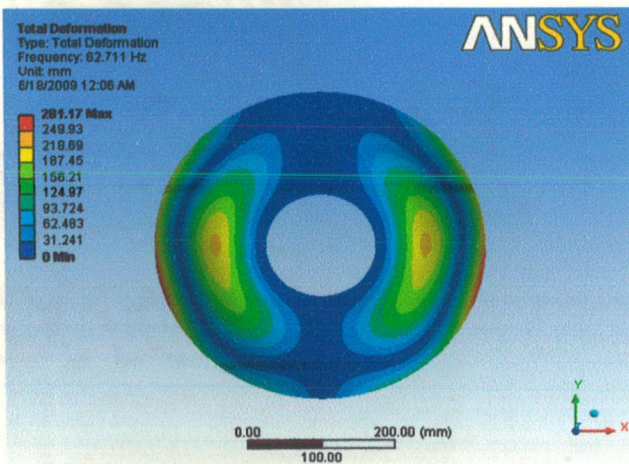
V Mode: $f_n = 43.726$ Hz
(Isometric view)



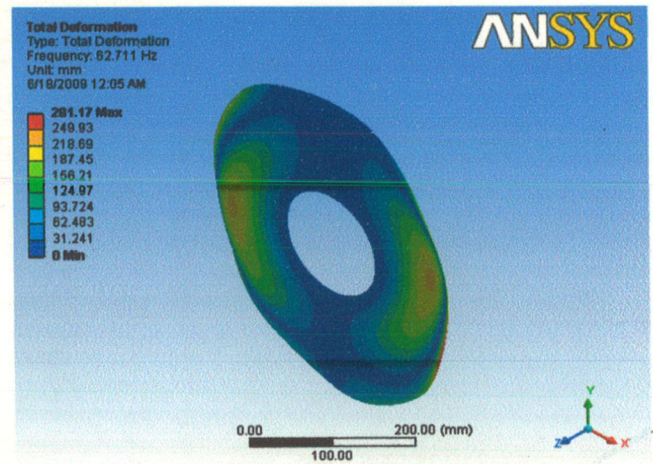
VI Mode: $f_n = 59.542$ Hz
(Front view)



VI Mode: $f_n = 59.542$ Hz
(Isometric view)



VII Mode: $f_n = 62.711$ Hz
(Front view)



VII Mode: $f_n = 62.711$ Hz
(Isometric view)

Figure 6.28: Mode shape of circular annular plate with PZT patches

In the experiment, one PZT patch is used as the sensor and four PZT patches are used as the actuator. The features of mode shapes with PZT patches are drastically changed as compared to without PZT patches due to un-symmetric structure.

7.1 Conclusion

In this work a finite element model of the piezolaminated composite plate based on the classical laminated plate theory is presented. In deriving the finite element model of piezolaminated composite plate first assumptions of the classical laminated plate theory is given followed by modeling of circular plate with PZT patches in which natural frequency equation with PZT patches and without PZT patches are discussed. Further, constitutive equation of piezoelectric materials, linear strain-displacement relations, electric field voltage relations, governing equation of motion, sensor voltage relations and actuator force relations are derived. Natural frequencies with different aspect ratio are calculated with the derived equations and compared with the available literature. It has been found that calculated value agree very well with the reference value. By *ANSYS* simulation it has been observed that natural frequency of plate is increases with PZT patches as compared to the without PZT patches, because addition of extra material with higher stiffness: mass ratio on the original structure. Mode shapes with PZT patches and without PZT patches both are presented and it is shown that the feature of mode shape with PZT patches are changed as compared to without PZT patches. It is due to structure becomes un-symmetric, because one patch is mounted as a sensor and four patch as the actuator.

Damping effect varies very much with the position of the piezoelectric patches on the surface of the plate. Hence, the most effective location of the PZT patches is determined to suppress the amplitude of vibration. It has been observed that when the sensor/actuator pairs are bonded near the fixed edge of the annular plate, where high strain region is the control effect is best. With the experiment it is concluded that damping effect increases with the increase in the control gain. But the practical limit of the control gain depends on the breakdown voltage of the piezoelectric material, because when the applied voltage is exceeds the breakdown voltage the piezoelectric material losses its piezoelectric properties. Also damping effect depends on the number of patches used but the covering area of the piezoelectric patches should be taken into consideration. Experiment shows that proportional control can achieve better active vibration control of the plate with

piezoelectric patches used as the sensor and actuator and piezoelectric sensor can be used to determine the natural frequency of the plate.

7.2 Scope for future work

- ✓ Experiment can be performed with different control logic for the same structure such as Proportional-Differential and Proportional-Integral-Differential.
- ✓ Classical controller should be replaced with non-classical controller to control the non-linear vibration.
- ✓ Experimental and theoretical analysis should be done to suppress up to higher mode of vibration by changing the location and number of patches used.
- ✓ The adhesive layer thickness should be taken into the analysis.
- ✓ Active control of smart structures can be studied using piezoelectric stack (multi-layer) actuators. Studies may be extended to micro-positioning applications by trajectory control.
- ✓ The control of structures having different types of actuators such as fluid power and servo motor can be used.
- ✓ Active vibration control of smart structure having complicated geometries such as two-dimensional structures should be studied. Also, it needs to be tested on real-life structures, such as airplane wings, helicopter blades, automotive applications, manufacturing processes, motion control, and measurement systems.

REFERENCES

1. Al-hazmi Mohammed W., "Finite Element Analysis of Cantilever Plate Structure Excited by Patches of Piezoelectric Actuators", Institute of Electrical and Electronics Engineers, Inc. Vol 978-1-4244-1701-8/08, 2008 ,pp 809-814
2. ANSYS User's Manual (version 11), *ANSYS Inc. Southpointe 275 Technology Drive Canonsburg, PA,15317.*
3. Alciatore David G.,Hiland Michael B., "Introduction to Mechatronics and Measurement Systems", IIIrd Edition, Tata McGraw-Hill Publishing Company Ltd, ISBN: 978-0-07-064814-2, pp 317-336
4. Akhras Georges, "Smart Materials and Smart Systems for the Future", Canadian Military Journal, Autumn 2000, pp 25-32
5. Bhattacharya P., Suhail H., and Sinha P.K., "Finite Element Free Vibration Analysis of Smart Laminated Composite Beams and Plates", Journal of Intelligent Materials Systems and Structures, Vol 9, 1998,pp 20-28
6. Barboni R., Mannini A., Fantini E., and Gaudenzi P, "Optimal Placement of PZT Actuators for the Control of Beam Dynamics", Journal of Smart Materials and Structures, Vol 9, 2000, pp 110-120
7. Behrens Sam, "Passive and Semi-active Vibration Control of Piezoelectric Laminates", M.E (Research) Thesis,2000, Department of Electrical and Computer Engineering, University of Newcastle, Australia
8. Bolton W., "Mechatronics- Electronic Control System in Mechanical and Electrical Engineering", IIIrd Edition, Pearson Education Ltd, ISBN: 81-7758-284-4, 2003,pp296-320
9. Bambill D.V., Laura P.A.A.A., and Rossi R.E., "The Fundamental Frequency of Transverse Vibrations of Rectangularly Orthotropic, Circular, Annular Plates with Several Combinations of Boundary Conditions", Journal of Sound and Vibration, Vol 216 (3), 1998, pp 543-551
10. Crawley E.F., and Luis Javier de, "Use of Piezoelectric Actuators as Elements of Integrated Structures", The American Institute of Aeronautics and Astronautics (AIAA) Journal, Vol 25, 1987, pp 1373-1385

11. Clayton L. Smith, "Analytical Modeling and Equivalent Electromechanical Loading Techniques for Adaptive laminated Piezoelectric Structures", PhD Thesis, 2001, Virginia Polytechnic Institute and State University, Blacksburg, Virginia.
12. Chiu Shyh-Rong, "Circular Plate Analysis using Finite Element Method", MS (Mechanical Engineering) Thesis, 1986, Graduate School of New Jersey Institute of Technology, USA
13. Chandrupatla T.R. and Belegundu A.D., "Introduction to Finite Element in Engineering", Pearson Education, IIIrd Edition, 2006, pp 23-38, 51-58, 230-240.
14. Dhuri K.D. and Seshu S., "Favorable locations for Piezo Actuators in Plates with good Control Effectiveness and Minimal Change in System Dynamics", Journal of Smart Materials and Structures, Vol 16,2007,pp2526-2542
15. Damaren Christopher J, "Optimal location of Collocated Piezo-actuator/sensor Combinations in Spacecraft Box Structures", Journal of smart Materials and Structures, Vol 12, 2003, pp494-499
16. Dimitriadis E.K, Fuller C. R and Rogers C. A, "Piezoelectric Actuators for Distributed Vibration Excitation of Thin Plates", Journal of Vibration and Acoustics, Vol 113, 1991, pp 100-106
17. Fei Juntao and Fang Yunmei, "Active Feedback Vibration Suppression of a Flexible Steel Cantilever Beam Using Smart Materials", Proceedings of the First International Conference on Innovative Computing, Information and Control (ICICIC'06), IEEE, 2006, pp 1-4
18. Gaudenzi P., Carbonaro R. and Benzi E., "Control of Beam Vibrations by means of Piezoelectric Devices: Theory and Experiments". Journal of Composite Structures, Vol- 50, 2000, pp 373-379.
19. Goswami S., Kant T., "Active Vibration Control of Intelligent Stiffened Laminates using Smart Piezoelectric Materials by Finite Element Method", Journal of Reinforced Plastics and Composites, Vol 17 (16),1998, pp 1472-1493
20. Gorman D.G., "Natural Frequencies of Polar Orthotropic Uniform Annular Plates", Journal of Sound and Vibration, Vol 80(1),1982, pp 145-154

21. Gaudenzi Paolo, Carbonaro Rolando and Benzi Edoardo, "Control of Beam Vibrations by means of Piezoelectric Devices: Theory and Experiments", *Journal of Composite Structures*, Vol 50, 2000, pp 373-379
22. Han J.B and Liew K.M., "Axisymmetric Free Vibration of Thick Annular Plates", *International Journal of Mechanical Sciences*, Vol 41,1999,pp1089-1109
23. Han Jae-Hung, Rew Keun-Ho and Lee In, " An Experimental Study of Active Vibration Control of Composite Structures with a Piezo-Ceramic Actuator and a Piezo-film Sensor", *Journal of Smart Materials and Structures*, Vol 6,1997,pp 549-558.
24. Halim Dunant, "Vibration Analysis and Control of Smart Structures", PhD Thesis, 2002, School of Electrical Engineering and Computer Science, The University of Newcastle, Australia.
25. Hsu Ming-Hung, "Vibration Analysis of Annular Plates", *Tamkang Journal of Science and Engineering*, Vol 10(3), 2007, pp 193-199
26. Harris C.M. and Crede C.E., "Shock and Vibration Handbook", Mc-Graw Hill Book Company Ltd, IInd Edition, 1976, pp 1.13-1.16, 7.26-7.32
27. Hutton David, "Fundamental of Finite Element Analysis", Mc-Graw Hill Higher Education, Ist Edition, ISBN 0-07-112231-1,pp 91-124
28. Hu Yan-Ru and Ng Alfred, "Active Robust Vibration Control of a Circular Plate Structure using Piezoelectric Actuators", 43rd American Institute of Aeronautics and Astronautics /ASME/ASCE/AHS/ASC Structures, Structural Dynamics, and Materials Conference, 22-25 April 2002, Denver, Colorado
29. Hwang Woo-Seok, Hwang Woonbong, and Park Hyun Chul, "Vibration Control of laminated Composite Plate with Piezoelectric sensor/actuator: Active and Passive Control Methods", *Journal of Mechanical System and Signal Processing*, Vol 8(5), 1994, pp 571-583.
30. Han Jae-Hung and Lee In, "Optimal Placement of Piezoelectric Sensor and Actuator for Vibration Control of a Composite Plate using Genetic Algorithms", *Journal of Smart Material and Structures*, Vol 8,1999,pp 256-267.

31. Halim Dunant and Moheimani S. O. Reza, "An Optimization Approach to Optimal Placement of Collocated Piezoelectric Actuators and Sensors on a Thin Plate", *Journal of Mechatronics*, Vol 13,2003,pp 27-47.
32. Hurlebaus S. and Gaul L., "Smart Structure Dynamics", *Journal of Mechanical Systems and Signal Processing*, Vol 20, 2006, pp 255-281
33. Kumar Ramesh K. and Narayanan S., "Active Vibration Control of Beam with Optimal Placement of Piezoelectric Sensor/ Actuator pairs", *Journal of Smart Materials & Structures*, Vol 17,2008,pp 1-15.
34. Kovalovs E.A., Barkanov S. and Gluhihs, "Active Control of Structures using Macro-fiber Composite (MFC)", *Functional Materials and Nanotechnologies (FM&NT 2007)*, *Journal of Physics: Conference Series*, Vol 93,2007, 012034
35. Karagulle H., Malgaca L. and Oktem H. F., "Analysis of Active Vibration Control in Smart Structures by *ANSYS*", *Journal of Smart Materials and Structures*, Vol 13, 2004, pp 661-667
36. Khanna Juhi, "Modeling and Control of Smart Cantilever Beam", M.Tech dissertation, 2004, System and Control Engineering Department, IIT, Bombay
37. Kang Wook, Lee Nam-Ho, Pang Shusheng and Chung Woo Yang, "Approximate Closed Form Solutions for Free Vibration of Polar Orthotropic Circular Plates", *Journal of Applied Acoustics*, Vol 66, 2005, pp 1162-1179
38. Lam K. Y., Peng X. Q., Liu G. R. and Reddy J. N., "A Finite-element Model for Piezoelectric Composite Laminates", *Journal of Smart Materials and Structures*, Vol 6,1997,pp 583-591
39. Lee Y. Y. and Yao J., "Structural Vibration Suppression using the Piezoelectric Sensors and Actuators", *Journal of Vibration and Acoustics*, Vol 125,2003,pp 109-113.
40. Liu Chorng-Fuh and Chen Ge-Tzung, "A Simple Finite Element Analysis of Axisymmetric Vibration of Annular and Circular Plates", *International Journal of Mechanical Science*, Vol 37, No 8, 1995, pp 861-871
41. Liu C. F., and Lee Y.T., "Finite Element Analysis of Three-dimensional Vibrations of Thick Circular and Annular Plates", *Journal of Sound and Vibration*, Vol 233(1),2000, pp 63-80

42. Lin C.C., and Tseng C.S., "Free Vibration of Polar Orthotropic laminated Circular and Annular Plates", *Journal of Sound and Vibration*, Vol 209(5), 1998, pp 797-810
43. LabVIEW User Manual, National Instruments Corporate Headquarters, 6504 Bridge Point Parkway, Austin , Texas, USA
44. LabVIEW Data Acquisition Basics Manual, National Instruments Corporate Headquarters, North Mopac Expressway, Austin, Texas, USA
45. Malgaca Levent and Karagulle Hira, "Active Control of Free and Forced Vibrations in Piezoelectric Smart Structures", 18th International Conference of Adaptive Structures and Technologies, October 3th,4th and 5th,2007. Ottawa, Ontario, Canada.
46. Mukherjee A., Joshi S.P. and Ganguli A., "Active Vibration Control of Piezolaminated Stiffened Plates", *Journal of Composite Structures*, Vol 55,2002, pp 435-443
47. Malgaca Levent, "Integration of Active Vibration Control Methods with Finite Element Models of Smart Structures", PhD Thesis, 2007, Graduate School of Natural and Applied Sciences of Dokuz Eylül University, İZMİR, Turkey
48. Meirovitch Leonard, "Elements of Vibration Analysis",IInd Edition, Tata McGraw-Hill Publishing Company Ltd.,ISBN 0-07-063431-9,2007, pp 519-530
49. Moita Jose M. Simoes, Soares Cristovao M. Mota and Soares Carlos A. Mota, "Active Control of Forced Vibrations in Adaptive Structures using a Higher Order Model", *Journal of Composite Structures*, Vol 71, 2005, pp 349-355.
50. Moita Jose M. Simoes, Correia Victor M. Franco, Martins Pedro G, Soares Cristovao M. Mota and Soares Carlos A. Mota, "Optimal Design in Vibration Control of Adaptive Structures using a Simulated Annealing Algorithm", *Journal of Composite Structures*, Vol 75, 2006, pp 79-87.
51. Nie G. J. and Zhong Z, "Semi-analytical Solution for Three-dimensional Vibration of Functionally Graded Circular Plates", *Journal of Computer Methods in Applied Mechanics and Engineering*, Vol 196, 2007, pp 4901-4910
52. Park Chan II., "Frequency Equation for the in-plane Vibration of a Clamped Circular Plate", *Journal of Sound and Vibration*", Vol 313, 2008, pp 325-333

53. Peng F., Ng Alfred and Ru Hu Yan, "Adaptive Vibration Control of Flexible Structures with Actuator Placement Optimization", Proceeding of IMECE'03, 2003 ASME International Mechanical Engineering. Congress, Washington, IMECE2003, pp 1-10
54. Preumont Andre, "Vibration Control of Active Structures", Kluwer Academic Publisher, IInd Edition, 2002, pp 30-33, 40-58.
55. Peng X.Q, Lam K.Y, and Liu G.R, "Active Vibration Control of Composite Beams with Piezoelectric: A Finite Element Model with Third Order Theory", Journal of Sound and Vibration, Vol 209(4), 1998, pp 635-650
56. Pankaj K. Langote and Seshu P., "Experimental Studies on Active Vibration Control of a Beam using Hybrid Active/Passive Constrained Layer Damping Treatments." Journal of Vibration and Acoustics, ISSN 1048-9002, Vol 127, no5, 2005, pp 515-518
57. Quek S. T., Wang S. Y. and Ang K. K., "Vibration Control of Composite Plates via Optimal Placement of Piezoelectric Patches", Journal of Intelligent Material Systems and Structures, Vol 14, 2003, pp 229-245.
58. Qiu Zhi-cheng, Zhang Xian-min, Wu Hong-xin and Zhang Hong-hua, "Optimal Placement and Active Vibration Control for Piezoelectric Smart Flexible Cantilever Plate", Journal of Sound and Vibration, Vol 301,2007,pp 521-543
59. Qiu Jinhao and Haraguchi Masakazu, "Vibration Control of a Plate using Self-sensing Piezoelectric Actuator and an Adaptive Control Approach", Journal of Intelligent Material System and Structures, Vol 17,2006,pp 661-669.
60. Reddy J.N., "Theory and Analysis of Elastic Plates", Taylor & Francis, Philadelphia, PA 19106, ISBN 1-56032-705-7, 1998, pp 179-247
61. Reddy J.N., "On Laminated Composite Plates with Integrated Sensors and Actuators", Journal of Engineering Structures, Vol 21, 1999, pp 568-593
62. Rao J.S., "Dynamics of Plates", Narosa Publishing House, New Delhi, 1999, ISBN 81-7319-250-2, pp 110-136
63. Rao S.S., "Mechanical Vibration", IVth Edition, Pearson Education (Singapore) Pte. Ltd., ISBN 81-297-0179-0, pp 49-61

64. Rao S.S., "The Finite Element Method in Engineering", IVth Edition, Elsevier Publisher, ISBN: 81-8147-885-1, 2005, pp 357-390
65. Sekouri El Mostafa, Hu Yan-Ru and Ngo Anh Dung, "Modeling of a Circular Plate with Piezoelectric Actuators", Journal of Mechatronics, Vol 14, 2004, pp 1007-1020.
66. Sun, D.C., Wu, H.X. and Wang D.J., "Modal Control of Smart Plates and Optimal Placement of Piezoelectric Actuators," In: Proceeding to International Conference in Vibration Engineering. 1998, pp 551-555, Northeastern University Press, Dalian, China.
67. Sethi Vineet and Song Gangbing, "Multimodal Vibration Control of a Flexible Structure using Piezoceramics", Proceedings of the 2005 IEEE/ASME, International Conference on Advanced Intelligent Mechatronics, Monterey, California, USA, 24-28 July, 2005
68. Tylikowski A, "Control of Circular Plate Vibrations via Piezoelectric Actuators Shunted with a Capacitive Circuit", Journal of Thin-Walled Structures, Vol 39,2001,pp 83-94
69. Tiersten H.F., "Linear Piezoelectric Plate Vibration", Plenum Press, New York, 1969, pp 33-36,51-61
70. Tiersten H.F., "Thickness Vibrations of Piezoelectric Plates", The Journal of the Acoustical Society of America, Vol 35(1), 1963,pp 53-58.
71. Thomson B.S., Gandhi M.V. and Kasiviswanathan S., "An Introduction to Smart Materials and Structures", Materials and Design, Vol 13, 1992,pp 3-9
72. Taher H. Rokni Damavand, Omidi M., Zadpoor A.A and Nikooyan A.A, "Free Vibration of Circular and Annular Plates with Variable Thickness and different Combinations of Boundary Conditions", Journal of Sound and Vibration, Vol 296 , 2006 ,pp 1084-1092
73. V. Nalbantoglu, "Robust Control and System Identification for flexible Structure", PhD Thesis, 1998, University of Minnesota, St. Paul, Minnesota, USA

74. Wang Q., Quek S. T., Sun C. T. and Liu X., "Analysis of Piezoelectric Coupled Circular Plate", *Journal of Smart Materials and Structures*, Vol 10, 2001, pp 229-239.
75. Wang S.Y., Quek S.T. and Ang K.K., "Dynamic Stability Analysis of Finite Element Modeling of Piezoelectric Composite Plates", *International Journal of Solids and Structures*, Vol 41, 2004, pp 745-764
76. Wang S. Y., Tai K., Quek S.T., "Topology Optimization of Piezoelectric Sensors/Actuators for Torsional Vibration Control of Composite Plates", *Journal of Smart Materials and Structures*, Vol 15, 2006, pp 253-269
77. Wang, S. Y., Quek, S.T., and Ang, K.K., "Vibration Control of Smart Piezoelectric Composite Plates", *Journal of Smart Materials and Structures*, Vol 10, 2001, pp 637-644
78. Wang C.M., Xiang Y., Watanabe E. and Utsunomiya T., "Mode Shapes and Stress-resultants of Circular Mindlin Plates with Free Edges", *Journal of Sound and Vibration*, Vol 276, 2004, pp 511-525.
79. Yalcin Hasan Serter, Arikoglu aytac and Ozkol Ibrahim, "Free Vibration Analysis of Circular Plates by Differential Transformation Method", *Journal of Applied Mathematics and Computation*, 2009, www.elsevier.com/locate/amc (article in press)
80. Yan Y.J. and Yam L.H., "Optimal Design of Number and Locations of Actuators in Active Control of a Space Truss", *Journal of Smart Materials and Structures*, Vol 11, 2002, pp 496-503
81. Yaman Yavuz, Caliskan Tarkan, Nalbantoglu Volkan, Prasad Eswar and Waechter David, "Active Vibration Control of a Smart Plate", *International Congress of Aeronautical Structures*, Canada, Oct 2002
82. Yaman Y., Caliskan T., Nalbantoglu V., Waechter D. and Prasad E., "Active Vibration Control of a Smart Beam", *Canada-US CanSmart Workshop Smart Materials and Structures* proceedings, Oct. 2001 Montreal Quebec, Canada
83. Yan S.U. and Ghasemi-Nejhad Mehrdad N, "Analytical Modeling and Active Vibration Suppression of Adaptive Composite Panels with Optimal Actuator

- Configurations”, Journal of Smart Materials and Structures, Vol 16, 2007, pp 2516-2525
84. Yun Wang, Rong-qiao XU and Hao-jiang DING, “Free Vibration of Piezoelectric Annular Plate”, ISSN 1009-3095, Journal of Zhejiang University Science, China, Vol 4, No4, 2003,pp 379-387
 85. Zhou D., Au F. T. K., Cheung Y. K and Lo S.H., “Three-dimensional Vibration Analysis of Circular and Annular Plates via the Chebyshev-Ritz Method”, International Journal of Solids and Structures, Vol 40, 2003, pp 3089-3105
 86. <http://www.sparklceramics.com>
 87. <http://www.ni.com/labview>
 88. <http://www.hk-phy.org>
 89. <http://www.smart.tamu.edu>
 90. <http://www.azom.com>
 91. <http://www.physikinstrumente.com>
 92. <http://www.virtualskies.arc.nasa.gov>
 93. <http://www.physicsmail.org>